

Emulsion Droplet Spreading at Air/Water Interfaces:
Mechanisms and Relevance to the Whipping of Cream

Promotor:

prof. dr. M. A. Cohen Stuart
hoogleraar fysische chemie
met bijzondere aandacht voor de kolloïdchemie

Co-promotoren:

dr. G. A. van Aken
projectleider WCFS
NIZO

dr. ir. T. van Vliet
projectleider WCFS
Agrotechnology & Food Innovations

Samenstelling promotiecommissie:

Prof. dr. H. D. Goff	University of Guelph, Canada
Prof. dr. W. G. M. Agterof	Universiteit Twente
Dr. ir. W. Kloek	Campina Innovation, Wageningen
Prof. dr. R.J. Hamer	Wageningen Universiteit

Dit onderzoek was uitgevoerd binnen de onderzoekschool VLAG.

Emulsion Droplet Spreading at Air/Water Interfaces:
Mechanisms and Relevance to the Whipping of Cream

Natalie Elizabeth Hotrum

Proefschrift
ter verkrijging van de graad van doctor
op gezag van de rector magnificus
van Wageningen Universiteit,
Prof. dr. ir. L. Speelman,
in het openbaar te verdedigen
op dinsdag 22 juni 2004
des namiddags te half twee in de Aula

ISBN: 90-8504-025-6

*Who has seen the wind?
Neither I nor you.
But when the leaves hang trembling,
The wind is passing through.*

*Who has seen the wind?
Neither you nor I.
But when the trees bow down their heads,
The wind is passing by.*

Christina Georgina Rossetti (1830-1894)

Hotrum, N.E. (2004)

Emulsion Droplet Spreading at Air/Water Interfaces: Mechanisms and Relevance to the Whipping of Cream.

Ph.D. Thesis, Wageningen University, The Netherlands

Keywords: emulsion, spreading coefficient, surface tension, emulsifier, whipped cream, dairy foam, partial coalescence

Abstract:

In this thesis, the interaction between emulsion droplets and expanding air/water interfaces was investigated. The objective was to deepen our knowledge concerning the physical processes that take place at the expanding air surfaces that form during aeration of emulsions. Emulsions can become aerated as a result of various processing operations, for example, stirring or pouring. Moreover, emulsions may be aerated with the intention of producing an aerated food product such as whipped cream or ice cream.

Emulsion droplet/air interaction can have important consequences for emulsion stability. For example, emulsion droplet spreading at the air/water interface can initiate a collective oil spreading mechanism, resulting in the spreading of many oil droplets. This may lead to coalescence of the emulsion droplets. The tendency for an oil droplet to spread at an expanding air/water interface depends on the values of the dynamic interfacial tensions at the air/water, oil/water and oil/air interfaces. This can be expressed in terms of a dynamic spreading coefficient; when the spreading coefficient is positive, oil spreads out of the droplets.

Experimental results confirmed that oil indeed only spreads out of emulsion droplets if the dynamic spreading coefficient is positive. The tendency for an emulsion droplet to spread at the air/water interface could be controlled by manipulating the surface expansion rate, the protein type and concentration, and type and concentration of emulsifier in the emulsion. The presence of crystalline fat, although relevant to the stability of emulsions exposed to shear, was not found to influence the spreading behaviour of emulsion droplets at the air/water interface. The results of the emulsion droplet spreading experiments lead to the development of a model that describes the whipping time of cream in terms of the proportion of the air bubble surface for which the spreading coefficient is positive. Experimental results for the whipping of model creams could be well explained by this model.

Table of Contents

1	Introduction	1
1.1	Scope	2
1.2	Aerating cream by whipping	2
1.3	Entering and spreading phenomena	4
1.4	Motivation and research objective	6
1.5	Outline of this thesis	7
	Acknowledgements	7
	References	7
2	Monitoring entering and spreading of emulsion droplets at an expanding air/water interface: a novel technique	9
2.1	Introduction	10
2.2	Materials and Methods	14
2.2.1	Materials	14
2.2.2	Solution and emulsion preparation	14
2.2.3	Roller trough technique and measurement of surface tension	15
2.2.4	Microscopy	17
2.3	Results	17
2.4	Discussion	21
2.5	Conclusions	24
	Acknowledgements	24
	References	24
3	Flow and fracture phenomena in adsorbed protein layers at the air/water interface in connection to spreading oil droplets	27
3.1	Introduction	28
3.2	Materials and Methods	32
3.2.1	Materials	32
3.2.2	Methods	33
3.3	Results	34
3.3.1	Definition of the wetting transition	34
3.3.2	Π/A curves of protein films and the wetting transition	34
3.3.3	Mechanical properties of protein films	39
3.4	Discussion	42
3.5	Concluding Remarks	44
	Acknowledgements	45
	References	46

4	Oil droplet spreading in the presence of proteins and low molecular weight surfactants	49
4.1	Introduction	50
4.2	Materials and Methods	52
4.2.1	Materials	52
4.2.2	Emulsion preparation	52
4.2.3	Determination of Π_{AW} at spreading	53
4.2.4	Determination of γ_{OW}	55
4.3	Results	55
4.3.1	Π_{AW} at spreading	55
4.3.2	γ_{OW} in the presence of lmw surfactants and proteins	57
4.4	Discussion	59
4.5	Concluding Remarks	64
	Acknowledgements	65
	Appendix	65
	References	65
5	Spreading of partially crystallised oil droplets on an air/water interface	69
5.1	Introduction	70
5.2	Materials and Methods	74
5.2.1	Materials	74
5.2.2	Determination of γ_{OW} and γ_{OA}	75
5.2.3	Determination of spreadability and spreading rate	75
5.2.4	Determination of Π_{AW} at spreading	76
5.3	Results	77
5.3.1a	Spreading at clean air/water interfaces: spreadability	77
5.3.1b	Spreading at clean air/water interfaces: spreading rate	79
5.3.2	Spreading in the presence of an adsorbed protein layer: Π_{AW} at spreading	82
5.4	Discussion	85
5.4.1a	Spreading at clean air/water interfaces: spreadability	85
5.4.1b	Spreading at clean air/water interfaces: spreading rate	86
5.4.2	Spreading in the presence of an adsorbed protein layer: Π_{AW} at spreading	87
5.5	Concluding Remarks	88
	Acknowledgements	89
	References	89

6	Elucidating the relationship between the spreading coefficient, surface-mediated partial coalescence and the whipping time of cream	91
6.1	Introduction	92
6.2	Materials and Methods	97
6.2.1	Materials	97
6.2.2	Emulsion preparation	97
6.2.3	Whipping of emulsions	98
6.3	Results	98
6.4	Discussion	104
6.5	Summary	109
	Acknowledgements	110
	References	110
	Summary	113
	Samenvatting	117
	List of Publications	121
	Acknowledgements	123
	Curriculum Vitae	125

Chapter 1:

Introduction

1.1 Scope

Aeration, or the incorporation of air bubbles, is one of the fastest growing processing operations in the food industry [1]. A wide variety of aerated food products are available; a few examples include whipped cream, ice cream, mousse, meringue, soufflé, bread, cake, carbonated soft drinks, beer, champagne and cappuccino foam. In this thesis we will concentrate on one class of aerated food system: the aerated emulsion. In aerated emulsions such as whipped cream, ice cream and milkshakes, a three-phase partially crystallised fat-in-water emulsion is transformed into a four-phase system as air bubbles are incorporated.

This thesis is focussed on the role of the interaction between emulsion (fat) droplets and air bubbles during the aeration of emulsions. We pay special attention to the role of emulsion droplet/air interaction in the development of structure in whipped cream. However, in a wider frame of reference, emulsion droplet/air interaction may be an important parameter controlling emulsion stability during any processing operation where emulsion droplets come into contact with air such as stirring, pouring or mastication.

In the present chapter, we begin by describing the main processes that take place during the aeration of cream by whipping (section 1.2). Since the interaction between emulsion droplets and the air bubble surface is one of the main steps in the development of whipped cream structure, we go on to describe the phenomenon of droplet entering and spreading at the air/water interface (section 1.3). Finally, the aim (section 1.4) and outline (section 1.5) of this thesis are presented.

1.2 Aerating cream by whipping

In whipped cream, air bubbles are incorporated into the cream by mechanically beating air into the system. This can be achieved, for example, by using a hand mixer. The processes that take place during the whipping of cream have been extensively studied, and a number of reviews can be found in the literature [2-5]. During whipping, foam containing large air bubbles stabilised by adsorbed proteins is initially formed [2,6]. As whipping continues, the air bubbles become smaller and fat globules (emulsion droplets) adsorb to the air bubble surface [7-10]. The adsorbed fat globules coexist with adsorbed protein at the air bubble surface [6,8,10]. Further,

during adsorption, fat globules appear to lose a portion of the fat globule membrane such that the fat comes in direct contact with the air [10,11]. The adsorbed fat globules form fat clumps by means of partial coalescence in the interface [3,5]. This implies that droplets fuse, but do not merge into a single droplet (or lens) due to the presence of a crystalline fat network within the droplets [12,13]. Thus, the presence of crystalline fat in the fat globules is critical for the formation of whipped cream. The final whipped cream structure is formed by the build-up of a network of partially coalesced fat globules, which hold the air bubbles in place and trap the aqueous phase by capillary action.

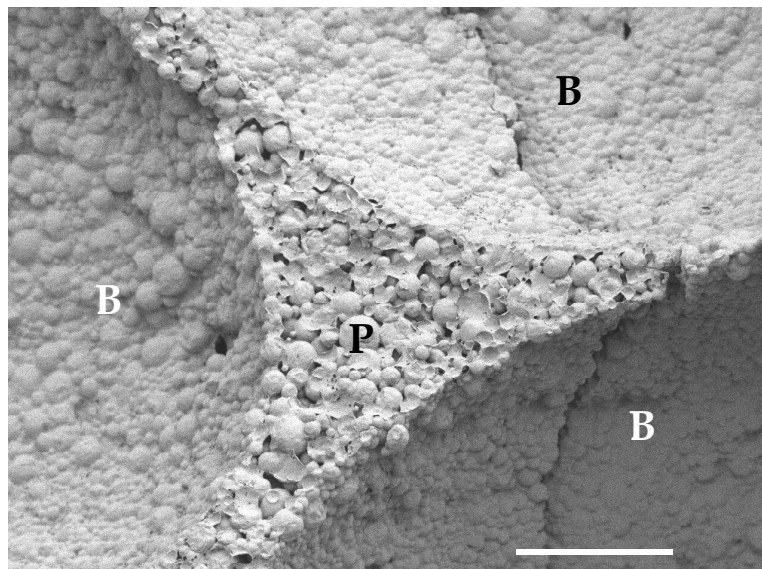


Figure 1.1: Scanning electron micrograph of whipped recombined cream containing 14 wt% hydrogenated palm fat, 26 wt% sunflower oil, stabilised by 1 wt% whey protein isolate. Bar = 10 μ m. Air bubbles, B, and the plateau border, P, are indicated.

Cream comes in several varieties. Natural cream is collected by centrifuging fresh milk. Further, cream may be homogenised, or recombined cream may be prepared. The fat droplets in homogenised and recombined cream are generally smaller than in natural cream. In homogenised cream, the fat droplets are stabilised by adsorbed casein and whey protein instead of by the milk fat globule membrane as is the case for natural cream [14]. In recombined cream, the protein and fat phase may differ considerably from that of natural cream. For example, recombined cream may consist of a butterfat emulsion stabilised by skim milk proteins [15]. Or, in order to make

creams more suitable for use in warm climates, it might be desirable to use a fat with a higher melting point, such as fractionated milk fat [16] or hydrogenated palm oil [17]. The whipping of homogenised and recombined cream follows the same process as that described above for natural cream and the final structure is similar to that of whipped natural cream. This can be observed in Figure 1.1 for the whipped model cream used in this thesis: fat droplets are attached to the air bubbles and connected via a partially coalesced fat droplet network; the triangular plateau border between the air bubbles is densely packed with fat droplets.

Although the same processes occur during the whipping of homogenised and recombined cream as during the whipping of natural cream, comparison of literature data reveals that homogenised and recombined creams often have much longer whipping times than natural cream [7,9,15]. This is considered undesirable. It is empirically known that emulsifiers (low molecular weight surfactants) can be added to improve the whipping properties of cream [15].

1.3 Entering and spreading phenomena

Adsorption of fat droplets at the air/water interface is a key step in the development of whipped cream structure. A fat droplet in the vicinity of an air/water interface can adopt one of three conformations: a non-entered droplet, a lens, or a spread oil layer. These conformations are depicted in Figure 1.2; for simplicity, we consider the interaction between a fat droplet containing only liquid fat (oil) and the air/water interface. Whether or not an oil droplet can enter or spread at an air/water interface is determined by the balance of three surface tensions (γ) between the air (A), water (W), and oil (O) phases. In addition, the mechanical properties of an adsorbed layer at the air/water or oil/water interfaces can play an important role.

Robinson and Woods [18] derived an entering coefficient, E , to predict whether a droplet will enter the air/water interface (Figure 1.2b) or remain submerged (Figure 1.2a). E is given by

$$E = \gamma_{AW} + (\gamma_{OW} - \gamma_{OA}) \quad (1.1)$$

Oil droplet entering is expected to occur if $E > 0$. For most oils, γ_{OW} is larger than γ_{OA} , meaning that the term $(\gamma_{OW} - \gamma_{OA})$ in Equation 1.1 will be positive. This means that negative γ_{AW} values are required for $E < 0$. Since this is

theoretically not possible, we expect $E > 0$ and oil droplet entering to occur for all oil/water systems where $\gamma_{OW} > \gamma_{OA}$.

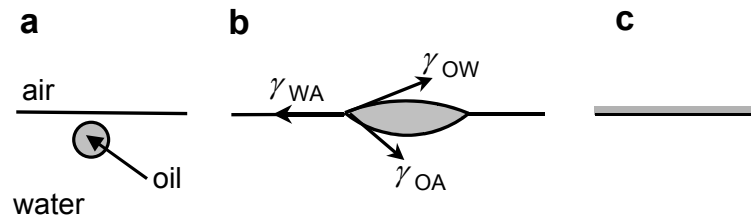


Figure 1.2: Schematic representation of the three possible conformations for an oil droplet in the vicinity of the air/water interface: (a) not entered, (b) entered and resting in the air/water interface and (c) spread.

More recently, however, it has been demonstrated that oil droplets do not always enter the air/water interface for systems where the condition $E > 0$ is satisfied. This has been explained by the formation of a thin film between an approaching oil droplet and the air/water interface, which can act as a kinetic barrier to droplet entering resulting in a metastable state [19,20]. Moreover, surfactants such as proteins can adsorb at the air/water and oil/water interfaces providing mechanical stability to the interface, thus inhibiting droplet entering [21,22]. In this thesis we do not specifically investigate the process of oil droplet entering. However, it is important to recognise that droplet entering is the precursor to oil droplet spreading.

During the whipping of cream, a limited amount of oil spreading out of fat droplets at the air bubble surface enables the droplets to partially coalesce giving rigidity to the air bubble surface [10]. The tendency for an oil lens (Figure 1.2b) to form a spread oil layer (Figure 1.2c) is predicted by the balance of interfacial tensions at the air/water/oil phase boundary [23]:

$$S = \gamma_{AW} - (\gamma_{OW} + \gamma_{OA}) \quad (1.2)$$

When S is positive, oil spreads. The presence of a spreading oil layer can facilitate the entering and spreading of more oil droplets, as these need now only coalesce with the spreading oil layer [24]. This mechanism of facilitated oil spreading could be of great importance to the stability of emulsions when they come into contact with air as a result of processing operations such as stirring or pouring. Admittedly, this mechanism is probably not applicable to the whipping of cream, where only limited oil spreading occurs.

Triglyceride oils such as soybean oil or butter oil can spread at the clean air/water interface, while paraffin oil, for which S is negative, cannot [25-27]. Surfactants such as proteins or low molecular weight surfactants (also called emulsifiers) can adsorb at air/water interfaces and lower the surface tension. This can cause S to become negative, thus inhibiting oil spreading [25-27]. In relation to whipped cream, the air bubbles are initially stabilised by adsorbed protein, and authors have recognised the need for expansion of the air bubble surface during whipping in order to reduce the air/water surface tension and allow the adsorption and spreading of fat globules at the air bubble surface [8,10]. Further, proteins or low molecular weight surfactants can adsorb at the oil/water interface, lowering the value of γ_{OW} ; this may also influence oil droplet spreading, and is a topic of investigation in this thesis.

1.4 Motivation and research objective

It is well established that system parameters such as whipping speed, protein concentration, protein type and the addition of low molecular weight surfactants influence the whipping properties (e.g. whipping time, overrun and firmness) of recombined cream [8,15,28]. Explanations for the influence of these system parameters on the whipping properties of cream have been sought in the way these parameters influence the susceptibility of fat droplets to shear-induced partial coalescence. However, when an emulsion containing both liquid and crystalline fat is sheared in the presence of air, a second and very effective type of partial coalescence can take place. During the whipping of cream fat globules adhere to the air bubble surface. Consequently, the oil present in the droplets comes into direct contact with air, which enhances the tendency of the droplets to coalesce so that interfacial droplet clumping takes place [3,5]. This can be denoted as surface-mediated partial coalescence. Authors have recognised that surface tension and the properties of adsorbed protein layers at both air bubble and emulsion droplet surfaces may be important factors influencing the interaction between emulsion droplets at the air bubble surface during the whipping of cream [3-5,8,10]. However, only a few studies have been reported that attempt to quantify this interaction [26,27,29], and the literature concerning surface-mediated partial coalescence is sparse. Therefore, the objective of this thesis is to identify the parameters that are of relevance to the adsorption and spreading of emulsion droplets at the air/water interface in general, and at the surface of air bubbles during

whipping in particular. Moreover, we aim to determine whether a link exists between the entering and spreading behaviour of emulsion droplets at the air/water interface and the whipping properties of cream.

1.5 Outline of this thesis

In Chapter 2 we describe a method developed in our laboratory for the study of surface pressure conditions at the moment when emulsion droplet spreading is initiated. The influence of bulk protein concentration and protein type on the spreading behaviour of emulsion droplets at the planar/air water interface is discussed. In Chapter 3 we take an in-depth look at the mechanism of droplet entering and spreading; attention is paid to the influence of rheological properties of the air/water interface and oil phase composition on emulsion droplet spreading behaviour. In Chapters 4 and 5 we investigate how the presence of low molecular weight surfactants and the presence of crystalline fat in the emulsion droplets influence the spreading behaviour of emulsion droplets at planar air/water interfaces, respectively. Finally, in Chapter 6 we make an attempt to describe the mechanism of emulsion droplet/air bubble interaction during the whipping of cream in terms of emulsion droplet spreading behaviour and to identify the parameters of relevance to this mechanism.

Acknowledgements

The scanning electron micrograph presented in Figure 1.1 was made by Henrie van Aalst, Unilever R&D, Vlaardingen, The Netherlands.

References

- [1] Campbell, G. M. and Mougeot, E. (1999). Creation and characterisation of aerated food products. *Trends in Food Science and Technology*, 10, 283-296.
- [2] Brooker, B. E. (1993). Stabilisation of air in foods containing fat - a review. *Food Structure*, 12, 115-122.
- [3] Darling, D. F. (1982). Recent advances in the destabilization of dairy emulsions. *Journal of Dairy Research*, 49, 695-712.
- [4] Goff, H. D. (1997). Instability and partial coalescence in whippable dairy emulsions. *Journal of Dairy Science*, 80, 2620-2630.
- [5] Mulder, H. and Walstra, P. (1974). *The Milk Fat Globule*. Wageningen: Pudoc.
- [6] Anderson, M., Brooker, B. E. and Needs, E. C. (1987). The role of proteins in the stabilization/destabilization of dairy foams. In E. Dickinson, *Food Emulsions and Foams* (pp. 100-109). London: Royal Society of Chemistry.
- [7] Graf, E. and Müller, H. R. (1965). Fine structure and whippability of sterilized cream. *Milchwissenschaft*, 20(6), 302-308.

- [8] Needs, E. C. and Huitson, A. (1991). The contribution of milk serum proteins to the development of whipped cream structure. *Food Structure*, 10, 353-360.
- [9] Schmidt, D. G. and van Hooydonk, A. C. M. (1980). A scanning electron microscopical investigation of the whipping of cream. *Scanning Electron Microscopy*, III, 653-658.
- [10] Brooker, B. E., Anderson, M. and Andrews, A. T. (1986). The development of structure in whipped cream. *Food Microstructure*, 5, 277-285.
- [11] Buchheim, W. (1978). Mikrostruktur von Geschlagenem Rahm [Microstructure of whipped cream]. *Gordian*, 78(6), 184-188.
- [12] Boode, K. and Walstra, P. (1993). Partial coalescence in oil-in-water emulsions 1. Nature of the aggregation. *Colloids and Surfaces A: Physicochemical and Engineering Aspects*, 81, 121-137.
- [13] van Boekel, M. A. J. S. and Walstra, P. (1981). Stability of oil-in-water emulsions with crystals in the disperse phase. *Colloids and Surfaces*, 3, 109-118.
- [14] Darling, D. F. and Butcher, D. W. (1978). Milk-fat globule membrane in homogenized cream. *Journal of Dairy Research*, 45, 197-208.
- [15] Zadow, J. G. and Kieseker, F. G. (1975). Manufacture of recombined whipping cream. *The Australian Journal of Dairy Technology*, 30(3), 114-117.
- [16] Jochems, A. M. P. and van Aken, G. A. (1997). Whippability of cream and recombined cream. *2nd World Congress on Emulsion, Bordeaux, France, September 23-26, 1997*.
- [17] Shamsi, K., Che Man, Y. B., Yusoff, M. S. A. and Jinap, S. (2002). A comparative study of dairy whipping cream and palm oil-based whipping cream in terms of FA composition and foam stability. *Journal of the American Oil Chemists' Society*, 79(6), 583-588.
- [18] Robinson, J. V. and Woods, W. W. (1948). A method of selecting foam inhibitors. *Journal of the Society of Chemical Industry*, 67, 361-365.
- [19] Koczko, K., Lobo, L. A. and Wasan, D. T. (1992). Effect of oil on foam stability: aqueous foams stabilized by emulsions. *Journal of Colloid and Interface Science*, 150(2), 492-506.
- [20] Lobo, L. and Wasan, D. T. (1993). Mechanisms of aqueous foam stability in the presence of emulsified non-aqueous-phase liquids: structure and stability of the pseudoemulsion film. *Langmuir*, 9, 1668-1677.
- [21] Dickinson, E., Murray, B. S. and Stainsby, G. (1988). Coalescence stability of emulsion-sized droplets at a planar oil-water interface and the relationship to protein films and surface rheology. *Journal of the Chemical Society of Faraday Transactions I*, 84(3), 871-883.
- [22] Hadjiiski, A., Dimova, R., Denkov, N. D., Ivanov, I. B. and Borwankar, R. (1996). Film trapping technique: precise method for three-phase contact angle determination of solid and fluid particles of micrometer size. *Langmuir*, 12, 6665-6675.
- [23] Harkins, W. D. and Feldman, A. (1922). Films. The spreading of liquids and the spreading coefficient. *The Journal of the American Chemical Society*, 44(12), 2665-2685.
- [24] Denkov, N. D., Tcholakova, S., Marinova, K. G. and Hadjiiski, A. (2002). Role of oil spreading for efficiency of mixed oil-solid antifoams. *Langmuir*, 18(15), 5810-5817.
- [25] Schokker, E. P., Bos, M. A., Kuijpers, A. J., Wijnen, M. E. and Walstra, P. (2003). Spreading of oil from protein stabilized emulsions at air/water interfaces. *Colloids and Surfaces B: Biointerfaces*, 26(4), 315-327.
- [26] Bisperink, C. G. J. (1997). *The influence of spreading particles on the stability of thin liquid films*. Thesis: Wageningen Agricultural University, The Netherlands.
- [27] Sirks, H. A. (1939). *Verslag van het Rijks-Landbouwproefstation te Hoorn over 1938* (pp. 11-15) The Hague: Algemeene Landsdrukkerij.
- [28] van Camp, J., van Calenberg, S., van Oostveldt, P. and Huyghebaert, A. (1996). Aerating properties of emulsions stabilized by sodium caseinate and whey protein concentrate. *Milchwissenschaft*, 51(6), 310-315.
- [29] King, N. (1955). *The Milk Fat Globule Membrane and Some Associated Phenomena*. Reading: Lampport Gilbert and Co.

Chapter 2:

Monitoring entering and spreading of emulsion droplets at an expanding air/water interface: a novel technique*

Abstract

The entering and spreading of emulsion droplets at quiescent and expanding air/water interfaces was studied using a new apparatus consisting of a modified Langmuir trough in which the air/water interface can be continuously expanded by means of rollers in the place of traditional barriers. When sodium caseinate and whey protein isolate-stabilised emulsion droplets were injected under the surface of sodium caseinate and whey protein isolate solutions, respectively, it appeared that the droplets entered the air/water interface only if the air/water surface pressure did not exceed a threshold value of ~ 15 mN/m. This condition was satisfied either under quiescent conditions for low protein concentrations or by continuous expansion of the interface at higher protein concentrations. According to equilibrium thermodynamics, entering of the droplets and the formation of lenses should occur for all the systems investigated, but this was not observed. At surface pressures higher than ~ 15 mN/m, immersed emulsion droplets were metastable. This is probably due to a kinetic barrier caused by the formation of a thin water film bounded by protein adsorption layers between the emulsion droplet and the air/water interface.

2.1 Introduction

Foam stability is strongly influenced by the presence of emulsion droplets. Spreading of emulsion droplets at the air/water interface is known to cause bubble collapse [1], which may be desirable (e.g. for antifoaming agents) or unwanted (e.g. the collapse of beer foam). Emulsion droplets are also known to stabilise foams, for example by accumulation in the plateau borders within a foam [2] or by adsorption to the bubble surface, as is the case in whipped cream [3,4]. In a good whipped cream, spreading of liquid fat is reduced by the presence of crystalline fat in the fat globules which helps to prevent oil from flowing out of the droplets when they adhere to the bubble surface [5].

Many researchers have postulated that interfacial tension [5,6] and the properties of the adsorbed protein layers at both the air bubble and the emulsion droplet surfaces [7-9] are main factors influencing the interaction between emulsion droplets and the air/water interface during the whipping of cream. However, very little work has been reported which quantifies this interaction. Sirks [10] reported that spreading of liquid fat on the air/water interface was not impeded by a pre-existing protein film provided the surface pressure (not specified) caused by the film was low enough. Schokker et al. [11] found 13 mN/m to be the limiting surface pressure for the spreading of oil-in-water emulsion droplets at quiescent air/milk protein interfaces. King [12] observed that fat globules could enter the milk/air interface if the interface was disturbed by touching it with a platinum loop. Before contact, the milk surface was free from fat globules, suggesting the existence of an energetic and/or kinetic barrier to fat globule insertion.

Thermodynamically, three conformations may arise for an oil droplet at the air/water interface. Robinson and Woods [13] derived an entering coefficient, E , which predicts whether a droplet will enter the air/water interface or remain submerged in the water phase. E is given by

$$E = \gamma_{AW} + (\gamma_{OW} - \gamma_{OA}) \quad (2.1)$$

where γ is interfacial tension and the subscripts W, A and O refer to water, air and oil, respectively. Entering of an oil droplet occurs when $E > 0$. When entered, a droplet may either form a lens or spread out into a film covering the air/water interface. The tendency of an emulsion droplet to spread at an air/water interface is predicted by the spreading coefficient, S , defined by

Harkins and Feldman [14] as

$$S = \gamma_{AW} - (\gamma_{OW} + \gamma_{OA}) \quad (2.2)$$

Thus, the three conformations can be predicted based on the balance of interfacial tensions for the initial system (i.e. before the oil droplet contacts the air/water interface) these are $E < 0$, $S < 0 < E$ and $S > 0$, respectively. E and S can also be calculated for the system once the air/water interface is in equilibrium (E_e and S_e) with the oil phase [15,16]. There are however, theoretical constraints on the possible values of E_e and S_e . This is due to the fact that the three-phase boundary depicted in Figure 2.1 disappears when $E < 0$, $S > 0$ and when $\gamma_{OW} + \gamma_{OA} - \gamma_{AW} < 0$ (expulsion of oil drop into air). Therefore, $S_e \leq 0$ and $0 \leq E_e \leq 2 \gamma_{OW}$. In this paper, references to E and S refer to the values calculated for the initial system, unless specifically indicated otherwise.

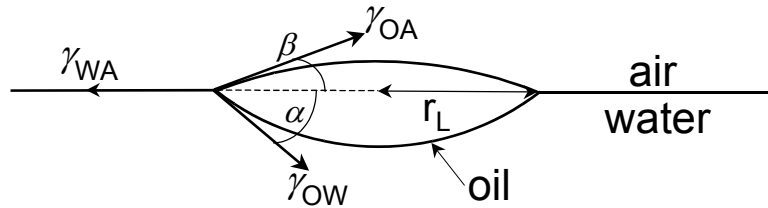


Figure 2.1: Schematic drawing of a sunflower oil lens resting in the air/water interface showing the relevant interfacial tensions and contact angles (α and β); γ is surface tension and the subscripts A, O and W refer to air, oil and water, respectively.

For a lens of oil resting in the air/water interface with the angles and interfacial tensions depicted in Figure 2.1, the three oil drop conformations can be illustrated by following the normalised lens radius, r_L , as a function of γ_{WA} , as shown in Figure 2.2. The assumptions that gravitational effects and line tension could be neglected were made in the calculation of lens radius. A summary of the relevant equations is given below.

Resolving the Neumann triangle of interfacial forces (Figure 2.1) horizontally at the three phase contact line yields

$$\gamma_{AW} = \gamma_{OW} \cos \alpha + \gamma_{OA} \cos \beta \quad (2.3)$$

From (2.3) it follows that the angles α and β are given by [17-19]

$$\cos \alpha = \frac{\gamma_{AW}^2 + \gamma_{OW}^2 - \gamma_{OA}^2}{2\gamma_{OW}\gamma_{AW}} \quad (2.4)$$

$$\cos \beta = \frac{\gamma_{AW}^2 + \gamma_{OA}^2 - \gamma_{OW}^2}{2\gamma_{OA}\gamma_{AW}} \quad (2.5)$$

The total volume of the drop before entering, $V_{\text{drop}} = V_1 + V_2$, where V_1 and V_2 are the volumes of the upper and lower lens caps (depicted in Figure 2.1) respectively. From geometry, V_1 and V_2 are given by [17,18]

$$V_1 = \frac{\pi r_L^3}{3 \sin^3 \beta} (\cos^3 \beta - 3 \cos \beta + 2) \quad (2.6)$$

$$V_2 = \frac{\pi r_L^3}{3 \sin^3 \alpha} (\cos^3 \alpha - 3 \cos \alpha + 2) \quad (2.7)$$

Thus, when V_{drop} and the respective interfacial tensions are known, r_L can be calculated. For the purpose of Figure 2.2, γ_{OW} and γ_{OA} were taken to be 29 and 28 mN/m, respectively, which were the values measured in our laboratory for an equilibrated sunflower oil/air/water system (Wilhelmy plate method).

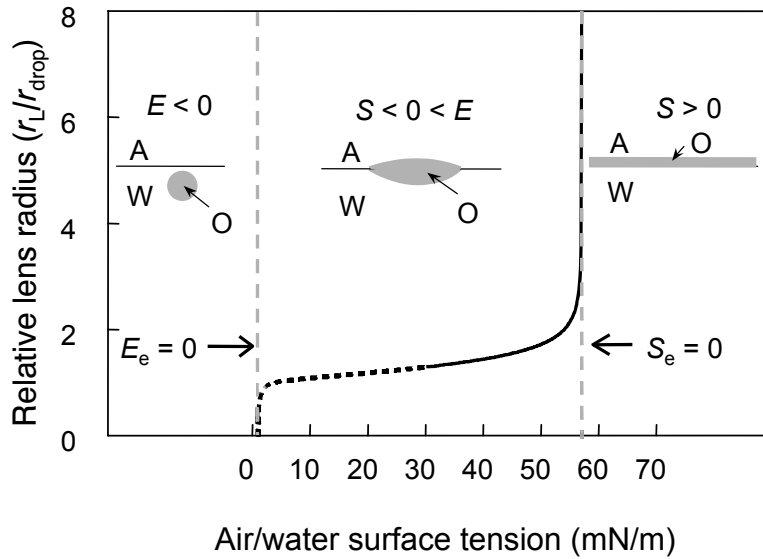


Figure 2.2: Relative lens radius for a sunflower oil droplet resting in the air/water interface vs. air/water surface tension. The radius of the lens, r_L , was calculated using Eqs. (2.6) and (2.7). Values of $\gamma_{OW} = 29$ mN/m and $\gamma_{OA} = 28$ mN/m have been used, which correspond to the water/sunflower oil/air system. For the purpose of illustration the curve is shown for a wide range of γ_{AW} values. A dotted line is used below $\gamma_{AW} = 30$ mN/m to denote that such low surface tension values are experimentally unrealistic for this system.

The curve in Figure 2.2 dives steeply to zero as E goes to 0, indicating that when $E < 0$ the droplet remains wetted by the aqueous phase (for the equilibrium situation, this occurs when $E_e = 0$). For the condition $S < 0 < E$, the oil droplet enters the air/water interface and forms a lens. The radius of the lens increases with increasing γ_{WA} until the condition $S = 0$ is reached. At this point, the curve increases asymptotically to ∞ . When S is greater than zero a spread oil film will form replacing the air/water interface with an oil/water interface (Figure 2.2). In the presence of adsorbed material at the air/water interface, the surface tensions may change as the oil spreads due to compression of the adsorbed layer by the expanding film. Spreading of the film may then stop when the condition $S_e = 0$ is reached.

It is important to mention that neither the spreading and entering coefficients nor the oil lens radius calculations account for the properties of a thin film that may form between an approaching emulsion droplet and the air/water interface. The presence of a thin film acting as a kinetic barrier introduces the possibility for a metastable state where the entering of emulsion droplets would not be observed even when the condition $E > 0$ is satisfied [2,20]. The stability of such a thin film against rupture is determined by disjoining pressure and film drainage, in addition to the properties of adsorption layers on both sides of the thin film. A number of authors [2,15,20-22] address the role of thin film forces in the entry of oil droplets into the air/water interface and their role in the destabilisation of foams in applications such as antifoaming and oil recovery. In these studies the entry barrier is investigated for static systems in the presence of adsorbed surfactants. Hadjiiski et al. [23] and Dickinson et al. [24] report on the oil droplet entry barrier for systems containing adsorbed proteins at the air/water and oil/water interfaces, respectively. Bergeron et al. [22] described a disjoining pressure cell in which the pressure required to rupture a thin water film sandwiched between bulk air and oil phases can be measured. The film trapping technique [16,23] enables similar pressure measurements with the added advantage that oil droplets can be used instead of a bulk oil phase. Using the film trapping technique, protein stabilised-emulsion droplets (diameter 1 – 3 μm) have been studied [23]. Lobo and Wasan [20] described the use of reflective light microscopy to observe the entering of oil droplets (diameter 300 – 800 μm) at the air/water interface.

The objective of our research was to deepen the understanding of interactions controlling the entering and spreading of protein-stabilised emulsion droplets at an expanding air/water interface. In this paper we report a new technique that enables the monitoring of entering and spreading of emulsion droplets and the conditions under which these occur by monitoring the surface tension of a dilating planar air/water interface. In contrast to studies carried out under static conditions where the system can reach equilibrium [2,16,22], we focus on the entering and spreading of oil droplets in systems that are kept out of equilibrium through expansion of the interface. Using this technique, we compare the surface pressure conditions required for the entering and spreading of oil-in-water emulsion droplets at sodium caseinate and whey protein isolate solution/air interfaces. To the best of our knowledge, these results represent the first reported attempt to quantify the physical requirements for the entering and spreading of protein-stabilized emulsion droplets at an expanding air/water interface.

2.2 Materials and Methods

2.2.1 Materials

Whey protein isolate, WPI, (BiPRO, Lot no. JE 052-9-420, Davisco Foods International, Le Sueur, MN 56058) and sodium caseinate (Sodium caseinate S, DMV International, Veghel, The Netherlands) were used in the preparation of protein solutions and emulsions. WPI and caseinate powders contained 95% and 86% protein, respectively (Biuret standard assay, in agreement with manufacturer's specifications). Sodium phosphate buffer, (30 mM, pH 6.7), was prepared from Na_2HPO_4 and $\text{NaH}_2\text{PO}_4 \cdot \text{H}_2\text{O}$ (Merck, Darmstadt, Germany, analytical grade) dissolved in distilled water. Commercial sunflower oil (Reddy NV Vandermoortele, Roosendaal, The Netherlands) was used for emulsion preparation.

2.2.2 Solution and Emulsion preparation

Protein stock solutions (1.0 or 2.0 wt%) were prepared by adding either WPI or caseinate to 30 mM sodium phosphate buffer and stirring at room temperature for 2 h to enable wetting of the protein powder. This was followed by stirring for 16 h at 4°C to dissolve of the protein. Protein concentration series were prepared by diluting stock solution with phosphate

buffer.

Oil-in-water emulsions (40 wt% oil, 1 wt% protein) were prepared by pre-homogenising the protein solution/oil mixture for 1 min using an Ultraturrax (T 25 basic, IKA, Staufen, Germany) equipped with an 18 mm dispersing element (S25KR-18 G, IKA). The pre-emulsion was then homogenised at room temperature for 10 passes at 7 MPa (homogeniser unit HU-2.0, Delta Instruments, Drachten, The Netherlands). The droplet size distribution of the emulsion droplets was measured by light scattering using a Coulter Laser LS230 (Coulter Electronics, Mijdrecht, The Netherlands). The $d_{3,2}$ and $d_{4,3}$ average droplet diameters were $1.2 \pm 0.1 \mu\text{m}$ and $2.2 \pm 0.1 \mu\text{m}$ for WPI-stabilised emulsions and $1.3 \pm 0.1 \mu\text{m}$ and $2.2 \pm 0.1 \mu\text{m}$ for caseinate-stabilised emulsions, respectively. One batch of each emulsion was prepared and used in all experiments. The average droplet size of the emulsions remained constant during the period of experimental work. Sodium azide (Merck, analytical grade) was added to the emulsions (0.02 wt%) to prevent microbial growth.

2.2.3 Roller trough technique and measurement of surface tension

The roller trough apparatus consisted of a modified Langmuir trough with cylindrical rollers in the place of traditional barriers. The trough (Figure 2.3) was made from 5 mm thick clear acrylic with inner dimensions of 270×110 mm, glued together with methyl methacrylate containing dibenzoyl-peroxide hardener (Agovit 1900 and Agovit Härterflüssigkeit, respectively, Rohm, Hanau, Germany). This glue did not influence the surface tension measurements. Two smooth, stainless steel rollers (diameter, 20 mm) were positioned 110 mm apart, with a 10 mm gap between the rollers and trough bottom. Teflon-coated axles were used to reduce friction. An O-ring, stretched over the drive wheels in a figure eight conformation, allowed the rollers to be rotated simultaneously in opposite directions, thus inducing expansion of the interface. A motor, (ADI 1012, Applikon, Schiedam, The Netherlands) attached to one axle was used to drive the rollers.

The roller trough technique allowed us to produce a continuously expanding air/water interface similar to the caterpillar trough and overflowing cylinder techniques [25]. Both the roller trough and caterpillar trough produce expansion in 1 dimension, whereas the overflowing cylinder gives 2D expansion. The main advantages of the roller trough over these other

techniques are the wide range of available expansion rates and that the roller trough is small enough to be fitted under a light microscope for qualitative observation of the air/water interface.

Surface tension was measured using the Wilhelmy plate technique. A roughened glass Wilhelmy plate ($20 \times 20 \times 1$ mm) was suspended over the center of the trough from a Q11 force transducer (Hottinger Baldwin Messtechnik (HBM), Darmstadt, Germany), which was connected to a *Spider8* control panel (HBM) and operated by *Spider8* control V1.3 (HBM) software. A measuring frequency of 10 Hz with Bessel filtering at a frequency of 1 Hz was found to be optimal. Data points were collected at a frequency of 5 s^{-1} .

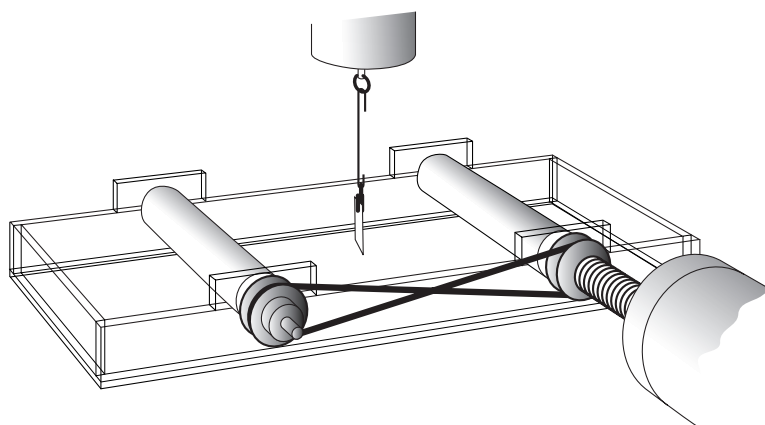


Figure 2.3: Schematic drawing of roller trough apparatus showing acrylic trough, rollers, motor drive and Wilhelmy plate suspended from force transducer. The Wilhelmy plate was oriented parallel to the trough rollers.

For each measurement, 300 mL solution was added to the trough, such that the solution was just touching the bottom of the rollers. This liquid level was chosen in order to reduce the occurrence of slip between the rollers and the protein solution. Slip would become more prevalent as the thickness of the liquid layer adhered to the roller during expansion increased. By using the largest possible distance between the liquid surface and the top of the roller, the thickness of the adhered fluid film was minimised. A relative expansion rate ($\lambda = d \ln A / dt$) of 0.12 s^{-1} was applied. The surface tension of the expanding interface was measured for a period of 30 s at the beginning of the experiment. The solution was then left undisturbed for 5 min at which point the surface tension of the quiescent interface was measured.

A 5- μL aliquot of undiluted emulsion was then injected under the quiescent surface of the protein solution using a micropipette. WPI- and caseinate-stabilised emulsions were added to WPI and caseinate solutions, respectively. When spontaneous, spreading of the emulsion occurred within 5 s after emulsion addition. If spreading of the emulsion was not observed within 20 s after emulsion addition, expansion ($\lambda = 0.12 \text{ s}^{-1}$) was applied.

2.2.4 Microscopy

An Olympus BX60 light microscope (Olympus Optical Co. GmbH, Hamburg, Germany) with 50 \times objective (LMPlanFl) was used for qualitative observation of the air/water interface. Using this microscope it was possible to view objects in both reflected (light source from above) and transmitted light. Only objects present in or on the air/water interface are visible in reflected light, making this technique good for the distinction between emulsion droplets that have entered the air/water interface and those just below the surface.

2.3 Results

All data are expressed in terms of surface pressure, $\Pi = \gamma^0_{\text{AW}} - \gamma_{\text{AW}}$ where γ^0_{AW} is equal to the surface tension of 30 mM sodium phosphate buffer (72 mN/m) and γ_{AW} is equal to the surface tension of the system.

The surface pressure values for the quiescent (Π_{q}) and expanding (Π_{e}) surfaces as a function of bulk protein concentration are given in Figures 2.4a and 2.4b for WPI and caseinate, respectively. For both proteins, the surface pressures increased with increasing protein concentration and the surface pressure of the system could be lowered by expansion of the interface ($\Pi_{\text{q}} > \Pi_{\text{e}}$). Because the quiescent values were measured after 5 min, they do not represent equilibrium values. At lower protein concentrations in particular, adsorption was incomplete and Π was still increasing.

Figure 2.4b shows that the difference between Π_{q} and Π_{e} was smaller at higher bulk caseinate concentrations. For lower protein concentrations (up to 1×10^{-2} wt% for WPI and 3.2×10^{-3} wt% for caseinate) Π_{e} was close to zero. Comparison of Figures 2.4a and 2.4b also shows that Π_{q} increased more rapidly as a function of bulk protein concentration for caseinate than for WPI. For example, $\Pi_{\text{q}} = 24 \text{ mN/m}$ was measured for 1 wt% caseinate (Figure 2.4b) compared to $\Pi_{\text{q}} = 20 \text{ mN/m}$ for the 1 wt% WPI solution (Figure 2.4a). These

results are in agreement with literature, where random coil proteins (e.g. caseins) are found to be more effective in lowering surface tension compared to globular proteins (e.g. whey proteins) for the same bulk concentration [26-29]. The higher Π_e values measured for caseinate during expansion at bulk protein concentrations above 3.2×10^{-3} wt% are also in agreement with literature. β -Casein has been found to lower the surface tension more effectively during expansion than β -lactoglobulin [28].

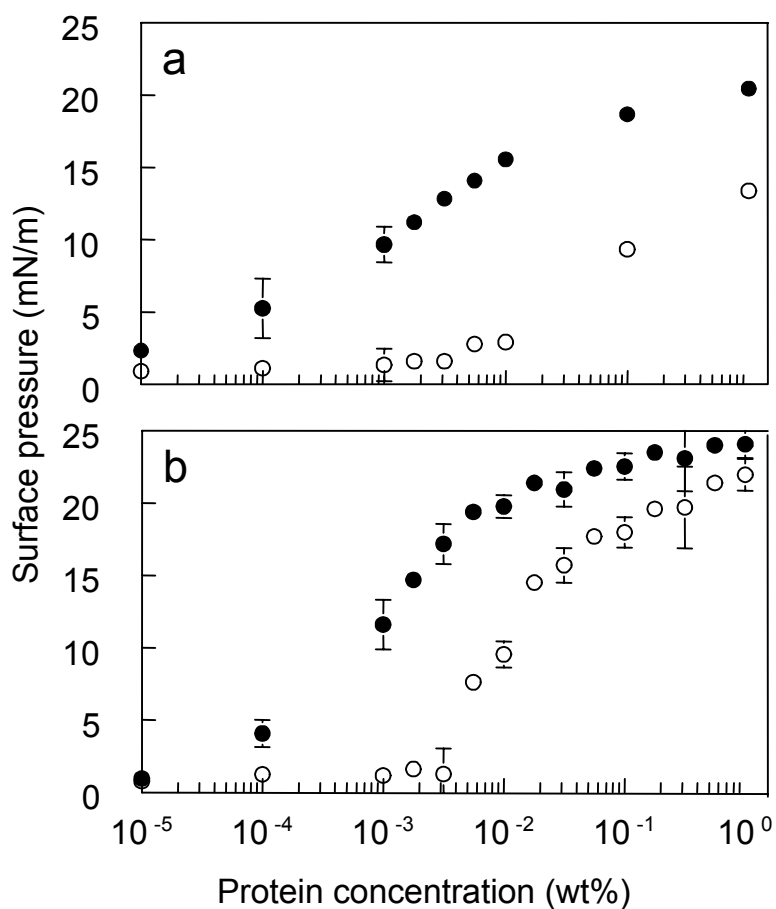


Figure 2.4: Surface pressure vs. (a) WPI and (b) sodium caseinate concentration for quiescent (●) and expanding (○) surfaces. Expanding surfaces: $\lambda = 0.12 \text{ s}^{-1}$. Points with error bars were measured in triplicate.

After the measurement of Π_q , emulsion was injected under the quiescent air/water interface. Due to their lower density, the emulsion droplets immediately creamed toward the surface after which two distinct types of behaviour were observed: either no entering or spontaneous entering and spreading out of the emulsion droplets, henceforth referred to as an entering/spreading event (E/S event). E/S events were detected by an

immediate increase in Π . During an E/S event, the injected emulsion was observed to spread out rapidly over the surface forming an opaque layer consisting of emulsion droplets both in and under the air/water interface. The occurrence of an E/S event was further supported by visual observation of the air/water interface using reflected light microscopy, which revealed the presence of tiny oil lenses in the surface, which were not present before the E/S event. In the case where an E/S event was not observed at the quiescent interface, expansion was applied. Again, either an E/S event was observed or neither entering nor spreading was detected. Typical Π vs. time profiles are shown for a spontaneous E/S event (Figure 2.5) and an E/S event during expansion (Figure 2.6) with WPI. Caseinate showed similar, albeit less pronounced, surface pressure profiles.

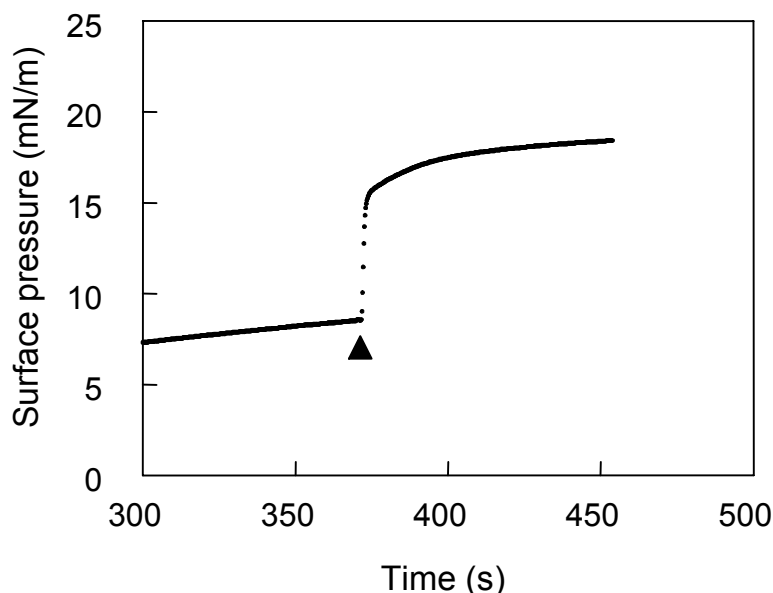


Figure 2.5: Surface pressure vs. time for 1×10^{-3} wt% WPI: spontaneous E/S event; \blacktriangle indicates the point when emulsion was injected.

When an E/S event could be induced by expansion of the interface (Figure 2.6), a peak was observed in the Π vs. time profile caused by the sudden entering and spreading out of the emulsion droplets. During expansion, Π was first observed to decrease, similar to the behaviour in the absence of emulsion droplets, until a critical surface pressure value, Π_{cr} , was reached at which the E/S event occurred. Then, Π began to increase in response to the additional surface-active material at the air/water interface. The surface pressure minimum, corresponding to Π_{cr} was recorded as the

surface pressure value at the point when the E/S event was initiated. When an E/S event did not occur at an expanding interface, a peak in the Π vs. time profile was not observed (graph not shown), nor were oil lenses observed in the air/water interface. In that case, the minimum surface pressure value achieved during expansion, Π_{\min} , was recorded.

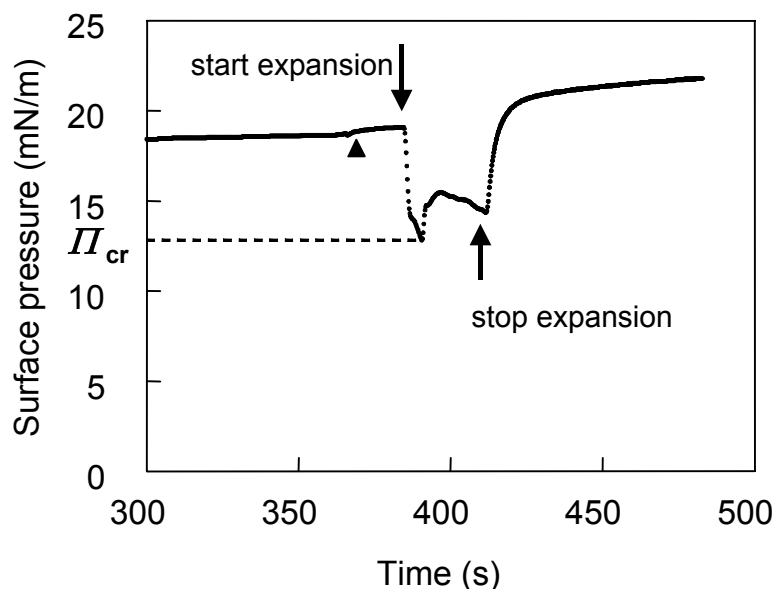


Figure 2.6: Surface pressure vs. time for 1×10^{-1} wt% WPI: E/S event induced by expansion ($\lambda = 0.12 \text{ s}^{-1}$) of the interface; \blacktriangle indicates the point when emulsion was injected. Π_{cr} equals the surface pressure at the point where the E/S event occurs.

Figures 2.7a and 2.7b show Π_{cr} as a function of protein concentration for WPI and caseinate, respectively. For the spontaneous E/S events (diamonds) $\Pi_{\text{q}} < \Pi_{\text{cr}}$, for E/S events during expansion (squares) Π_{cr} is given, while for the cases where an E/S event did not occur Π_{min} (triangles) is given. In these figures, a threshold Π -value appears to be present, above which E/S events no longer occur spontaneously. For both WPI and caseinate, this threshold is approximately equal to 15 mN/m. The existence of a surface pressure boundary agrees with the observation of Sirks [10] that entering and spreading under quiescent conditions was only observed at surface pressures below a critical value (i.e. $\Pi_{\text{q}} \leq \Pi_{\text{cr}}$). The value of 15 mN/m is close to the value of 13 mN/m measured as the limiting surface pressure for the spreading of oil-in-water emulsions at quiescent air/milk protein interfaces by Schokker et al. [11]. Our results also agree with those of Bisperink [30] who

reported that spreading of soy oil droplets at a quiescent air/water interface was observed for $\Pi_{AW} < 14$ mN/m. In Bisperink's research [30], the equilibrium air/water surface tension was controlled by varying the concentration of a commercially available anionic detergent (Teepol). E/S events during expansion (squares) were observed at $\Pi_{cr} = 14 \pm 1$ mN/m for WPI (Figure 2.7a) and at $\Pi_{cr} = 16 \pm 1$ mN/m for caseinate (Figure 2.7b). E/S events were never observed at $\Pi_e > 18$ mN/m, which was observed for the caseinate system only (7b, triangles). Additional experiments were performed with caseinate where the emulsion was introduced under an already expanding interface to see if this had an effect on Π_{cr} (data not shown). Again, E/S events were never observed when Π_e was greater than 18 mN/m.

2.4 Discussion

Spontaneous E/S events were not observed for $\Pi_q > 15$ mN/m and E/S events during expansion were found to occur at a Π_{cr} of 14 ± 1 and 16 ± 1 mN/m for WPI and caseinate, respectively. The similarity of these values suggests that Π_{AW} plays a leading role in the entering and spreading of emulsion droplets at the air/water interface. The measured Π_{cr} required for E/S events and the known values for γ_{OW} and γ_{OA} can be used to calculate E and S at the moment of spreading.

Substituting the Π_{cr} values measured for our system and values of $\gamma_{OW} = 11$ mN/m (as may be the case in the presence of an adsorbed protein layer) and $\gamma_{OA} = 28$ mN/m (i.e. the value for the pure interface as may be expected for a newly formed oil/air interface) into Equation (2.1) yields a positive entering coefficient. In fact, E is positive under quiescent and expanding conditions for all bulk protein concentrations studied in this paper. Hence, thermodynamically, the entering of droplets in the air/water interface should be favoured. Nevertheless, we were unable to observe inserted emulsion droplets in reflected light microscopy before the occurrence of an E/S event. An inserted droplet would be expected to form a lens with $r_L \geq r_{drop}$ (Figure 2.2), which would be large enough to be visible in light microscopy. Since the droplets do not appear to enter the air/water interface, it is likely that entering is kinetically impeded. This may be explained by the formation of a relatively stable thin film between an approaching emulsion droplet and the air/water interface [20]. Adsorbed proteins probably

contribute to the stability of the thin film through electrostatic and steric repulsion. Moreover, proteins are known to form viscoelastic films [31], which may provide extra resistance against the entering of oil droplets. Dickinson et al. [24] reported that when the planar oil/water interface is aged (72 h) in the presence of protein (lysozyme, κ -casein or β -casein) coalescence of oil droplets with the oil/water interface ceases altogether due to the strength of the adsorbed protein layer.

Substituting $\gamma_{OW} = 11$ mN/m and $\gamma_{OA} = 28$ mN/m into Equation (2.2), it follows that the condition $S > 0$ is satisfied when $\Pi_{AW} < 33$ mN/m. This would predict that once the kinetic barrier to entering is overcome, spreading should occur under quiescent conditions in all our experiments. However, this was not the case. As mentioned above, E/S events were only observed after Π_{AW} had been lowered to ~ 15 mN/m. This difference may be due to the highly dynamic character of the system during an E/S event. When an entered emulsion droplet begins to spread, both γ_{OW} and γ_{OA} will increase. At the same time, γ_{AW} will decrease due to compression of the air/water interface surrounding the spreading emulsion droplet. As a consequence, the respective surface tensions deviate considerably from their initial and equilibrium values. Due to the relatively slow adsorption of proteins at expanding interfaces [28] we may expect that during spreading, γ_{OW} and γ_{OA} will be approximately equal to the values measured for the pure interfaces. Substituting the values of $\gamma_{OW} = 29$ mN/m and $\gamma_{OA} = 28$ mN/m (i.e. for the pure interfaces) into Equation (2.2) predicts a positive value for the dynamic spreading coefficient, S_{dyn} , when $\Pi_{AW} < 15$ mN/m. This value coincides with the experimental threshold for the observation of an E/S event (Π_{cr}), thus pointing to S_{dyn} rather than S as the important parameter controlling E/S events.

We may hypothesise as to why E/S events are only observed once $S_{dyn} > 0$. Using surface tension as a detector for droplet insertion has the disadvantage that surface tension is likely to be much more sensitive to droplet spreading than to droplet insertion in the absence of spreading. It may be that although droplet entering is kinetically impeded, from time to time a single droplet is able to overcome the kinetic barrier and enter the air/water interface. A single entered droplet would not be expected to cause a measurable change in Π and may go undetected if this entering occurs out of the microscope field of view.

At the point when Π_{AW} is such that $S_{\text{dyn}} > 0$, the single droplet will begin to spread causing a change in the surface pressure and surface composition of the system. Droplets just below the air/water interface will then encounter the bare oil/water interface of the spreading emulsion droplet instead of an air/water interface. Such an encounter may lead to immediate coalescence of the still intact droplets with the spreading droplet. In this way, the initial spreading of a single droplet may trigger the entering and spreading of more droplets, the collective effect manifesting itself as a large measurable change in Π_{AW} . A detailed study of the conditions at which entering occurs in the absence of spreading for both static and dynamic conditions is the subject of ongoing research.

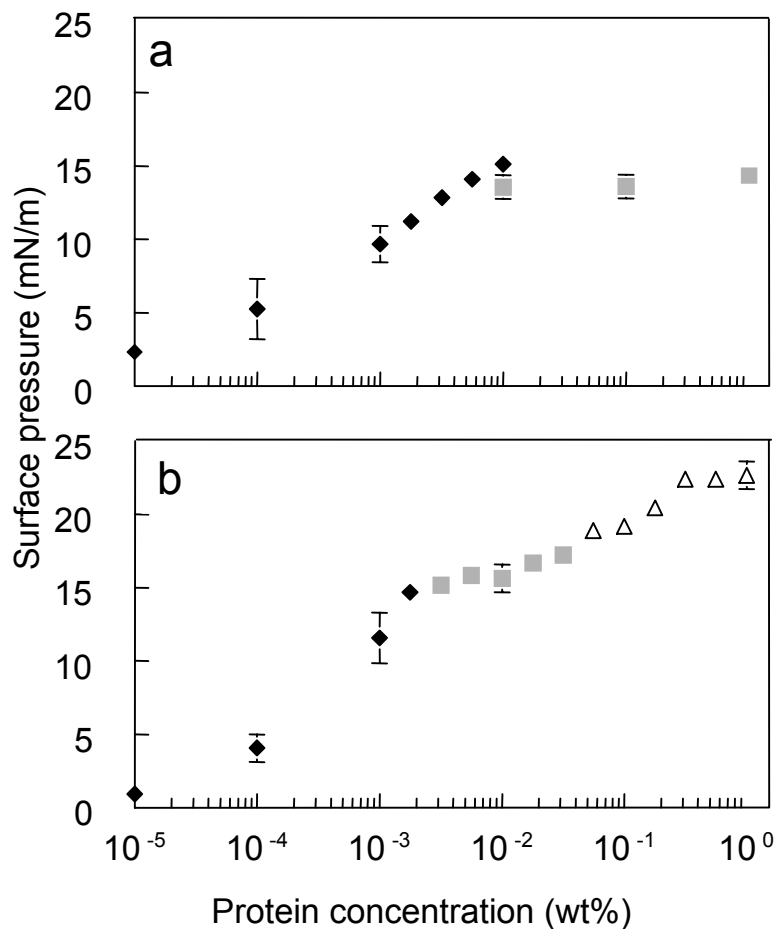


Figure 2.7: Surface pressure when an E/S event is initiated vs. (a) WPI and (b) sodium caseinate concentration; (◆) spontaneous entering and spreading; (■) E/S event after expansion ($\lambda = 0.12 \text{ s}^{-1}$); (△) no E/S event observed, values reported correspond to minimum surface pressure achieved during expansion.

2.5 Conclusions

A new technique has been developed for studying the entering and spreading of emulsion droplets at the air/water interface. Using this technique a threshold value of $\Pi_{cr} \sim 15$ mN/m has been measured for the spreading of emulsion droplets at the air/water interface. The measured surface pressure threshold seems to coincide with the air/water surface pressure value (15 mN/m) required for a positive dynamic spreading coefficient in the sunflower oil/protein solution/air system. Although the thermodynamic entering coefficient can be shown to be larger than the spreading coefficient, no cases were found where the droplets entered the air/water interface and formed lenses without evidence of spreading. This result suggests that the entering process is strongly inhibited by the formation of a metastable thin film between the emulsion droplet and the air/water interface.

Acknowledgements

The authors wish to thank Martin Bos (WCFS/TNO Voeding, The Netherlands) and Erix Schokker (Friesland Coberco Dairy Foods, The Netherlands) for valuable discussions. We also thank Ronald Wegh (Wageningen University) for technical expertise and advice pertaining to the design of the roller trough and Gert Buurman (Wageningen University) for the roller trough drawing (Figure 2.3).

References

- [1] Prins, A. (1986). Some physical aspects of aerated milk products. *Netherlands Milk and Dairy Journal*, 40, 203-215.
- [2] Koczko, K., Lobo, L. A. and Wasan, D. T. (1992). Effect of oil on foam stability: aqueous foams stabilized by emulsions. *Journal of Colloid and Interface Science*, 150(2), 492-506.
- [3] Anderson, M. and Brooker, B. E. (1988). Dairy Foams. In E. Dickinson and G. Stainsby, *Advances in Food Emulsions and Foams* (pp. 221-255). London: Elsevier.
- [4] Mulder, H. and Walstra, P. (1974). *The Milk Fat Globule*. Wageningen: Pudoc.
- [5] Darling, D. F. (1982). Recent advances in the destabilization of dairy emulsions. *Journal of Dairy Research*, 49, 695-712.
- [6] Besner, H. and Kessler, H. G. (1998). Interfacial interaction during the foaming of non homogenized cream. *Milchwissenschaft*, 53(12), 682-686.
- [7] Brooker, B. E., Anderson, M. and Andrews, A. T. (1986). The development of structure in whipped cream. *Food Microstructure*, 5, 277-285.
- [8] Goff, H. D. (1997). Instability and partial coalescence in whippable dairy emulsions. *Journal of Dairy Science*, 80, 2620-2630.
- [9] Needs, E. C. and Huitson, A. (1991). The contribution of milk serum proteins to the development of whipped cream structure. *Food Structure*, 10, 353-360.
- [10] Sirks, H. A. (1939). *Verslag van het Rijks-Landbouwproefstation te Hoorn over 1938* (pp. 11-15) The Hague: Algemeene Landsdrukkerij.

- [11] Schokker, E. P., Bos, M. A., Kuijpers, A. J., Wijnen, M. E. and Walstra, P. (2003). Spreading of oil from protein stabilized emulsions at air/water interfaces. *Colloids and Surfaces B: Biointerfaces*, 26(4), 315-327.
- [12] King, N. (1955). *The Milk Fat Globule Membrane and Some Associated Phenomena*. Reading: Lampport Gilbert and Co.
- [13] Robinson, J. V. and Woods, W. W. (1948). A method of selecting foam inhibitors. *Journal of the Society of Chemical Industry*, 67, 361-365.
- [14] Harkins, W. D. and Feldman, A. (1922). Films. The spreading of liquids and the spreading coefficient. *The Journal of the American Chemical Society*, 44(12), 2665-2685.
- [15] Aveyard, R., Binks, B. P., Fletcher, P. D. I., Peck, T.-G. and Garrett, P. R. (1993). Entry and spreading of alkane drops at the air/surfactant solution interface in relation to foam and soap foam stability. *Journal of the Chemical Society of Faraday Transactions*, 89(24), 4313-4321.
- [16] Basheva, E. S., Ganchev, D., Denkov, N. D., Kasuga, K., Satoh, N. and Tsujii, K. (2000). Role of betaine as foam booster in the presence of silicone oil drops. *Langmuir*, 16, 1000-1013.
- [17] Aveyard, R. and Clint, J. H. (1997). Liquid lenses at fluid/fluid interfaces. *Journal of the Chemical Society of Faraday Transactions*, 93(7), 1397-1403.
- [18] Retter, U. and Vollhardt, D. (1993). Formation of lenticular nuclei from an insoluble monolayer at the air/water interface: a model. *Langmuir*, 9, 2478-2480.
- [19] Pujado, P. R. and Scriven, L. E. (1972). Sessile lenticular configurations: translationally and rotationally symmetric lenses. *Journal of Colloid and Interface Science*, 40(1), 82-98.
- [20] Lobo, L. and Wasan, D. T. (1993). Mechanisms of aqueous foam stability in the presence of emulsified non-aqueous-phase liquids: structure and stability of the pseudoemulsion film. *Langmuir*, 9, 1668-1677.
- [21] Garrett, P. R. (1993). In P. R. Garrett, *Defoaming: Theory and Industrial Applications* (p. 1). New York: Marcel Dekker.
- [22] Bergeron, V., Fagan, M. E. and Radke, C. J. (1993). Generalized entering coefficients: a criterion for foam stability against oil in porous media. *Langmuir*, 9, 1704-1713.
- [23] Hadjiiski, A., Dimova, R., Denkov, N. D., Ivanov, I. B. and Borwankar, R. (1996). Film trapping technique: precise method for three-phase contact angle determination of solid and fluid particles of micrometer size. *Langmuir*, 12, 6665-6675.
- [24] Dickinson, E., Murray, B. S. and Stainsby, G. (1988). Coalescence stability of emulsion-sized droplets at a planar oil-water interface and the relationship to protein films and surface rheology. *Journal of the Chemical Society of Faraday Transactions I*, 84(3), 871-883.
- [25] Prins, A. (1995). Dynamic Surface Tension and Dilational Interfacial Properties. In E. Dickinson, *New Physico-Chemical Techniques for the Characterization of Complex Food Systems* (pp. 214-239). London: Blackie Academic & Professional.
- [26] Graham, D. E. and Phillips, M. C. (1979). Proteins at liquid interfaces III. Molecular structures of adsorbed films. *Journal of Colloid and Interface Science*, 70(3), 427-439.
- [27] Tornberg, E. (1978). The interfacial behaviour of three food proteins studied by the drop volume technique. *Journal of the Science of Food and Agriculture*, 29, 762-776.
- [28] van Aken, G. A. and Merks, M. T. E. (1996). Adsorption of soluble proteins to dilating surfaces. *Colloids and Surfaces A: Physicochemical and Engineering Aspects*, 114, 221-226.
- [29] Walstra, P. and de Roos, A. L. (1993). Proteins at air-water and oil-water interfaces: static and dynamic aspects. *Food Reviews International*, 9(4), 503-525.
- [30] Bisperink, C. G. J. (1997). *The influence of spreading particles on the stability of thin liquid films*. Thesis: Wageningen Agricultural University, The Netherlands.
- [31] Lucassen-Reynders, E. H. and Benjamins, J. (1999). Dilational rheology of proteins adsorbed at fluid interfaces. In E. Dickinson and J. M. Rodríguez Patino, *Food Emulsions and Foams: Interfaces, Interactions and Stability* (pp. 195-206). Cambridge: Royal Society of Chemistry.

Chapter 3:

Flow and Fracture Phenomena in Adsorbed Protein Layers at the Air/Water Interface in Connection with Spreading Oil Droplets*

Abstract

Oil spreading at the air/water interface was studied for protein-stabilised emulsion droplets added under the surface of a spread protein layer. The initial transition from entered oil lens to spread oil layer can be thought of as a wetting transition, which is a surface tension-controlled phenomenon. The essentially irreversible nature of protein adsorption allows manipulation of the air/water surface tension by compression and expansion of the air/water surface such that the wetting transition can be induced. The initial wetting initiates a co-operative spreading process; it is this spreading process that is the subject of investigation. From the morphology of the spreading emulsion, clear differences in the flow behaviour of different protein films can be observed. The proteins investigated represent a series exhibiting an increased tendency to form a coherent protein film at the air/water interface in the order β -casein < β -lactoglobulin < soy glycinin. In the case of β -casein, the film flows and oil spreads in a radial fashion. The β -lactoglobulin and soy glycinin films on the other hand fracture during expansion and oil spreads in the cracks in the protein film, making the broken structure visible. This observation serves as strong visual evidence for the inhomogeneity of protein films during large-scale deformation.

3.1 Introduction

Insertion and spreading of oil droplets at the air/water interface is of practical relevance to a wide range of industrial applications ranging from antifoaming action to the stability of food foams. In relation to antifoams, spreading of oil serves to break the foam films between air bubbles resulting in collapse of the foam [1-3]. In food applications, however, a limited amount of spreading of oil (fat) at the air/water interface can be beneficial to the stability of many systems including whipped cream, ice cream and cake batters [4-6]. Protein is often also present in these systems, and due to the smaller size of protein molecules compared to oil droplets, protein generally adsorbs first at newly formed air/water surfaces. Depending on variables such as adsorbed amount, expansion rate and fat crystal habit, to name a few, oil droplets may attach to or even rupture the protein layer. Understanding the influence of the protein film on the behaviour of oil droplets at the air/water interface is, thus, central to understanding and predicting food foam stability.

Proteins are known to form strongly adsorbed layers at the air/water interface. These layers can be classified based on their method of preparation as either spread or adsorbed layers. For convenience, we often assume that in spread layers the proteins are irreversibly adsorbed to the air/water interface. Another special property of adsorbed proteins is that they tend to form coherent layers. As a result of this, a protein layer can remain stagnant when the liquid under the layer is subjected to flow; this is in contrast to surfactant layers, which tend to flow with the sub-phase under the same conditions [7,8]. This coherence is generally attributed to the formation of a network between adsorbed protein molecules that gives mechanical strength to the adsorbed layer; this is often referred to as a protein "film". Mechanical properties of protein films may result in yielding or fracturing when the film is exposed to large deformation either in shear or in dilation [9-15]. The maximum stress that can be sustained by the protein film differs strongly from one protein to another. For example, protein film fracture has been reported for shear and dilational deformation of adsorbed protein layers of the globular proteins β -lactoglobulin and soy glycinin; however, β -casein, a random coil protein, appears to behave as a predominantly fluid film [13-15]. Bos and van Vliet [12] hypothesised that protein film fracture resulting from dilational deformation would lead to an inhomogeneous air/water surface with regions depleted of protein. This is relevant to aeration of emulsions since fat droplets

are expected to attach most easily to clean interfaces. Once attached, fat droplets may enter and spread over the air bubble surface.

The subject of droplet entering is a much-debated point that has received a lot of attention, see for example papers by Aveyard and Binks [1], Hadjiiski et al. [16] and Lobo and Wasan [17]. In this paper, we do not examine the entering process specifically; however, it is important to recognise that entering is the precursor to spreading. In the classical spreading theory, entering is predicted from equilibrium thermodynamics [18]. Moreover, it has been shown that entering is influenced by the kinetic aspect of rupture of the thin film separating the oil droplet from the air/water interface [17,19]. Due to their coherent nature, protein films can effectively inhibit droplet entering by lending mechanical stability to the thin film [16,20,21].

Assuming a droplet has entered the air/water interface, spreading may occur. The driving force for oil spreading is the balance of interfacial tensions (γ) at the air (A)–water (W)–oil (O) phase boundary. The transition from an oil lens to a spread oil layer can be thought of as a specialised case of a wetting transition occurring in a gas/liquid/liquid system rather than in the more common gas/liquid/solid system [22]. When the oil forms a lens, it is said to partially wet the air/water surface. In contrast, when spreading occurs, the oil layer completely wets the air/water surface. The balance of interfacial tensions at the three-phase boundary favours complete wetting of the air/water interface by oil when the spreading coefficient,

$$S = \gamma_{AW} - (\gamma_{OW} + \gamma_{OA}) \quad (3.1)$$

is zero or positive [23], and partial wetting when S is negative. Many food grade oils have $S > 0$ on clean water, whereas the less polar higher alkanes often have $S < 0$. In the presence of an adsorbed protein layer, γ_{AW} may be sufficiently lowered to bring S to negative values. Because protein adsorption is essentially irreversible, γ_{AW} can be manipulated by simply expanding or compressing the air/water interface [20,24,25]. In an earlier paper [20], we have shown that expansion of the interface results in the spreading of oil droplets at the air/water interface. The wetting transition coincided with the γ_{AW} required for $S = 0$. It is important to note that the wetting transition refers exclusively to the initiation of the lens-to-oil-layer transition. In the same paper [20], we hypothesised that the wetting transition initiates a co-operative entering and spreading process. In this process, oil droplets just under the

interface of the spreading oil droplet coalesce with the bare oil/water interface of the spreading oil (see Figure 3.1). This self-amplifying spreading process showed up as a sharp peak in the surface tension response measured for these systems. In support of this co-operative spreading model, it has since been shown for antifoaming agents that the presence of a spread oil layer facilitates the entering and spreading of additional oil droplets [2].

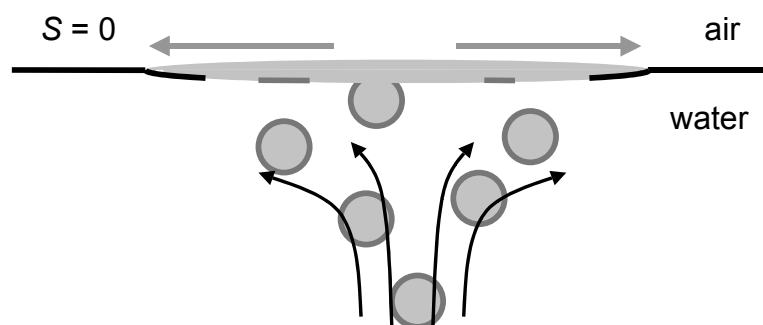


Figure 3.1: Schematic representation of the co-operative entering and spreading process that occurs when an entered droplet begins to spread; based on the description given by Hotrum et al. [20]. The surface tension in the air/water protein film (black) is such that the non-equilibrium criterion $S > 0$ is met. The dynamic spreading oil lens (indicated by grey arrows) leads to droplet transport toward the spreading oil (indicated by black arrows). Newly arrived emulsion droplets (light grey, with a dark grey adsorbed protein layer) easily coalesce with the bare oil/water interface provided by the spreading lens. This leads to further spreading which leads to more coalescence and so on as long as the condition $S > 0$ is maintained.

In the sunflower oil/protein solution/air system [20], there was an important difference in the surface tension response to emulsion spreading between the studied whey protein (or β -lactoglobulin) and caseinate (or β -casein) systems that we were unable to explain based on the co-operative model. Specifically, even though spreading occurred for both systems at $S = 0$, we observed a much sharper peak in the surface tension response at the point of spreading for the whey protein (or β -lactoglobulin) system than for the caseinate (or β -casein) system (Figure 3.2). This observation suggests that spreading in the presence of an adsorbed protein layer is not purely a surface tension phenomenon. In this paper, we show that in addition to the role of surface tension, the spreading of oil droplets at the air/water interface is

influenced by the rheological properties of the protein film. We study the spreading of protein-stabilised oil-in-water emulsion droplets at the air/water interface in the presence of a spread protein layer. Layers of β -lactoglobulin (pH 6.7), β -casein (pH 6.7), and soy glycinin (pH 3) are investigated. These three proteins represent a series exhibiting an increased tendency to form a coherent protein film at the air/water interface in the order β -casein < β -lactoglobulin < soy glycinin (pH 3) [13]. Using spread layers enables us to study the behaviour of the protein film during expansion without having to account for protein adsorption from the bulk, and to show that the spreading of oil from emulsion droplets follows very different scenarios for these three proteins.

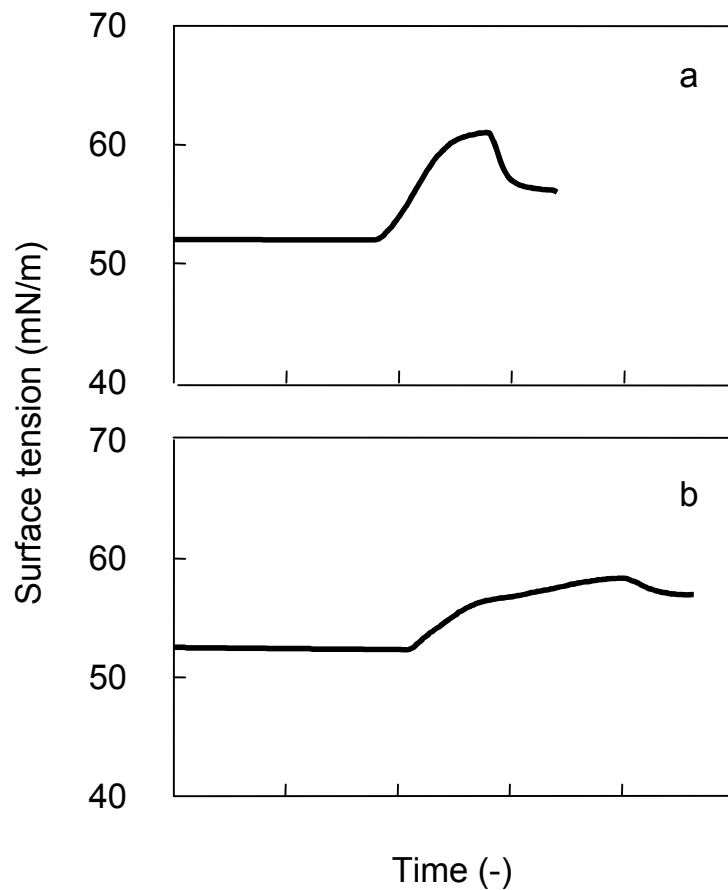


Figure 3.2: Air/water surface tension response to spreading of protein-stabilised sunflower oil-in-water emulsion droplets at the surface of 0.1 g protein/L bulk (a) β -lactoglobulin and (b) β -casein solutions. The response was measured during continuous expansion of the air/water interface in the roller trough [20]. Emulsion droplet spreading occurs at $S = 0$, as detected by a peak in the surface tension response.

3.2 Materials and Methods

3.2.1 Materials

β -Lactoglobulin was purified according to the method of de Jongh et al. [26]. β -Casein was purified from acid-precipitated casein based on the method described by Christensen and Munksgaard [27] and Swaisgood [28]. Soy glycinin was isolated from soybeans according to the fractionation scheme given by Thanh and Shibasaki [29] and was further prepared as described by Martin et al. [30].

β -Lactoglobulin and β -casein were dissolved in 20 mM imidazole buffer (pH 6.7) containing 0.1 M NaCl by stirring for 1 h at room temperature. For soy glycinin, 30mM citric acid/di-sodium phosphate buffer (pH 3) was used. The chemicals used for the buffers were purchased from Merck (Darmstadt, Germany, analytical grade).

Table 3.1: Oil/water and oil/air interfacial tensions (γ) of sunflower oil and *n*-tetradecane at room temperature (22°C) and the corresponding air/water surface tension (γ_{AW}) and surface pressure (Π_{AW}) required for complete wetting of the air/water interface by oil^a

oil	γ_{OW} (mN/m)	γ_{OA} (mN/m)	γ_{AW} (mN/m) required for $S = 0$	Π_{AW} (mN/m) required for $S = 0$
sunflower oil	29	28	57	15
<i>n</i> -tetradecane	47	26	73	-1

^aSurface pressure is defined as $\Pi = \gamma^0_{AW} - \gamma_{AW}$, where γ_{AW} is the surface tension of the system and γ^0_{AW} is the surface tension of the clean air/water interface (72 mN/m at 22°C).

For the emulsions, sunflower oil (Reddy, Vandermoortele, Roosendaal, The Netherlands) and *n*-tetradecane (Janssen Chimica, Geel, Belgium, 99% pure) were used. A summary of relevant interfacial tensions for these two oils is given in Table 3.1. The sunflower oil was further purified using silica gel 60 (70–230 mesh, Merck, Germany) based on the method described by Smulders [31]. This procedure was performed twice. Purified sunflower oil was flushed with N₂ gas and stored at –20°C until required. Emulsions were prepared as described by Hotrum et al. [20]. To yield comparable droplet sizes, sunflower oil-in-water emulsions were homogenised at 7 MPa, while *n*-tetradecane emulsions were homogenised at 2.5 MPa; this resulted in a droplet diameter ($d_{3,2}$) of ~1 μ m. After homogenisation, emulsions were washed in order to remove excess protein. Emulsions were centrifuged at 11 000g for 10 min, and

the subnatant phase was removed with a syringe and replaced with fresh buffer solution. The emulsion droplets were re-suspended by gentle shaking for a period of 1 h. The washing procedure was repeated twice.

3.2.2 Methods

In this work we monitored the air/water surface pressure Π_{AW} , defined as $\Pi_{AW} \equiv \Pi = \gamma_{AW}^0 - \gamma_{AW}$, where γ_{AW}^0 is the surface tension of a clean air/water interface (72 mN/m at 22°C) and γ_{AW} is the air/water surface tension of the system. Experiments were performed in a Teflon Langmuir trough equipped with a computer-controlled barrier. The surface area was varied between 600 and 150 cm² at a constant barrier speed of 55 mm²/s, this corresponded to a relative expansion rate (dlnA/dt) ranging from ~0.001 to 0.0035 s⁻¹ with decreasing area. During the experiments, Π was monitored by means of a platinum Wilhelmy plate. Before each experiment, the Wilhelmy plate was flamed to red-hot with an ethanol flame to remove any impurities and the Teflon trough was wiped clean with acetone followed by chloroform.

Curves of Π versus trough area were obtained by spreading a layer of protein solution over the surface of a buffer solution according to the Trurnit method [25,32]. With the trough at its maximum area, a solution of 0.1 g protein/L was allowed to flow down the sides of a wetted, roughened glass rod (diameter, 10 mm; length, 150 mm) until a Π -value of 1 mN/m was reached. Immediately following application of the spread protein layer, the surface was compressed to 150 cm² and allowed to equilibrate for a period of 5 min. This was followed by expansion of the interface back to 600 cm². In the case where the spreading of emulsion droplets was to be monitored, a 5- μ L aliquot of emulsion was added immediately following the equilibration period. To avoid contamination of the surface, the emulsion was added using a flexible pipette tip by passing the tip underneath the barrier from the side of the barrier where no protein film was present. The protein compositions of the emulsion and the spread layers were identical (e.g., β -casein-stabilised emulsion was added under the surface of a β -casein spread layer, etc.). The emulsion was then allowed to cream to the surface for 2 min. Subsequently, the surface was expanded to its maximum value. The shape and appearance of the emulsion sample were monitored during the expansion using a CCD

camera, set to take images at a rate of 1 image every 10 s. A plate of dark glass was placed on the bottom of the trough to improve contrast.

3.3 Results

3.3.1 Definition of the wetting transition

Assuming the values of γ_{OA} and γ_{OW} for sunflower oil and *n*-tetradecane (Table 3.1) are equal to those of the pure interfaces, which is a reasonable assumption for a quick droplet-to-lens shape change as a consequence of droplet entering [20], a diagram can be constructed showing the relationship between the spreading coefficient, S , and γ_{AW} . This is depicted in Figure 3.3. The wetting transition is defined as the point beyond which the slope of the curve becomes zero. For sunflower oil, the wetting transition will occur when $\gamma_{AW} = 57$ mN/m ($\Pi_{AW} = 15$ mN/m). For an air/water interface in equilibrium with the oil phase, S cannot be positive since the air/water interface is eliminated when the system goes through the wetting transition. For systems where γ_{AW} exceeds the minimum required to satisfy the complete wetting criterion, oil always spreads, this is the meaning of the plateau at $S = 0$. For *n*-tetradecane, a negative surface pressure ($\Pi_{AW} = -1$ mN/m) would be required in order for the system to go through the wetting transition. Clearly, this is outside the experimentally accessible range. Thus, *n*-tetradecane oil is not capable of completely wetting an air/water surface.

3.3.2 Π/A curves of protein films and the wetting transition

The surface pressure as a function of area (Π/A) curves for the spread layers of the various proteins can be found in Figure 3.4. These curves show the behaviour of the protein layer in the absence of emulsion; they can be considered as the “blanks” for our wetting experiments. β -Lactoglobulin (Figure 3.4b) and soy glycinin (Figure 3.4c) display a significant hysteresis between the dilation and compression curves, but for β -casein (Figure 3.4a) the hysteresis is negligible. Hysteresis tends to increase with increasing elastic modulus of the film and is generally attributed to relaxation processes in the protein film [24]. In the Π/A curve for soy glycinin, the expansion curve crosses the compression curve at around $\Pi = 12$ mN/m. To check that this crossover was not due to a change in wetting of the Wilhelmy plate, we repeated the experiment using a film balance trough. In this method, the

surface pressure is determined by measuring the lateral force exerted on a barrier, which separates the spread protein layer from a clean air/water interface. The crossover was observed with both the film balance and the Wilhelmy plate techniques. Moreover, we observed that somewhat more soy glycinin was required to form a spread layer with $\Pi = 1$ mN/m as compared to β -casein or β -lactoglobulin. Soy glycinin is known to adsorb relatively slowly, so that part of the protein applied by the Trurnit method may have entered the bulk solution rather than adsorbing to the air/water interface. This may explain the crossover in the Π/A curve: excess protein remaining in the bulk solution just under the interface may adsorb at the air/water interface upon its expansion.

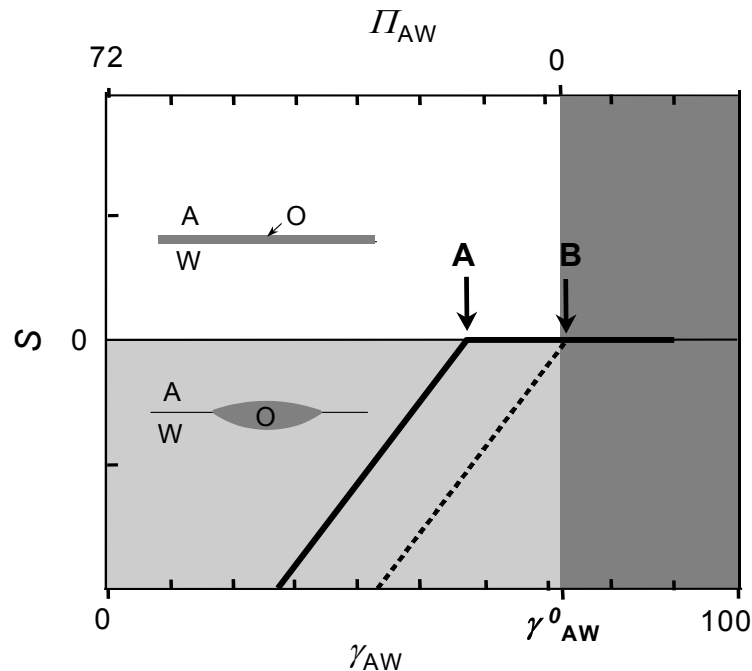


Figure 3.3: Schematic representation of the wetting transition for two oils, sunflower (solid line) and *n*-tetradecane (dotted line). The spreading coefficient ($S = \gamma_{AW} - (\gamma_{OW} + \gamma_{OA})$) is shown as a function of Π_{AW} and γ_{AW} . When $S < 0$, the oil droplet partially wets the air/water interface; a lens is formed (light grey shaded region). When $S = 0$, the wetting transition takes place, and the oil fully wets the water surface; a spread oil layer is formed (not shaded). The point of wetting transition is indicated with an arrow for the two oils (see also Table 3.1). The sunflower oil (A) goes through the wetting transition when $\Pi_{AW} = 15$ mN/m. For *n*-tetradecane (B) a wetting transition will not occur, as a negative surface pressure is required (dark grey shaded region).

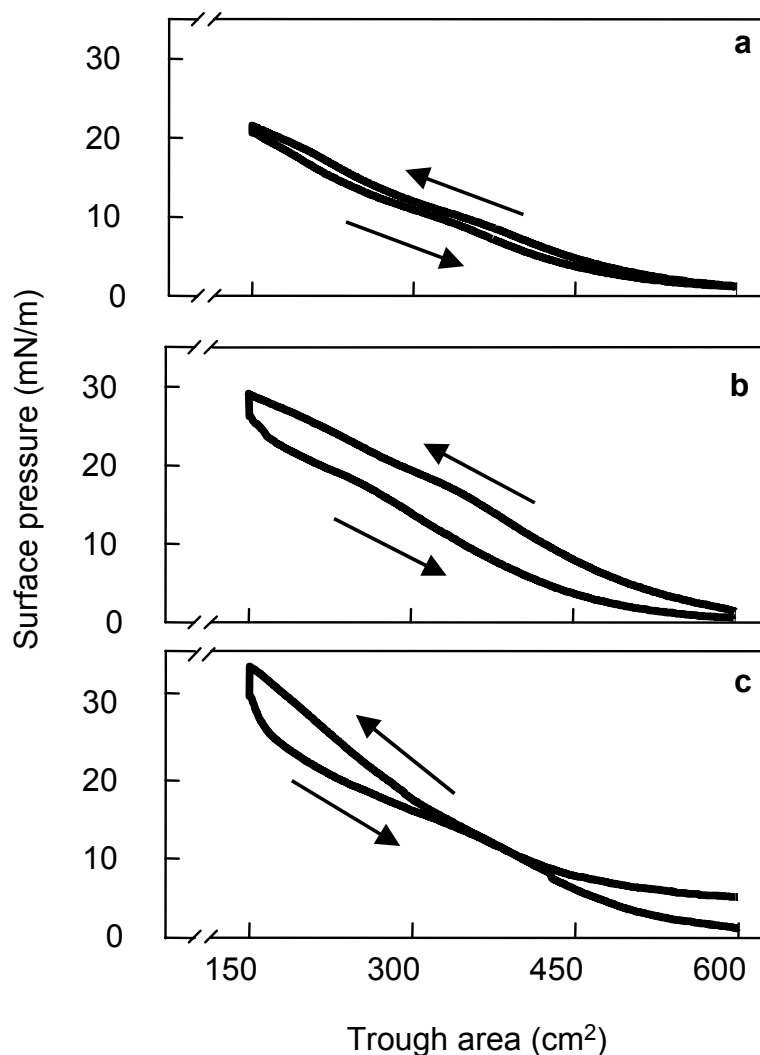


Figure 3.4: Π vs. trough area for spread layers of β -casein (a), β -lactoglobulin (b), and soy glycinin (c). Compression was followed by expansion at constant barrier speed (55 mm²/s). There was a 5 min equilibration time before application of expansion. Arrows indicate the direction of the change in area.

Based on the Π/A curves of the three proteins, we expect that a wetting transition will occur for the sunflower oil system. In Figure 3.5, the Π/A curves for the three proteins in the presence of the sunflower oil-in-water emulsions are shown. Emulsion was added after compression of the interface. The expansion curves in the presence of emulsion (Figure 3.5a–c) differ from those in the absence of emulsion (Figure 3.4a–c). During expansion in the presence of sunflower oil emulsion, the Π/A curves level off at $\Pi \sim 15$ mN/m for all three protein systems. This Π -value corresponds to the surface pressure where $S = 0$ (Figure 3.3) and is in agreement with our previous findings for

entering and spreading at the surface of a bulk protein solution [20,21]. After initiation of the wetting transition Π becomes constant because a further increase in the trough area just leads to more oil spreading. The trough is small enough that even at its maximum area, the oil supply from the emulsion droplets is not exhausted. It is important to note that while the oil completely wets the air/water interface, the protein film does not seem to be wetted by the oil. A sharp boundary can be observed between protein-free regions of spread oil and oil-free regions of spread protein.

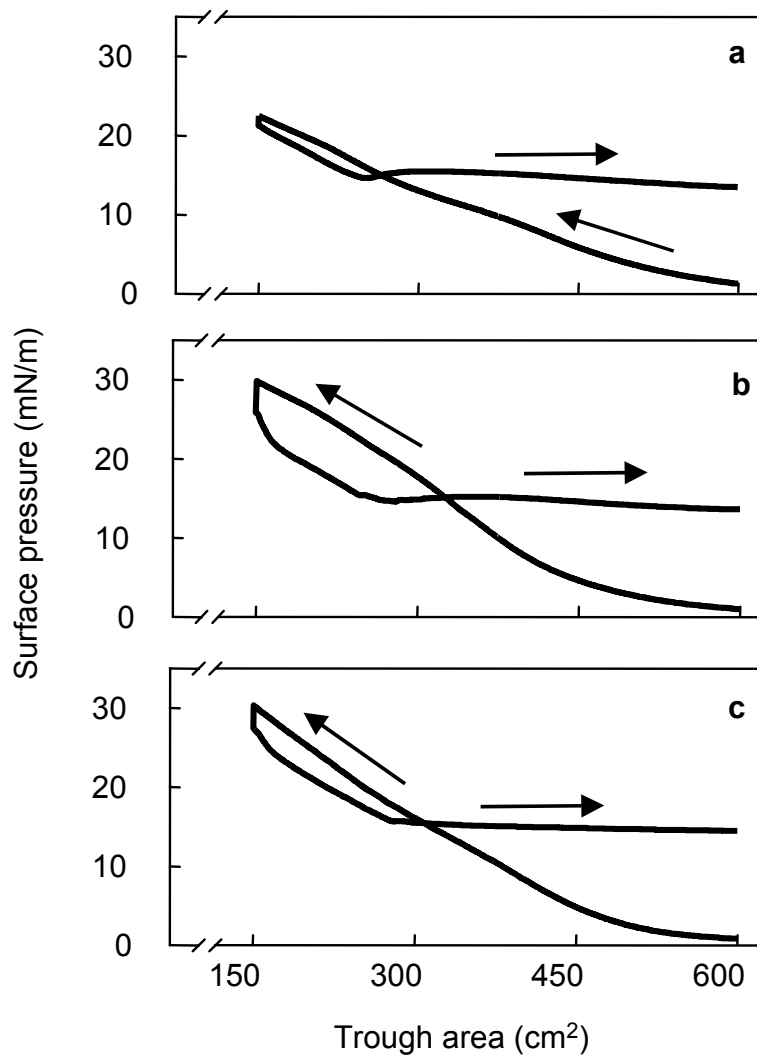


Figure 3.5: Π vs. trough area for spread layers of β -casein (a), β -lactoglobulin (b), and soy glycinin (c). Sunflower oil-in-water emulsion was added 5 min after compression was completed; after waiting a further 2 min to allow creaming of the sample, expansion was applied. The barrier speed was constant ($55 \text{ mm}^2/\text{s}$). Arrows indicate the direction of the change in area.

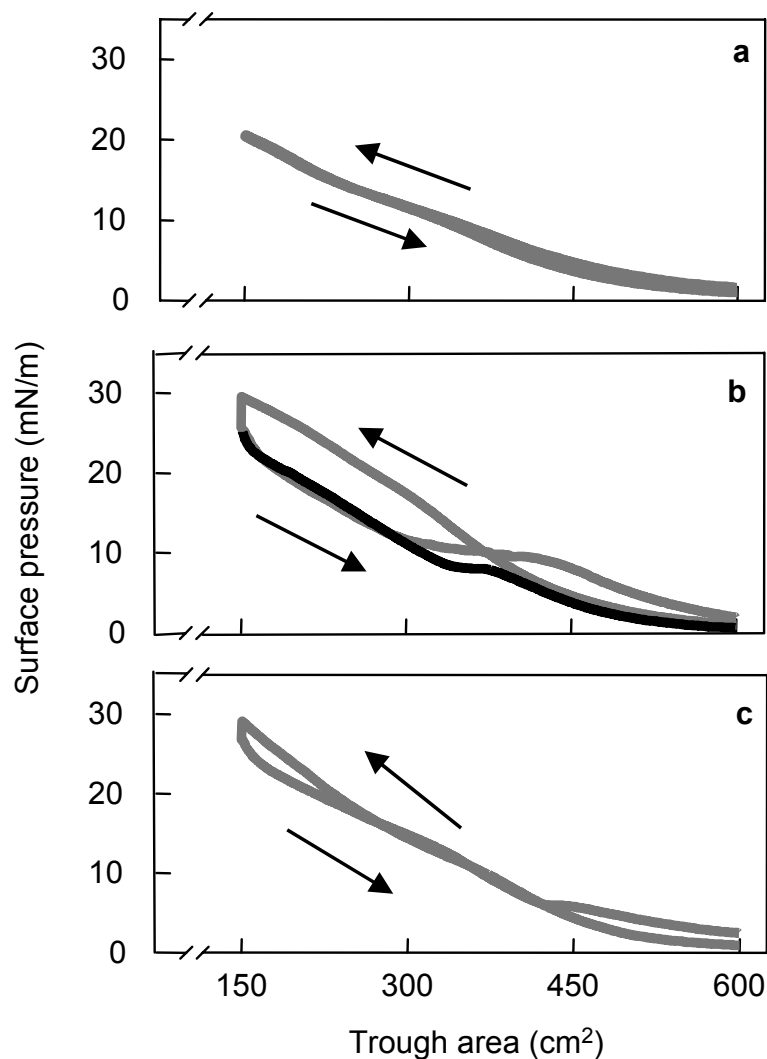


Figure 3.6. Π vs. trough area for spread layers of β -casein (a), β -lactoglobulin (b), and soy glycinin (c). *n*-Tetradecane oil-in-water emulsion was added 5 min after compression was completed; after waiting a further 2 min to allow creaming of the sample, expansion was applied. The barrier speed was 55 mm²/s. Arrows indicate the direction of the change in area. For comparison, in panel b, an additional expansion curve is given (black line) for a system where a 2.5- μ L aliquot of β -lactoglobulin-stabilised *n*-tetradecane emulsion was added instead of the usual 5- μ L aliquot. The compression curves for these two systems were very similar and for simplicity only that of the 5 μ L system is given.

In Figure 3.3, we showed that *n*-tetradecane should be unable to spread at the air/water interface. This is confirmed by the Π/A curves measured for the spread protein layers in the presence of *n*-tetradecane emulsion (Figure 3.6). For all three systems, the surface pressure returns to the starting value upon emulsion injection and subsequent expansion. With the exception of β -lactoglobulin (Figure 3.6b), the presence of emulsion has a negligible effect on the Π/A curve. An explanation for the behaviour of the β -lactoglobulin system is given in the discussion section.

3.3.3 Mechanical properties of protein films

Based on the Π/A curves presented in Figures 3.4–3.6, it would appear that the wetting transition in protein systems is governed purely by the thermodynamic quantities γ_{AW} , γ_{OA} , and γ_{OW} . Thermodynamic equilibrium would imply that surface tension (stress) gradients in the surface are excluded. However, in the presence of an adsorbed protein layer, local stresses may develop in the interface. As such, the influence of the surface rheological properties of the protein film should not be neglected. The rheological properties of protein films are generally categorised according to the film's response to dilational and shear deformation.

In dilational deformation, the response of the protein film to changes in area is measured. The relationship between the change in surface pressure with changing area is known as the interfacial dilational modulus (E), where:

$$E = -\left(\frac{\delta \ln A}{\delta \Pi}\right)_T \quad (3.2)$$

The interfacial dilational modulus gives an indication of the stiffness of the film. The steeper slopes of the Π/A curves for β -lactoglobulin (Figure 3.4b) and soy glycinin (Figure 3.4c) suggest that these films are more rigid than the β -casein film for which a less steep slope is measured (Figure 3.4a). This is in qualitative agreement with the results of Martin et al. [13] who measured the dilational modulus for adsorbed β -lactoglobulin and soy glycinin films to be 3 times greater than the dilational modulus of an adsorbed β -casein film. In the experiment reported here, the applied deformation is an order of magnitude larger.

Shear deformation of a protein film gives an even more sensitive indication of the stiffness of the protein molecules and the strength of the

intermolecular interactions between them. In the same paper, Martin et al. [13], reported that based on interfacial shear rheology, β -casein (pH 6.7) formed very weak protein networks compared to β -lactoglobulin (pH 6.7) and soy glycinin (pH 3), both of which formed stiff protein networks that were prone to fracture. In particular, soy glycinin (pH 3) formed very stiff but brittle protein films. These results indicate that random coil protein (β -casein) films are considerably more liquid-like than those of globular proteins (β -lactoglobulin or soy glycinin), which is in agreement with previous studies [24,33]. In this section, the differing rheological properties of the three protein films can be clearly observed in the morphology of the spreading oil layer in the air/water interface.

Images of the emulsion samples at various stages during surface expansion are given for the β -casein, β -lactoglobulin, and soy glycinin systems in Figures 3.7, 3.8, and 3.9, respectively. Due to the contrast between the opaque emulsion sample and the transparent protein film, it is possible to visually observe changes in the position and morphology of the emulsion sample during surface expansion. Upon expansion of the adsorbed β -casein layer (Figure 3.7), the emulsion flows in a radial fashion with increasing trough area. This indicates that the surface pressure is nearly homogeneous in the film and that shear stress components are negligible, typical for a fluid adsorbed layer. At $\Pi = 15$ mN/m the first black spots appear in the interface (Figure 3.7a). These black spots are circular regions of oil film, which increase in size with increasing surface area of the protein film (Figure 3.7b,c). The circular shape generally remains intact, indicating that the protein film between the spots is continuous: holes in the protein film have formed independently of one another to accommodate the spreading oil.

For the globular proteins, a strikingly different spreading scenario is observed. For both the β -lactoglobulin (Figure 3.8) and soy glycinin (Figure 3.9) systems the emulsion sample is stagnant during initial expansion. Upon further expansion, the protein film abruptly breaks up, forming cracks in the film, which fill with oil. The oil completely wets the air/water interface in the crack and no individual emulsion droplet lenses remain in this area, as can be deduced from the absence of turbidity. With continued expansion, the initially small cracks (Figures 3.8a and 3.9a) grow (Figures 3.8b and 3.9b). For the β -lactoglobulin system, small sections of the creamed emulsion are

observed to “break off” (Figure 3.8b,c). In the images of the soy glycinin system, the crack propagation process can clearly be observed: features that start out as a small cracks (Figure 3.9a) become larger (Figure 3.9b) and more branched (Figure 3.9c) as the film is further expanded.

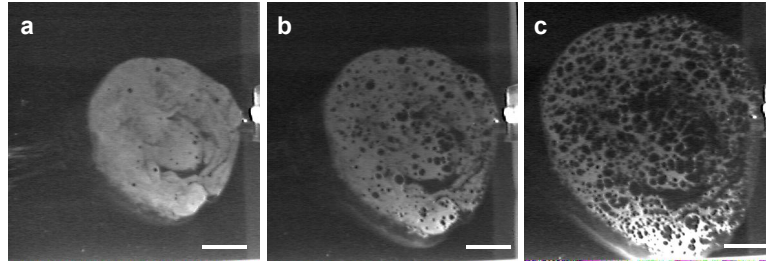


Figure 3.7: CCD camera images showing the spreading behaviour of β -casein-stabilised emulsion in a β -casein spread layer at various points on the Π/A curve depicted in Figure 3.5a: (a) at (244.5 cm², 14.8 mN/m), (b) at (255.5 cm², 14.7 mN/m) and (c) at (266.5 cm², 15.0 mN/m). The bar is 1 cm.

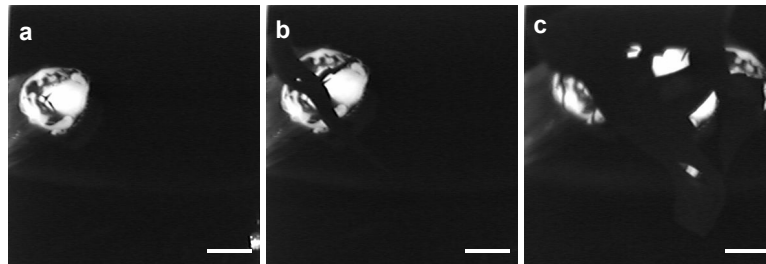


Figure 3.8: CCD camera images showing the spreading behaviour of β -lactoglobulin-stabilised emulsion in a β -lactoglobulin spread layer at various points on the Π/A curve depicted in Figure 3.5b: (a) at (245.4 cm², 15.5 mN/m), (b) at (251.3 cm², 15.4 mN/m) and (c) at (283.7 cm², 14.9 mN/m). The bar is 1 cm.

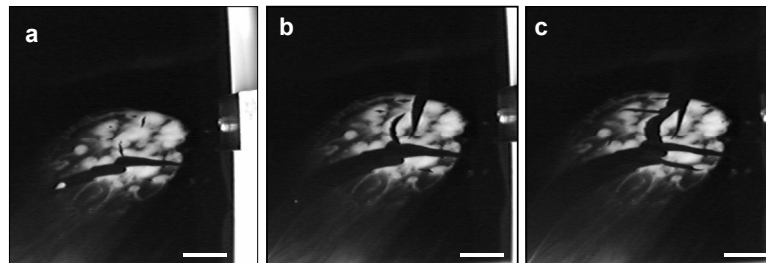


Figure 3.9: CCD camera images showing the spreading behaviour of soy glycinin stabilised emulsion in a soy glycinin spread layer at various points on the Π/A curve depicted in Figure 3.5c: (a) at (279.6 cm², 15.7 mN/m), (b) at (285.2 cm², 15.7 mN/m) and (c) at (290.7 cm², 15.7 mN/m). The bar is 1cm.

3.4 Discussion

The images of spreading emulsion show that, for protein-containing systems, the spreading process is influenced by the mechanical properties of the air/water film in addition to the thermodynamic parameters γ_{AW} , γ_{OA} , and γ_{OW} . The results are consistent with the conclusion formulated by various authors that random coil proteins (β -casein) form mobile, easily flowing films, which display largely viscous flow behaviour, while globular proteins (β -lactoglobulin and soy glycinin) form immobile, more rigid, strongly viscoelastic adsorbed layers, which have a predominantly elastic flow behaviour [13,24,25,33]. For β -casein spread layers, droplets enter and spread collectively at many independent points in the protein film. Each of these points acts as a nucleation site for the wetting transition. The result is the radial pattern of emulsion spreading characterised by many growing holes in the protein film (Figure 3.7). For the β -lactoglobulin and soy glycinin spread layers, we observed that the protein films fracture and that the oil droplets enter and spread in the cracks, possibly contributing to crack propagation. Fracture in a protein film is a result of local stresses that build up when the film is exposed to shear and/or dilational deformation [11,13,14]. The presence of emulsion serves to make the broken structure visible by filling up the cracks with oil. Because these protein films fracture rather than flow, erratic spreading patterns are observed (Figures 3.8 and 3.9).

In light of this new information regarding protein film failure, we can expand our co-operative model for the spreading of emulsion droplets in the sunflower oil/protein solution/air system [20] to account for the mechanical properties of the protein layer. For a coherent interface, such as for β -lactoglobulin and soy glycinin, the protein film fractures, promoting simultaneous entering and spreading over a much larger area at once. Much more oil spreads in a single event. This may explain the sharp peak in the surface tension response observed in the earlier roller trough experiments [21] for the β -lactoglobulin system (Figure 3.2a). For a fluid interface, such as is the case for β -casein, the process of droplet insertion and spreading occurs more gradually and at many separate points in the protein film, and thus a more gradual surface tension response was observed for these systems (Figure 3.2b).

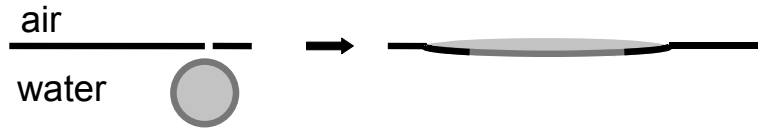


Figure 3.10: Schematic representation of the composition of the air/water interface in the case where entered lenses contain non-spreading oil. After rupture of the air/water protein film (left), emulsion droplets enter the air/water interface (right). Because the oil does not spread, the oil/water protein film remains intact and may attach to the surrounding air/water protein film forming a continuous protein film. The increase in protein film area provided by the oil/water protein film corresponds to the sum of the surface area of the original droplets that make up the oil lens. For simplicity, it is assumed that protein desorption can be neglected, the specific area of the adsorbed protein is the same at the air/water and oil/water interfaces and protein is not adsorbed to the newly formed oil/air interface, but remains adsorbed to the oil/water interface.

The film fracture phenomenon can also be used to explain the levelling off in the Π/A curve observed for the *n*-tetradecane emulsion system in the presence of β -lactoglobulin (Figure 3.6b). During expansion of the air/water interface, the emulsion droplets of the β -lactoglobulin/*n*-tetradecane system appeared to enter the interface at the same place, presumably in a crack, and subsequently coalesce with one another, resulting in a single large oil lens. Coalescence was confirmed in the case of the β -lactoglobulin/*n*-tetradecane system by compressing the trough surface, after which the cracks closed, leaving a transparent millimetre-sized oil lens at the surface. In the β -casein system, an opaque emulsion cloud was observed after this compression step, indicating that a significant proportion of emulsion droplets were still intact.

After entering of the *n*-tetradecane droplets and their coalescence into a large lens, the protein layer that was originally adsorbed at the droplet surface can become incorporated into a continuous protein film at the air/water interface and the oil/water interfaces (Figure 3.10). The incorporation of additional protein from the surface of entering droplets would keep Π approximately constant with increasing area up to the point that the supply of emulsion droplets is exhausted. For our system, we estimate that this corresponds to a maximum additional 60 or 120 cm² of protein film depending on whether a 2.5- or 5- μ L aliquot of emulsion is used (i.e., this is

the total area of droplet surface for 2.5- and 5- μL aliquots of 40% oil-in-water emulsion with a $d_{3,2}$ of 1 μm , respectively). This estimate agrees well with the experimental results: the plateau's in the Π/A curves (Figure 3.6b) range from ~ 335 to 380 cm^2 and from ~ 310 to 430 cm^2 for the case where a 2.5- μL (solid black line) and a 5- μL (solid grey line) aliquot of emulsion is added, respectively. Some coalescence was also observed for the *n*-tetradecane system in the presence of soy glycinin; however, analysis of the Π/A curve (Figure 3.6c) is complicated due to the crossover effect observed for the soy glycinin protein system (see Figure 3.4c).

The large proportion of intact droplets remaining after expansion of the interface for the β -casein/*n*-tetradecane system suggests that droplet entering was limited for this system. Further, based on the homogeneous nature of the β -casein film during expansion one may expect that entered droplets remain surrounded by an air/water protein film, thus limiting droplet coalescence. As a result, very little protein originating from the emulsion droplets is available to contribute area to the air/water protein film in this system. Thus, the shape of this Π/A curve (Figure 3.6a) is unaffected.

As an aside, the occurrence of film fracture does offer an explanation as to the source of the crossover measured for the soy glycinin system in the absence of emulsion (Figure 3.4c). Excess soy glycinin, present in the bulk solution due to incomplete adsorption during application of the spread protein layer, may adsorb at the "clean" spots in the air/water interface that are created when the film fractures during subsequent expansion, causing a levelling off in Π .

3.5 Concluding Remarks

The different spreading patterns observed for the three protein systems gives us new insight into the behaviour of adsorbed protein layers exposed to large-scale dilational deformation. It has been postulated that protein films can fracture [12]; however, only recently has concrete evidence of protein fracture been reported in the literature [10,13-15]. In the work presented here, protein film fracture in dilation is made visible by the presence of emulsion in the system.

When the emulsion is formed from a spreading oil, such as sunflower oil, expansion of the protein film leads to a lowered surface pressure such that the

oil in the emulsion droplets undergoes a wetting transition from lens to oil layer; this initiates a co-operative spreading process. Depending on the rheological properties of the protein film, different oil spreading scenarios take place. In the case of β -casein, the film flows and spreading proceeds gradually and in a radial fashion. The β -lactoglobulin and soy glycinin films on the other hand demonstrate fracture behaviour and oil spreads catastrophically to fill the cracks. Thus, we have shown that for protein-containing systems the wetting transition as such is determined by thermodynamics, but the morphology of the coexisting spread oil and spread protein domains is controlled by the mechanical properties of the protein film.

The experiments with the non-spreading oil, *n*-tetradecane, support the role of the mechanical properties of the protein film in droplet entering and spreading. Fracture in the β -lactoglobulin film creates a crack where many droplets enter the interface simultaneously and coalesce, forming a large lens. The protein film previously adsorbed to the emulsion droplet form a continuous protein layer at the oil/water interface of the *n*-tetradecane lens that exerts a pressure on the surrounding air/water interface. This is not observed in the presence of the more liquid-like β -casein film for which droplet entering is limited as a result of the homogeneous character of the air/water protein film during expansion.

This work offers clear evidence that in certain protein films, the surface pressure is inhomogeneous upon deformation, leading to the development of stress gradients, even for films with relatively short (5 min) ageing times. This has important consequences for the interpretation of surface rheological measurements in general. In addition, the fracture behaviour of different proteins is expected to be of practical relevance to the stability of emulsions exposed to air, for example, during whipping or oral processing.

Acknowledgements

The authors gratefully acknowledge ir. R.A. Ganzevles for her contribution to the development of the combined Langmuir trough/video technique used in this study.

References

- [1] Aveyard, R., Binks, B. P., Fletcher, P. D. I., Peck, T.-G. and Garrett, P. R. (1993). Entry and spreading of alkane drops at the air/surfactant solution interface in relation to foam and soap foam stability. *Journal of the Chemical Society of Faraday Transactions*, 89(24), 4313-4321.
- [2] Denkov, N. D., Tcholakova, S., Marinova, K. G. and Hadjiiski, A. (2002). Role of oil spreading for efficiency of mixed oil-solid antifoams. *Langmuir*, 18(15), 5810-5817.
- [3] Kruglyakov, P. M. and Vilкова, N. G. (1999). The relation between stability of asymmetric films of the liquid/liquid/gas type, spreading coefficient and surface pressure. *Colloids and Surfaces A: Physicochemical and Engineering Aspects*, 156, 475-487.
- [4] Brooker, B. E. (1993). Stabilisation of air in foods containing fat - a review. *Food Structure*, 12, 115-122.
- [5] Darling, D. F. (1982). Recent advances in the destabilization of dairy emulsions. *Journal of Dairy Research*, 49, 695-712.
- [6] Goff, H. D. (1997). Instability and partial coalescence in whippable dairy emulsions. *Journal of Dairy Science*, 80, 2620-2630.
- [7] Prins, A., Jochems, A. M. P., van Kalsbeek, H. K. A. I., Boerboom, F. J. G., Wijnen, M. E. and Williams, A. (1996). Skin formation on liquid surfaces under non-equilibrium conditions. *Progress in Colloid and Polymer Science*, 100, 321-327.
- [8] Prins, A., Boerboom, F. J. G. and van Kalsbeek, H. K. A. I. (1998). The use of overflowing cylinder technique to measure stagnant surface behaviour. *Colloids and Surfaces*, 143, 395-401.
- [9] van Vliet, T., van Aken, G. A., Bos, M. A. and Martin, A. H. (2003). Failure behaviour of adsorbed protein layers, consequences for emulsion and foam stability. In E. Dickinson and T. van Vliet, *Food Colloids: Biopolymers and Materials* Cambridge: Royal Society of Chemistry.
- [10] Murray, B. S., Cattin, B., Schüler, E. and Sonmez, Z. O. (2002). Response of adsorbed protein films to rapid expansion. *Langmuir*, 18, 9476-9484.
- [11] Benjamins, J. (2000). *Static and dynamic properties of proteins adsorbed at liquid interfaces*. Thesis: Wageningen University, The Netherlands.
- [12] Bos, M. A. and van Vliet, T. (2001). Interfacial rheological properties of adsorbed protein layers and surfactants: a review. *Advances in Colloid and Interface Science*, 91, 437-471.
- [13] Martin, A. H., Grolle, K., Bos, M. A., Cohen Stuart, M. A. and van Vliet, T. (2002). Network forming properties of various proteins adsorbed at the air/water interface in relation to foam stability. *Journal of Colloid and Interface Science*, 254, 175-183.
- [14] Bos, M. A., Grolle, K., Kloek, W. and van Vliet, T. (2003). Determination of fracture stresses of adsorbed protein layers at air-water interfaces. *Langmuir*, 19, 2181-2187.
- [15] Martin, A. H., Bos, M. A., Cohen Stuart, M. A. and van Vliet, T. (2002). Stress-strain curves of adsorbed protein layers at the air/water interface measured with surface shear rheology. *Langmuir*, 18, 1238-1243.
- [16] Hadjiiski, A., Dimova, R., Denkov, N. D., Ivanov, I. B. and Borwankar, R. (1996). Film trapping technique: precise method for three-phase contact angle determination of solid and fluid particles of micrometer size. *Langmuir*, 12, 6665-6675.
- [17] Lobo, L. and Wasan, D. T. (1993). Mechanisms of aqueous foam stability in the presence of emulsified non-aqueous-phase liquids: structure and stability of the pseudoemulsion film. *Langmuir*, 9, 1668-1677.
- [18] Robinson, J. V. and Woods, W. W. (1948). A method of selecting foam inhibitors. *Journal of the Society of Chemical Industry*, 67, 361-365.
- [19] Bergeron, V., Fagan, M. E. and Radke, C. J. (1993). Generalized entering coefficients: a criterion for foam stability against oil in porous media. *Langmuir*, 9, 1704-1713.
- [20] Hotrum, N. E., van Vliet, T., Cohen Stuart, M. A. and van Aken, G. A. (2002). Monitoring entering and spreading of emulsion droplets at an expanding air/water interface: a novel technique. *Journal of Colloid and Interface Science*, 247(1), 125-131.

- [21] Hotrum, N. E., Cohen Stuart, M. A., van Vliet, T. and van Aken, G. A. (2003). Entering and Spreading of Protein Stabilised Emulsion Droplets at the Expanding Air/Water Interface. In E. Dickinson and T. van Vliet, *Food Colloids, Biopolymers and Materials* Cambridge: Royal Society of Chemistry.
- [22] Aveyard, R. and Clint, J. H. (1997). Liquid lenses at fluid/fluid interfaces. *Journal of the Chemical Society of Faraday Transactions*, 93(7), 1397-1403.
- [23] Harkins, W. D. and Feldman, A. (1922). Films. The spreading of liquids and the spreading coefficient. *The Journal of the American Chemical Society*, 44(12), 2665-2685.
- [24] MacRitchie, F. (1986). Spread monolayers of proteins. *Journal of Colloid and Interface Science*, 25, 341-385.
- [25] van Aken, G. A. and Merks, M. T. E. (1996). Adsorption of soluble proteins to dilating surfaces. *Colloids and Surfaces A: Physicochemical and Engineering Aspects*, 114, 221-226.
- [26] de Jongh, H. H. J., Gröneveld, T. and de Groot, J. (2001). Mild isolation procedure discloses new protein structural properties of β -lactoglobulin. *Journal of Dairy Science*, 84, 562-571.
- [27] Christensen, M. I. E. and Munksgaard, L. (1989). Quantitative fractionation of casein by precipitation or ion exchange chromatography. *Milchwissenschaft*, 44, 480-484.
- [28] Swaisgood, H. E. (1982). Chemistry of Milk Proteins. In P. F. Fox, *Developments in Dairy Chemistry - 1* (pp. 1-57). London: Applied Science Publishers.
- [29] Thanh, V. H. and Shibasaki, K. (1976). Major proteins of soybean seeds. A straightforward fractionation and their characterization. *Journal of Agricultural and Food Chemistry*, 24, 1117-1121.
- [30] Martin, A. H., Bos, M. A. and van Vliet, T. (2002). Interfacial rheological properties and conformational aspects of soy glycinin at the air/water interface. *Food Hydrocolloids*, 16, 63-71.
- [31] Smulders, P. E. A. (2000). *Formation and stability of emulsions made with proteins and peptides*. Thesis: Wageningen University.
- [32] Trurnit, H. J. (1960). A theory and method for the spreading of protein monolayers. *Journal of Colloid Science*, 15, 1-13.
- [33] Graham, D. E. and Phillips, M. C. (1980). Proteins at liquid interfaces IV. Dilational properties. *Journal of Colloid and Interface Science*, 76(1), 227-239.

Chapter 4:

Oil droplet spreading in the presence of proteins and low molecular weight surfactants*

Abstract

In this paper we investigate the influence of low molecular weight (lmw) surfactant on the spreading behaviour of emulsified sunflower oil at the air/water interface. Two non-ionic lmw surfactants, polyoxyethylene sorbitan monolaurate (Tween 20, water-soluble) and sorbitan monooleate (Span 80, oil-soluble), were used in combination with β -lactoglobulin. The value of the air/water surface pressure, Π_{AW} , required for oil spreading was significantly higher in the presence of Span 80 (17 mN/m) and Tween 20 (22 mN/m), than in the absence (or at low concentrations) of lmw surfactant (15 mN/m). The results show that the presence of lmw surfactants can facilitate oil droplet spreading at the air/water interface. The increase in the value of Π_{AW} at spreading implies a shift in the balance of forces at the oil/water/air phase boundary. We demonstrate that this is likely due to the ability of lmw surfactants to be more effective than proteins in lowering the oil/water surface tension under the dynamic conditions encountered during oil droplet spreading. This may be relevant to aerated emulsions, where droplet entering and spreading precedes the formation of a layer of partially coalesced droplets at the air/water interface. In these systems, the increase in the value of Π_{AW} at spreading of emulsion droplets in the presence of surfactant may explain their higher rate of partial coalescence during aeration compared to protein-stabilised emulsions. For aerated systems, this explanation can be seen as an alternative to the explanation that decreased stability against coalescence results from a decrease in the mechanical strength of the adsorbed protein layer when lmw surfactant molecules adsorb and displace protein molecules from the oil/water interface.

4.1 Introduction

The mutual interaction between emulsion droplets at the air bubble surface during churning or whipping plays an important role in the development of structure and stability in aerated emulsions [1,2]. This, in turn, is dependent on the ease of droplet adsorption and spreading of oil out of the emulsion droplets when they contact the air/water interface [3]. A small amount of spread oil enables adjacent emulsion droplets to fuse, or partially coalesce giving rigidity to the interface, which is beneficial to air bubble stability in products such as whipped cream and ice cream [4]. However, excessive oil spreading may lead to the formation of a continuous oil layer, which cannot stabilise the air bubble, yielding poor quality foam [4]. The tendency for an oil lens, resting in an air/water interface, to spread is governed by the balance of interfacial tensions (γ) at the three-phase boundary that exists between the oil (O), water (W) and air (A), phases. When the spreading coefficient

$$S = \gamma_{AW} - (\gamma_{OW} + \gamma_{OA}) \quad (4.1)$$

is positive, oil spreading (also referred to as complete wetting) occurs [5]. Many food emulsions contain proteins and low molecular weight surfactants, which lower γ_{AW} and γ_{OW} by adsorption to the air/water or oil/water interface. The extent of oil spreading at the air bubble surface during aeration will depend on the values of γ_{AW} , γ_{OW} and γ_{OA} for a given system under dynamic conditions. In the case of sunflower oil, γ_{OW} and γ_{OA} are equal to 29 and 28 mN/m, for the pure oil/water (γ_{OW}^0) and oil/air (γ_{OA}^0) interfaces, respectively. The value of γ_{OW} for the static oil/water interface of a protein-stabilised emulsion would undoubtedly be lower than γ_{OW}^0 , due to the presence of adsorbed protein. However, entering and spreading at the air/water interface is a dynamic process during which an oil droplet will experience a sudden large increase in area. In an earlier paper [6], we proposed that in the case of a protein-stabilised emulsion, this large area increase would lead to the condition $\gamma_{OW} \sim \gamma_{OW}^0$ since protein adsorption is relatively slow compared to the spreading process. Since proteins do not adsorb to the oil/air interface we further assumed that γ_{OA} would be equal to γ_{OA}^0 . Using the values for γ_{OW}^0 and γ_{OA}^0 , then according to Equation (4.1) $S > 0$ when $\gamma_{AW} > 57$ mN/m for the sunflower oil/water/air system. This corresponds to a critical air/water surface pressure $\Pi_{cr} = 72 - 57 = 15$ mN/m, meaning that we do not expect oil spreading to occur for the sunflower oil system if $\Pi_{AW} > 15$ mN/m. Previous

experimental results supported these assumptions: for protein systems, we found that emulsion droplets did not spread at the air/water interface if $\Pi_{AW} > 15\text{mN/m}$ [6-8].

In this paper we extend our work on the entering and spreading behaviour of triglyceride oil droplets at the air/water interface by adding low molecular weight (lmw) surfactants to the system. Lmw surfactants are known to displace proteins from interfaces [9-20]. Protein displacement tends to increase gradually with increasing surfactant concentration. With respect to oil-in-water emulsions, water-soluble surfactants are known to be more effective in displacing protein from the oil/water interface than oil-soluble surfactants [12-15,18,19]. Further, the adsorption of surfactant has been shown to effectively reduce the cohesiveness of adsorbed protein layers at both the oil/water and air/water interfaces [9-11]. Weakening of the adsorbed layer has been thought to be the cause of the decrease in stability against coalescence under shear [21] and the enhanced partial coalescence during aeration [19,22-24] observed for emulsions stabilised by a mixture of protein and lmw surfactant, as compared to purely protein-stabilised emulsions.

In the case of aerated emulsions, however, a different explanation for the observation of enhanced partial coalescence may be considered. Compared to proteins, lmw surfactants tend to adsorb faster than proteins. Further, they tend to give higher surface pressures at lower adsorbed amounts than proteins [25]. Likely, this implies that lmw surfactants have the potential to facilitate droplet spreading by means of a mechanism dependent on the kinetics of surfactant adsorption to an expanding oil/water interface. If enough lmw surfactant molecules remain adsorbed to the oil/water interface during oil spreading to keep $\gamma_{OW} < \gamma_{OW}^0$, oil spreading will be easier and occur at higher Π_{AW} values than for the protein system. For aerated systems, where partial coalescence takes place predominantly at the air/water interface [4], facilitated droplet spreading may accelerate this type of partial coalescence leading to shorter churning/whipping times in systems such as ice cream and whipped cream. Thus, an investigation into the influence of surfactants on droplet spreading behaviour is of vital importance to our understanding of the influence of surfactants on the stability of emulsions during aeration. In this work, we investigate and compare the influence of the presence of a water-soluble surfactant, Tween 20, and an oil-soluble surfactant, Span 80, on the spreading behaviour of sunflower oil emulsion droplets at the air/water

interface. Emulsion composition conditions were consistent with those of previous work in this research group [26]. Our aim was to determine if, and to what extent, the presence of low molecular weight surfactants can facilitate oil spreading at the air/water interface.

4.2 Materials and Methods

4.2.1 Materials

β -Lactoglobulin (MW 18 300 g/mol) purified according to the method of de Jongh et al. [27], was dissolved in 20 mM imidazole buffer (pH 6.7) containing 0.1 M NaCl by stirring for 1 h at room temperature. The chemicals used for the buffer were purchased from Merck (Darmstadt, Germany, analytical grade). Two types of non-ionic low molecular weight surfactant, Tween 20 (polyoxyethylene sorbitan monolaurate, Merck, MW 1227.72 g/mol), and Span 80 (sorbitan monooleate, Fluka, Switzerland, MW 428.62 g/mol), were used without any further purification.

Sunflower oil (Reddy, Vandermoortele, Roosendaal, The Netherlands) was purified using silica gel 60 (70 - 230 mesh, Merck, Germany) based on the method described by Smulders [28]. The purification procedure was performed twice. Purified sunflower oil was flushed with N₂ gas and stored at -20 °C until required.

4.2.2 Emulsion preparation

For all emulsions, after preparation of the aqueous and oil phases, a pre-emulsion was formed using an Ultraturrax (T 25 basic, IKA, Staufen, Germany) equipped with an 18 mm dispersing element (S25KR-18 G, IKA). This step was followed by homogenisation using a bench-top homogeniser [6] for 10 passes at a homogenisation pressure of 10 MPa. Four different emulsion systems were prepared: (i) mixed β -lactoglobulin/Span 80, (ii) mixed β -lactoglobulin/Tween 20, (iii) β -lactoglobulin only and (iv) Tween 20 only. Systems i, ii and iii all contained 1 wt% β -lactoglobulin. System iv contained 1 wt% Tween 20. All emulsions contained 40 wt% sunflower oil.

Different aqueous and oil phase preparation schemes were followed depending on the emulsion composition. In the case of the mixed β -lactoglobulin/Span 80 system, the amount of surfactant required to give the desired Span 80 concentration, ranging from 1.4×10^{-4} to 2.7×10^{-2} M in the oil

phase, was dissolved in sunflower oil by gentle stirring for 1 h. β -Lactoglobulin was dissolved in buffer under gentle stirring for 1 h. This was followed by homogenisation as described above. The emulsions containing Span 80 were equilibrated for 14 h before performing the experiments. For the mixed β -lactoglobulin/Tween 20 system, a stock emulsion with a slightly higher oil and protein content was prepared. After homogenisation, the stock emulsion was diluted with Tween 20 dissolved in buffer in order to give the desired surfactant concentration ranging from 1.4×10^{-4} to 9.1×10^{-3} M in the aqueous phase of the emulsion. The emulsions with added Tween 20 were stirred gently for 14 h, after which the measurements were performed. Finally, for the emulsions containing 1 wt% β -lactoglobulin or 1 wt% Tween 20, the protein or lmw surfactant was dissolved for 1 h in buffer, followed by homogenisation with oil.

The average droplet diameter ($d_{3,2}$) of the emulsions measured by light scattering using a Coulter Laser LS230 (Coulter Electronics, The Netherlands) was found to be 1.3 ± 0.1 μm for all emulsions. The droplet size distribution was normally distributed. The $d_{3,2}$ was not significantly influenced by the addition of surfactant within the experimental concentration range.

4.2.3 Determination of Π_{AW} at spreading

The air/water surface pressure (Π_{AW}) at the point of spreading was determined for 5- μL aliquots of emulsion injected under a quiescent air/water interface that had been aged for 5 min. In the experiments with the mixed β -lactoglobulin/Span 80 and β -lactoglobulin/Tween 20 emulsion systems, the emulsion was injected under the surface of a 5.4×10^{-5} M (0.1 wt%) β -lactoglobulin solution. This concentration was chosen because previous work on the spreading of protein-stabilised emulsion droplets at the air/water interface indicated that, under quiescent conditions, this bulk concentration was sufficient to inhibit oil droplets from spreading [7]. In order to lower Π_{AW} and induce oil spreading, the surface was expanded at a rate of $\lambda = 0.12$ s^{-1} . The occurrence of oil spreading during expansion showed up as a minimum in the Π_{AW} vs. time curve [6]. We define this minimum as the maximum empirical value of Π_{AW} at which oil spreading was observed for the system, henceforth referred to as Π_{AW} at spreading. For some of the systems studied in this paper, oil spreading occurred spontaneously, meaning that

spreading was observed under quiescent conditions (expansion of the interface was not required).

Further, experiments were performed on emulsions stabilised by Tween 20 (1 wt%) added under the quiescent surface of Tween 20 solutions (ranging in concentration from 4×10^{-7} to 8×10^{-5} M) and on emulsions stabilised by β -lactoglobulin (1 wt%) added under the quiescent surface of β -lactoglobulin solutions (ranging in concentration from 6×10^{-8} to 1×10^{-4} M).

All these experiments were performed using the roller trough set-up, a detailed description of which is given by Hotrum et al. [6]. This rectangular trough, similar to a Langmuir trough, is equipped with computer-controlled cylindrical barriers instead of the more conventional sliding barrier (Figure 2.3). The main advantage of the roller trough set-up compared to a conventional Langmuir trough is that continuous and high steady-state expansion rates can be obtained. In the work reported here, a Teflon trough with the same inner dimensions replaced the acrylic trough described previously.

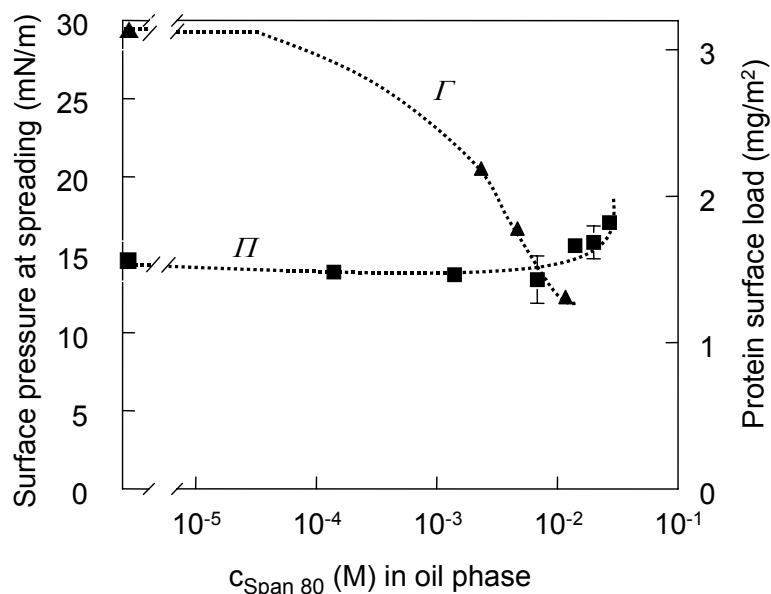


Figure 4.1: Surface pressure at spreading (■) during expansion of the air/water interface ($\lambda = 0.12 \text{ s}^{-1}$) and β -lactoglobulin surface load (▲) vs. Span 80 concentration in the emulsion. Lines are drawn for illustrative purposes. For reference, Π_{AW} at spreading and Γ β -lactoglobulin in the absence of surfactant are shown on the primary y-axis before the break. Γ values (▲) were re-plotted from [13].

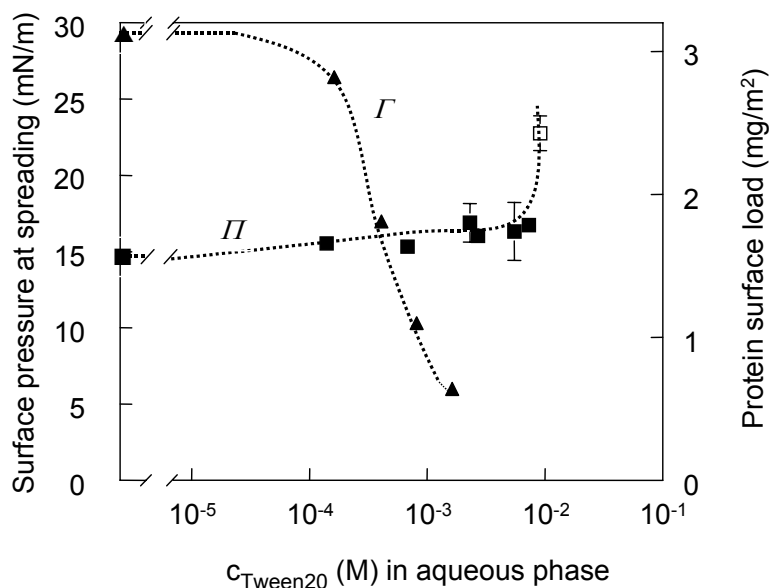


Figure 4.2: Surface pressure at spreading (■) during expansion of the air/water interface ($\lambda = 0.12 \text{ s}^{-1}$) and β -lactoglobulin surface load (▲) vs. Tween 20 concentration. For surface pressure: open symbol (□), spreading under quiescent conditions. Lines are drawn for illustrative purposes. For reference, Π_{AW} at spreading and $\Gamma_{\beta\text{-lactoglobulin}}$ in the absence of surfactant are shown on the primary y-axis before the break. Γ values (▲) were re-plotted from [13].

4.2.4 Determination of γ_{OW}

An automated drop tensiometer, ADT, (IT Concept, Longessaigne, France) [29,30] was used for the determination of γ_{OW} . In this method, an oil droplet is formed in an aqueous solution. The γ_{OW} is determined by axi-symmetric drop-shape analysis. All experiments were performed in the rising drop configuration. We determined γ_{OW} for systems containing Tween 20, Span 80, and mixtures of surfactant and protein. The γ_{OW} values determined after 60 min equilibration time are reported. All experiments were performed at 22°C.

4.3 Results

4.3.1 Π_{AW} at spreading

In Figures 4.1 and 4.2 it can be seen that, for low concentrations of added surfactant, the value of Π_{AW} at spreading is $\sim 15 \text{ mN/m}$. This is in agreement with our previous results for the spreading of protein-stabilised emulsion droplets at the air/water interface [6,7]. However, the value of Π_{AW} at

spreading increases at low surfactant concentrations larger than $\sim 1 \times 10^{-2}$ M and 1×10^{-3} M in the case of added Span 80 (Figure 4.1) or Tween 20 (Figure 4.2), respectively. For the Span 80 systems, a maximum value for Π_{AW} at spreading of 17 mN/m was measured for the emulsion containing 2.7×10^{-2} M Span 80. At higher Span 80 concentrations, emulsions became unstable to coalescence, making it impossible to perform spreading experiments. Emulsion instability above this Span 80 concentration has been reported in the literature [13,26]. For the mixed β -lactoglobulin/Tween 20 systems, the value of Π_{AW} at spreading increased to such an extent that oil spreading was observed under quiescent conditions at $\Pi_{AW} = 23 \pm 1$ mN/m for the emulsion containing 9.1×10^{-3} M Tween 20 (Figure 4.2, open square). For reference, in Figures 4.1 and 4.2, we re-plotted the protein surface load of β -lactoglobulin stabilised sunflower oil-in-water emulsions in the presence of increasing concentrations of Span 80 (Figure 4.1) or Tween 20 (Figure 4.2) reported by de Feijter et al. [13]. It seems that the increase in the value of Π_{AW} at spreading becomes apparent once a significant amount of protein has been displaced from the oil droplet surface. However, the composition of the oil/water interface of the emulsion droplets under static conditions is probably of little consequence to the value of Π_{AW} at spreading. This will be addressed in the discussion section.

In order to further investigate the apparent influence of low surfactants on the value of Π_{AW} at spreading, we compared the oil spreading behaviour observed for a β -lactoglobulin-only system with that observed for a Tween 20-only system. The results are shown in Figure 4.3. For the β -lactoglobulin system, oil spreading is observed under quiescent conditions up to a β -lactoglobulin concentration of 2.75×10^{-6} M (Figure 4.3, open triangles). Above this concentration, Π_{AW} under quiescent conditions (after 5 min equilibration) is larger than 15 mN/m and expansion of the interface is required in order to lower Π_{AW} and induce oil spreading. For the β -lactoglobulin systems subjected to expansion of the interface (Figure 4.3, closed triangles), spreading is observed at $\Pi_{AW} \sim 15$ mN/m. The results for the β -lactoglobulin system are in agreement with previous results [7]. The Tween 20 system displays different oil spreading behaviour. For this system, oil spreading is observed under quiescent conditions up to $\Pi_{AW} = 22$ mN/m for the 8×10^{-6} M Tween 20 solution (Figure 4.3, open squares). Further, when

expansion of the interface is required, spreading occurs when $\Pi_{AW} = 22 \text{ mN/m}$ (Figure 4.3, closed squares).

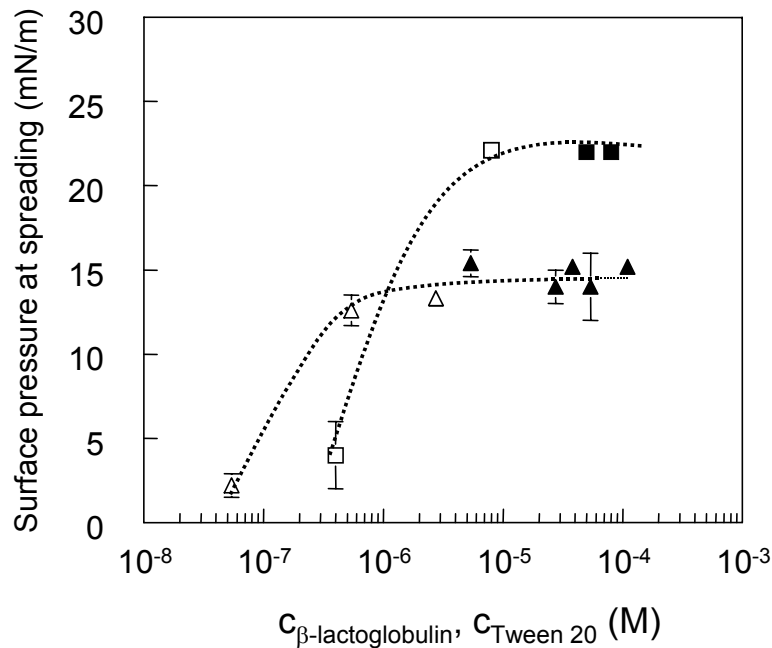


Figure 4.3: Surface pressure at spreading vs. concentration of the solution to which emulsion was added. Two systems are represented: β -lactoglobulin-stabilised emulsion added under the surface of β -lactoglobulin solutions (\blacktriangle) and Tween 20-stabilized emulsion added under the surface of Tween 20 solutions (\blacksquare). Open symbols, spreading under quiescent conditions; closed symbols, spreading during expansion of the air/water ($\lambda = 0.12 \text{ s}^{-1}$).

4.3.2 γ_{OW} in the presence of lmw surfactants and proteins

For both Span 80 and Tween 20, in the absence of β -lactoglobulin, the γ_{OW} vs. log concentration curves (Figures 4.4 and 4.5) have a shape characteristic of that expected for lmw surfactants. Above a minimum concentration, saturation adsorption is reached and γ_{OW} decreases linearly with the logarithm of concentration, followed by a levelling off in γ_{OW} as a result of micelle formation at the critical micelle concentration (CMC). For Span 80 (Figure 4.4), we find a CMC $\sim 0.1 \text{ M}$ in oil. For Tween 20 (Figure 4.5), we find a CMC of $\sim 1 \times 10^{-5} \text{ M}$ in water in the absence of protein. Our experimental results are in reasonable agreement with values for the CMC of Tween 20 and Span 80 that are reported in the literature [31,32]. Tween 20 is more surface active than Span 80, which can be seen by the decrease in γ_{OW} at much lower

concentrations for Tween 20 compared to Span 80, which has also been observed by Owusu and Zhu [31].

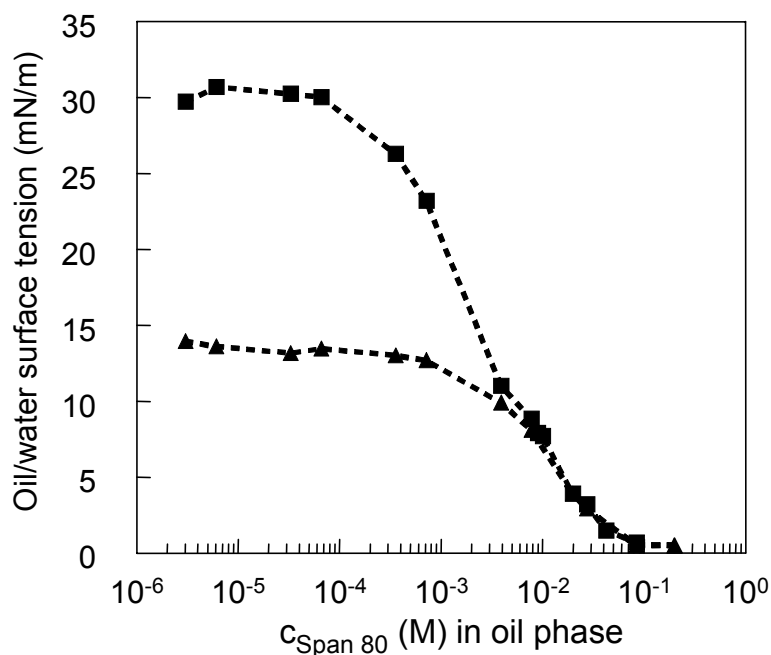


Figure 4.4: Oil/water surface tension (22°C) vs. Span 80 concentration for oil measured against either buffer solution (■) or 5.4×10^{-5} M β -lactoglobulin (▲).

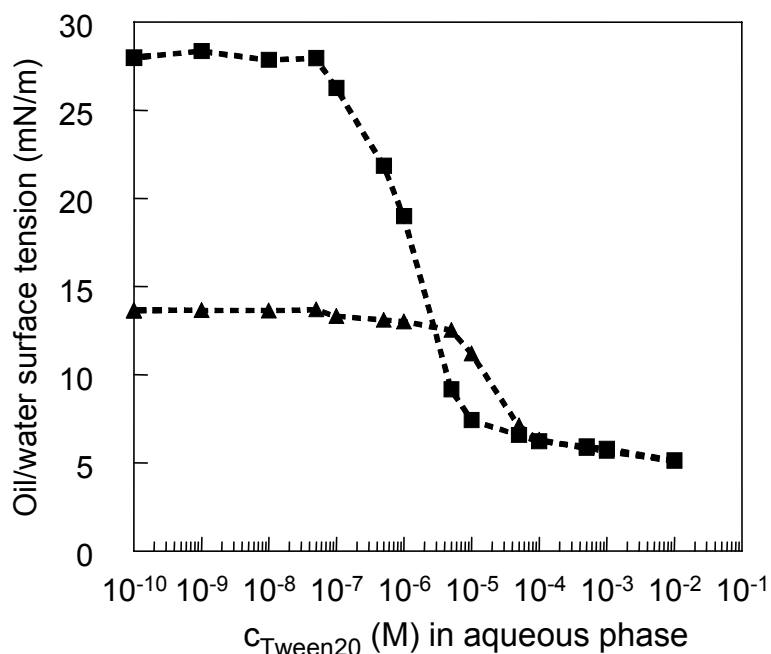


Figure 4.5: Oil/water surface tension (22°C) vs. Tween 20 concentration for oil measured against either Tween 20 (■) or a mixture of Tween 20 and 5.4×10^{-5} M β -lactoglobulin (▲).

In the presence of 5.4×10^{-5} M (0.1 wt%) β -lactoglobulin and in the absence of surfactant, we measured $\gamma_{OW} = 13$ mN/m for the sunflower oil/water interface (data not shown). This value is in reasonable agreement with de Feijter et al. [13] who reported $\gamma_{OW} = 14$ mN/m for the same system. For the mixed β -lactoglobulin/surfactant systems (Figures 4.4 and 4.5), we observed that at low surfactant concentrations $\gamma_{OW} = 13$ mN/m, which is the same γ_{OW} value as for 5.4×10^{-5} M β -lactoglobulin. As the surfactant concentration increases, γ_{OW} further decreases, reaching values as low as $\gamma_{OW} = 1$ mN/m and $\gamma_{OW} = 5$ mN/m for the Span 80 (above 0.1 M) and Tween 20 (above 1×10^{-4} M) systems, respectively. This suggests that above the respective surfactant concentrations, there is a shift from a protein-dominated to a surfactant-dominated oil/water interface. Further, in the presence of protein, the CMC of Tween 20 appears to be shifted by one order of magnitude to $\sim 1 \times 10^{-4}$ M, which can be explained by a lowering of the concentration of Tween 20 in solution due to the formation of a 1:1 surfactant:protein complex, as suggested in the literature [10,11].

4.4 Discussion

The value of Π_{AW} at spreading measured for the Tween 20-stabilized emulsion (22 mN/m) is considerably higher than the value measured for the β -lactoglobulin-stabilised emulsion (15 mN/m) (Figure 4.3). For the mixed protein/surfactant systems, values of Π_{AW} at spreading > 15 mN/m are also measured above a certain lmw surfactant concentration (Figures 4.1 and 4.2). These experimental results offer clear evidence that surfactants can facilitate emulsion droplet spreading at the air/water interface.

According Equation (4.1), an increase in the value of Π_{AW} at spreading indicates that there has been a shift in the balance of interfacial tensions at the three-phase boundary. Since at freshly formed air/oil interface $\gamma_{OA} = \gamma_{OA}^0$, this implies that $\gamma_{OW} < \gamma_{OW}^0$ for the surfactant containing systems. We expect that lmw surfactants, facilitate oil spreading due to a kinetic effect related to their higher rate of adsorption [25], and ability to effectively lower γ_{OW} [33], under dynamic conditions such as those associated with droplet entering and spreading. Below we give a physical argument to defend the validity of this explanation.

First, we need an estimation of the relative expansion rate, $d \ln A / dt = \theta$, of the oil/water interface for a spreading oil droplet. In another paper [34], we determined that the spreading rate, dz/dt , of sunflower oil on a clean air/water interface could range from 0.04 to 0.16 m/s, depending on the distance, z , from the origin of spreading. For the estimation of θ we will use an intermediate value of $dz/dt = 0.1$ m/s. For an oil droplet spreading in a radial fashion, θ will be:

$$\theta = \frac{d \ln(4\pi z^2)}{dt} = \frac{2}{z} \frac{dz}{dt} \quad (4.2)$$

Thus, θ is dependent on the distance that the oil has spread. For example, for $z = 0.005$ m, $\theta = 40$ s⁻¹ while for $z = 0.05$ m, $\theta = 4$ s⁻¹. This means that on the length-scales relevant to oil droplet spreading, we can expect the relative expansion rate of the oil/water interface to be on the order of 1 - 10 s⁻¹.

Having established an expected range for θ of the spreading oil/water interface, we can now estimate if it is realistic to expect β -lactoglobulin or Tween 20 to be present at the oil/water interface in sufficient amounts for $\gamma_{OW} < \gamma_{OW}^0$ at the concentrations used in the experiments. Using the same approach as van Voorst Vader [35], we can derive an expression for the steady-state surface concentration, Γ_{SS} , of protein or surfactant molecules at an expanding air/water interface:

$$\Gamma_{SS} = \frac{k_a c}{\theta + k_d + k_a \sqrt{\frac{\pi\theta}{2D}}} \quad (4.3)$$

where k_a and k_d are the adsorption and desorption rate constants as defined by the Langmuir isotherm (see Appendix) and c and D are the concentration and diffusion coefficient, respectively of surface active molecules in the aqueous phase surrounding the oil droplets. In this model, we assume that adsorption is surface-controlled [36] and that there is no local equilibrium between the adsorbed layer and the subsurface. Equation (4.3) can be further simplified for the individual cases of protein and lmw surfactant.

For proteins layers, which tend to be strongly adsorbed, desorption is negligible. Thus, we will set $k_d = 0$. Further, for β -lactoglobulin, we may expect $k_a \approx 1 \times 10^{-7}$ m/s (see Appendix); given that we expect that θ is on the order of 1 - 10 s⁻¹, and that $D \sim 7 \times 10^{-11}$ m²/s, we can expect that $\theta \gg k_a \sqrt{\pi\theta / 2D}$, allowing us to simplify Equation (4.3) to:

$$\Gamma_{\text{SS,protein}} = \frac{k_a c}{\theta} \quad (4.4)$$

For proteins, a minimum surface coverage of $\sim 1 \text{ mg/m}^2$ is required in order to measure a surface pressure [37]. Thus, for a given value of c , we can calculate the value of θ that will allow $\Gamma_{\text{SS, protein}} = 1 \text{ mg/m}^2$ at the expanding oil/water interface. For the case of a 40% oil-in-water emulsion with a droplet diameter of $1 \mu\text{m}$, stabilised by 10 g/L (1 wt%) β -lactoglobulin, with a droplet surface coverage of 3 mg protein/m^2 [13], the concentration of protein in the continuous phase would be, $c = 4.7 \text{ g/L} = 4700 \text{ g/m}^3$. Substituting this value for c and the above defined values for k_a and Γ_{SS} into Equation (4.4) gives $\theta = 0.47 \text{ s}^{-1}$. This means that for the case of β -lactoglobulin adsorption to an expanding oil/water interface, we expect $\gamma_{\text{OW}} < \gamma_{\text{OW}}^0$ only if $\theta < 0.47 \text{ s}^{-1}$. Since we expect θ to be on the order of $1 - 10 \text{ s}^{-1}$ during oil droplet spreading, we therefore expect that $\gamma_{\text{OW}} = \gamma_{\text{OW}}^0$ under these expansion conditions; thus it follows that $S \geq 0$ is satisfied when $\Pi_{\text{AW}} \leq 15 \text{ mN/m}$. The experimental results for β -lactoglobulin (Figure 4.3) confirm this. Earlier results on the dynamic surface pressure of whey protein isolate at the air/water interface [7] indicate that at $\theta = 0.47 \text{ s}^{-1}$ significant surface pressures can be measured, however this does not necessarily apply to a dynamic oil/water surface. Certainly, for $\theta = 10 \text{ s}^{-1}$ we could expect the surface pressure to be very small.

Next, we will use the same approach as above to estimate if we can expect $\gamma_{\text{OW}} < \gamma_{\text{OW}}^0$ at the spreading oil/water interface in the presence of Tween 20. In this case, we need to simplify Equation (4.3) to reflect the adsorption behaviour of lmw surfactants. For these systems, k_d cannot be neglected, as these molecules are known to easily diffuse between the bulk and the surface. However, we can express k_d as $k_d = k_a/K$, where K is the equilibrium constant between adsorption and desorption of surfactant molecules. Substituting k_a/K for k_d in Equation (4.3) and dividing the numerator and denominator by k_a yields:

$$\Gamma_{\text{SS,surfactant}} = \frac{c}{\frac{\theta}{k_a} + \frac{1}{K} + \sqrt{\frac{\pi\theta}{2D}}} \quad (4.5)$$

Equation (4.5) can then be further simplified. Low molecular weight surfactants tend to adsorb very fast, such that k_a is expected to be very large. Further, lmw surfactants are very surface active, so that K is very large. Therefore, in the denominator, the terms θ/k_a and $1/K$ are expected to be very

small and the term $\sqrt{\pi\theta/2D}$ will dominate. Thus, for a low molecular weight surfactant, equation (4.3) can be simplified to:

$$\Gamma_{SS, \text{surfactant}} = c\sqrt{\frac{2D}{\pi\theta}} \quad (4.6)$$

For Tween 20, based on the Stokes-Einstein equation ($D = kT/6\pi\eta a$), we can estimate $D \sim 2 \times 10^{-10}$ m²/s, which appears to be a reasonable approximation compared to the diffusion coefficients reported in the literature for various water soluble, non-ionic surfactants [38,39]. Further, we can expect $\gamma_{OW} < \gamma^0_{OW}$ when $\Gamma_{SS, \text{surfactant}} > 3 \times 10^{-6}$ mol/m², which is a modest estimate if we assume that the surfactant behaves as a 2D gas ($\Pi = \Gamma RT$). Given this, we can calculate the value of θ that will allow $\Gamma_{SS, \text{surfactant}} = 3 \times 10^{-6}$ mol/m² at the expanding oil/water interface, for a given value of c . Estimating $c = 4700$ g/m³ = 3.8 mol/m³ for a 40 wt% emulsion stabilised by 1 wt% Tween 20 with a surface coverage of 3 mg/m² [13] and substituting this value together with the above defined values for D and Γ_{ss} into Equation (4.6), gives $\theta = 200$ s⁻¹. This is much larger than our estimate of $\theta = 1 - 10$ s⁻¹ for the oil/water interface of a spreading droplet, and based on the above calculation it is reasonable to assume that $\gamma_{OW} < \gamma^0_{OW}$ during oil spreading for the case of a Tween 20 stabilised emulsion. In reality, c is above the CMC of Tween 20, which may change the result of the estimation somewhat. Still, we would expect the critical Π_{AW} required to meet the condition $S \geq 0$ to be shifted to higher values of Π_{AW} for the Tween 20 system compared to the β -lactoglobulin system, which is supported by the experimental results (Figure 4.3).

The above approximations support our hypothesis that lmw surfactants facilitate oil spreading due to their ability to effectively lower γ_{OW} under the dynamic conditions associated with oil droplet spreading. One could argue that for the mixed systems (Figures 4.1 and 4.2), the effect of lmw surfactant on the value of Π_{AW} at spreading is due to protein displacement from the oil/water interface in the emulsions, and comparison of displacement data reported by de Feijter et al. [13] might appear to confirm this. However, the comparatively static case of protein displacement in emulsions should not be confused with the highly dynamic case of adsorption of surfactant to an expanding oil/water interface, as is the case for spreading oil. For the mixed β -lactoglobulin/Tween 20 emulsions, the increase in Π_{AW} at spreading begins

at $\sim 1 \text{ mol/m}^3$ ($1 \times 10^{-3} \text{ M}$). At this concentration sufficient surfactant is present in the continuous phase of the emulsion so that $\gamma_{\text{OW}} < \gamma_{\text{OW}}^0$ during the oil spreading process (Equation (4.6)). In our opinion, it is merely a coincidence that this concentration is similar to that at which Tween 20 has displaced β -lactoglobulin from the oil/water interface under static conditions (Figure 4.2). For the mixed β -lactoglobulin/Span 80 emulsions, a similar argument applies. For this system, at $c = 1 \text{ mol/m}^3$ ($1 \times 10^{-3} \text{ M}$), we expect a significant amount of protein to be displaced from the static oil/water interface (Figure 4.1). However, we do not measure an increase in the value of Π_{AW} at spreading for the mixed β -lactoglobulin/Span 80 systems until $c > 10 \text{ mol/m}^3$ ($1 \times 10^{-2} \text{ M}$). We can evaluate whether $\gamma_{\text{OW}} < \gamma_{\text{OW}}^0$ for these systems. For Span 80 we might expect $D \approx 2 \times 10^{-12} \text{ m}^2/\text{s}$, which is the value reported by Campanelli and Wang [38] corrected for the viscosity of sunflower oil of $22.7 \text{ mPa}\cdot\text{s}$ [40]. Substituting this D -value and $\Gamma_{\text{SS, surfactant}} = 3 \times 10^{-6} \text{ mol/m}^2$ into Equation (4.6) predicts that for $c = 1 \text{ mol/m}^3$, $\gamma_{\text{OW}} < \gamma_{\text{OW}}^0$ if $\theta < 2 \text{ s}^{-1}$ and that for $c = 10 \text{ mol/m}^3$, $\gamma_{\text{OW}} < \gamma_{\text{OW}}^0$ if $\theta < 100 \text{ s}^{-1}$. The θ -value of 2 s^{-1} is on the same order of magnitude as the θ -value predicted by Equation (4.2) for the expanding oil/water interface of a spreading oil droplet, while $\theta = 100 \text{ s}^{-1}$ is an order of magnitude larger than the predicted θ -value. This explains why we measure an increase in the value of Π_{AW} at spreading for the mixed β -lactoglobulin/Span 80 emulsions when $c > 10 \text{ mol/m}^3$ but not when $c = 1 \text{ mol/m}^3$.

Our proposal that oil droplet spreading in the presence of surfactants is facilitated due to a kinetic effect has important consequences for our understanding of the influence of surfactants on processes where air is incorporated into emulsions such as during the whipping of cream and ice-cream-making. For example, in their work on the influence of lmw surfactants on partial coalescence during the churning of ice cream, Goff and Jordan [24] found that the most surface active surfactant was also the most effective in promoting partial coalescence. They suggested that this might be due to a relationship between surface activity and the extent to which a lmw surfactant can displace protein from the interface, but were unable to fully explain their observation. In light of the evidence presented in this paper for facilitated oil droplet spreading in the presence of surfactants, we can more fully account for the phenomenon observed by Goff and Jordan [24]. It is not so much the

ability of the surfactant to adsorb to the oil/water interface under static conditions, thus displacing protein that is important. Rather, lmw surfactants are able to facilitate droplet spreading at the air/water interface by effectively lowering γ_{OW} under the dynamic conditions encountered during the spreading process. The larger the diffusion coefficient of the surfactant molecule, the better it will be at facilitating droplet spreading, as we observed for Tween 20 ($D \sim 1 \times 10^{-10} \text{ m}^2/\text{s}$, Π_{AW} at spreading = 22 mN/m) compared to Span 80 ($D \sim 2 \times 10^{-12}$, Π_{AW} at spreading = 17 mN/m) in this work. During aeration, partial coalescence takes place at the air bubble surface when oil spreading out of adjacent adsorbed oil droplets meets and the droplets fuse [2]. If droplet spreading is facilitated, as is the case in the presence of sufficient lmw surfactant, droplets will spread more easily and thus coalesce more easily and a greater degree of partial coalescence will be measured after the same churning time. This mechanism can also explain the shorter whipping times observed for protein-stabilised recombined cream with added lmw surfactant [3].

An alternative explanation for facilitated droplet spreading is that surfactants decrease the stability of emulsion droplets against coalescence under shear [21] and enhance partial coalescence during aeration [19,22-24] by lowering the mechanical strength of the adsorbed protein layers at both the oil/water and air/water interfaces [9-11]. While this mechanism may explain the influence of surfactants on the stability against coalescence of emulsions sheared in the absence of air, we do not feel that this mechanism can explain the facilitated oil spreading at the air/water interface described in this paper. Moreover, in our study of the spreading behaviour of oil droplets at a fluid-like interface (β -casein) compared to at a more rigid interface (β -lactoglobulin) [8] the value of Π_{AW} at spreading for the two systems did not appear to be influenced by the mechanical properties of the adsorbed protein layer.

4.5 Concluding Remarks

The fast adsorption and strong surface activity of lmw surfactants such as Span 80 and Tween 20 compared to the protein β -lactoglobulin means that the assumption made for protein containing systems that $\gamma_{OW} = \gamma_{OW}^0$ upon emulsion droplet entering and spreading does not hold in the presence of surfactants. We propose that lmw surfactants facilitate oil spreading due to a

kinetic effect related to their ability to effectively lower γ_{OW} under the dynamic conditions associated with droplet entering and spreading. As a consequence, there is a shift in the balance of interfacial tensions at the three-phase boundary leading to an increase in the value of Π_{AW} at spreading. The effect is stronger for Tween 20 than for Span 80, which can be explained by the larger diffusion coefficient expected for Tween 20.

Acknowledgements

The authors thank Franklin Zoet for performing experiments and Els de Hoog and Maria Nezery for allowing us to use their data for γ_{OW} in the presence of Span 80.

Appendix

Estimation of k_a for β -lactoglobulin

According to the Langmuir isotherm [41]:

$$\frac{d\Gamma}{dt} = k_a c(1 - \phi) - k_d \phi \quad (4.A1)$$

where, ϕ is the fraction of the surface that is occupied by the adsorbed molecules. In the case of a protein, we can assume $k_d = 0$. Further, for initial adsorption, we can assume $\phi = 0$. Equation (4.A1) simplifies to:

$$\frac{d\Gamma}{dt} = k_a c \quad (4.A2)$$

For proteins, a minimum surface coverage of ~ 1 mg/m² is required to give a detectable surface pressure [37]. This corresponds to 5.5×10^{-8} mol/m², in the case of β -lactoglobulin. According to van Aken and Merks [36], this condition is reached for a 1.1×10^{-3} mol/m³ (20 mg/L) β -lactoglobulin solution after ~ 500 s. This corresponds to a value for $d\Gamma/dt$ of 1.1×10^{-10} mol/m²s. Substituting this value for $d\Gamma/dt$ and $c = 1.1 \times 10^{-3}$ mol/m³ into Equation (4.A2) yields a value for $k_a = 1 \times 10^{-7}$ m/s. Note that k_a is dependent on the value of Γ and c .

References

- [1] Brooker, B. E. (1993). Stabilisation of air in foods containing fat - a review. *Food Structure*, 12, 115-122.
- [2] Darling, D. F. (1982). Recent advances in the destabilization of dairy emulsions. *Journal of Dairy Research*, 49, 695-712.

- [3] Hotrum, N. E., Cohen Stuart, M. A., van Vliet, T. and van Aken, G. A. (2004). Elucidating the relationship between the spreading coefficient, surface-mediated partial coalescence and the whipping time of cream. *To be submitted*.
- [4] Brooker, B. E., Anderson, M. and Andrews, A. T. (1986). The development of structure in whipped cream. *Food Microstructure*, 5, 277-285.
- [5] Harkins, W. D. and Feldman, A. (1922). Films. The spreading of liquids and the spreading coefficient. *The Journal of the American Chemical Society*, 44(12), 2665-2685.
- [6] Hotrum, N. E., van Vliet, T., Cohen Stuart, M. A. and van Aken, G. A. (2002). Monitoring entering and spreading of emulsion droplets at an expanding air/water interface: a novel technique. *Journal of Colloid and Interface Science*, 247(1), 125-131.
- [7] Hotrum, N. E., Cohen Stuart, M. A., van Vliet, T. and van Aken, G. A. (2003). Entering and Spreading of Protein Stabilised Emulsion Droplets at the Expanding Air/Water Interface. In E. Dickinson and T. van Vliet, *Food Colloids, Biopolymers and Materials* Cambridge: Royal Society of Chemistry.
- [8] Hotrum, N. E., Cohen Stuart, M. A., van Vliet, T. and van Aken, G. A. (2003). Flow and fracture phenomena in adsorbed protein layers at the air/water interface in connection with spreading oil droplets. *Langmuir*, 19, 10210-10216.
- [9] Courthaudon, J.-L., Dickinson, E. and Matsumura, Y. (1991). Competitive adsorption of β -lactoglobulin + Tween 20 at the oil-water interface. *Colloids and Surfaces*, 56, 293-300.
- [10] Coke, M., Wilde, P. J., Russell, E. J. and Clark, D. C. (1990). The influence of surface composition and molecular diffusion on the stability of foams formed from protein/surfactant mixtures. *Journal of Colloid and Interface Science*, 138(2), 489-504.
- [11] Wilde, P. J. and Clark, D. C. (1993). The competitive displacement of β -lactoglobulin by Tween 20 from oil-water and air-water interfaces. *Journal of Colloid and Interface Science*, 155, 48-54.
- [12] Courthaudon, J.-L., Dickinson, E., Matsumura, Y. and Williams, A. (1991). Influence of emulsifier on the competitive adsorption of whey proteins in emulsions. *Food Structure*, 10, 109-115.
- [13] de Feijter, J. A., Benjamins, J. and Tamboer, M. (1987). Adsorption displacement of proteins by surfactants in oil-in-water emulsions. *Colloids and Surfaces*, 27, 243-266.
- [14] Dickinson, E. and Tanai, S. (1992). Protein displacement from the emulsion droplet surface by oil-soluble and water-soluble surfactants. *Journal of Agricultural and Food Chemistry*, 40, 179-183.
- [15] Dickinson, E., Owusu, R. K., Tan, S. and Williams, A. (1993). Oil-soluble surfactants have little effect on competitive adsorption of α -lactalbumin and β -lactoglobulin in emulsions. *Journal of Food Science*, 58(2), 295-298.
- [16] Mackie, A. R., Gunning, A. P., Wilde, P. J. and Morris, V. J. (1999). Orogenic displacement of protein from the air/water interface by competitive adsorption. *Journal of Colloid and Interface Science*, 210, 157-166.
- [17] Mackie, A. R., Gunning, A. P., Wilde, P. J. and Morris, V. J. (2000). Orogenic displacement of protein from the oil/water interface. *Langmuir*, 16, 2242-2247.
- [18] Oortwijn, H. and Walstra, P. (1979). The membranes of recombined fat globules. 2. Composition. *Netherlands Milk and Dairy Journal*, 33, 134-154.
- [19] Pelan, B. M. C., Watts, K. M., Campbell, I. J. and Lips, A. (1997). The stability of aerated milk protein emulsions in the presence of small molecule surfactants. *Journal of Dairy Science*, 80, 2631-2638.
- [20] Dickinson, E. (1992). *An Introduction to Food Colloids*. Oxford: Oxford University Press.
- [21] Chen, J., Dickinson, E. and Iveson, G. (1993). Interfacial interactions, competitive adsorption and emulsion stability. *Food Structure*, 12, 135-146.
- [22] Barfod, N. M., Krog, N., Larsen, G. and Buchheim, W. (1991). Effects of emulsifiers on protein/fat interaction in ice cream mix during ageing. 1. Quantitative analyses. *Fat Science Technology*, 93(24), 29.
- [23] Dickinson, E. and Stainsby, G. (1982). *Colloids in Food*. London: Applied Science.
- [24] Goff, H. D. and Jordan, W. K. (1989). Action of emulsifiers in promoting fat destabilization during the manufacture of ice cream. *Journal of Dairy Science*, 72, 18-29.

- [25] Walstra, P. and de Roos, A. L. (1993). Proteins at air-water and oil-water interfaces: static and dynamic aspects. *Food Reviews International*, 9(4), 503-525.
- [26] van Aken, G. A. (2003). Competitive adsorption of protein and surfactants in highly concentrated emulsions: effect on coalescence mechanisms. *Colloids and Surfaces A: Physicochemical and Engineering Aspects*, 213, 209-219.
- [27] de Jongh, H. H. J., Gröneveld, T. and de Groot, J. (2001). Mild isolation procedure discloses new protein structural properties of β -lactoglobulin. *Journal of Dairy Science*, 84, 562-571.
- [28] Smulders, P. E. A. (2000). *Formation and stability of emulsions made with proteins and peptides*. Thesis: Wageningen University.
- [29] Benjamins, J., Cagna, A. and Lucassen-Reynders, E. H. (1996). Viscoelastic properties of triacylglycerol/water interfaces covered by proteins. *Colloids and Surfaces A: Physicochemical and Engineering Aspects*, 114, 245-254.
- [30] Martin, A. H., Grolle, K., Bos, M. A., Cohen Stuart, M. A. and van Vliet, T. (2002). Network forming properties of various proteins adsorbed at the air/water interface in relation to foam stability. *Journal of Colloid and Interface Science*, 254, 175-183.
- [31] Owusu, R. K. and Zhu, Q.-H. (1996). Interfacial parameters for selected Spans and Tweens at the hydrocarbon-water interface. *Food Hydrocolloids*, 10(1), 27-30.
- [32] Rodríguez Patino, J. M., Rodríguez Niño, R. and Alvarez Gómez, J. M. (1997). Interfacial and foaming characteristics of protein-lipid systems. *Food Hydrocolloids*, 11(1), 49-58.
- [33] Boerboom, F. J. G. (2000). *Proteins and protein/surfactant mixtures at interfaces in motion*. Thesis: Wageningen University, The Netherlands.
- [34] Hotrum, N. E., Cohen Stuart, M. A., van Vliet, T. and van Aken, G. A. (2004). Spreading of partially crystallized oil droplets on an air/water interface. *Accepted to Colloids and Surfaces A: Physicochemical and Engineering Aspects*.
- [35] van Voorst Vader, F., Erkens, Th. F. and van den Tempel, M. (1964). Measurement of dilational surface properties. *Transactions of the Faraday Society*, 60, 1170-1177.
- [36] van Aken, G. A. and Merks, M. T. E. (1996). Adsorption of soluble proteins to dilating surfaces. *Colloids and Surfaces A: Physicochemical and Engineering Aspects*, 114, 221-226.
- [37] Benjamins, J. (2000). *Static and dynamic properties of proteins adsorbed at liquid interfaces*. Thesis: Wageningen University, The Netherlands.
- [38] Campanelli, J. R. and Wang, X. (1998). Comments on modelling the diffusion-controlled adsorption of surfactants. *The Canadian Journal of Chemical Engineering*, 76(February), 51-57.
- [39] Kjellin, U. R. M., Reimer, J. and Hansson, P. (2003). An investigation of dynamic surface tension, critical micelle concentration, and aggregation number of three nonionic surfactants using NMR, time-resolved fluorescence quenching, and maximum bubble pressure tensiometry. *Journal of Colloid and Interface Science*, 262, 506-515.
- [40] Kloek, W. (1998). *Mechanical properties of fats in relation to their crystallization*. Thesis: Wageningen Agricultural University, The Netherlands.
- [41] Hiemenz, P. C. and Rajagopalan, R. (1997). *Principles of Colloid and Surface Chemistry*. New York: Marcel Dekker.

Chapter 5:

Spreading of partially crystallised oil droplets on an air/water interface*

Abstract

The influence of crystalline fat on the amount and rate of oil spreading out of emulsion droplets onto either a clean or a protein-covered air/water interface was measured for β -lactoglobulin stabilised emulsions prepared with either anhydrous milk fat or a blend of hydrogenated palm fat and sunflower oil. At a clean interface, the liquid oil present in the emulsion droplets was observed to completely spread out of the droplets unimpeded by the presence of a fat crystal network. Further, the presence of a fat crystal network had no effect on the rate of oil spreading out of the droplets. At a protein-covered interface, the spreading behaviour of emulsion droplets containing crystalline fat was evaluated in terms of the surface pressure (Π_{AW}) at the point of spreading, Π_{AW} at spreading was unaffected by the presence of crystalline fat. We conclude it is unlikely that the role of crystalline fat in stabilising aerated emulsions such as whipped cream is to reduce oil spreading at the air/water interface. However, the temperature of the system did have an effect: spontaneous spreading of emulsion droplets at clean air/water interfaces occurred for systems measured at 5°C, but not for those measured at 22 or 37°C. Thus, temperature may play a more important role in the whipping process than commonly thought: the entering and spreading of emulsion droplets was favoured at lower temperatures because the surface pressure exerted by protein adsorbed at the air/water interface was reduced. This effect may facilitate the whipping process.

5.1 Introduction

Emulsion droplets play an important role in the stability of aerated food emulsions. In order to be effective in providing stability and structure to this special class of foam, emulsion droplets must contain a significant proportion of crystalline fat [1,2]. For example, in natural and recombined whipped cream, partially coalesced emulsion droplets adhere to the air bubbles, giving structural integrity to the air bubbles; in the final whipped cream, a network of partially coalesced droplets connects fat clumps in the bulk to droplets adhered to the air bubble surface giving structural integrity to the foam [3-5]. Another aspect of importance is the interaction between emulsion droplets and air bubbles during aeration. In particular, spreading of liquid oil at the air/water interface should be limited, as oil spreading results in thinning of the lamellae between bubbles, which may ultimately lead to film destabilisation and air bubble collapse [6].

Thus, we arrive at the question of how to control spreading of liquid oil out of emulsion droplets when they enter the air/water interface. For an oil lens resting in an air/water interface, the tendency to spread is predicted from the balance of interfacial tensions (γ) at the three-phase boundary that exists between the air (A), water (W) and oil (O) phases. When the spreading coefficient

$$S = \gamma_{AW} - (\gamma_{OW} + \gamma_{OA}) \quad (5.1)$$

is positive, oil spreading (also called complete wetting) occurs [7]. For example, in the absence of surface active material, sunflower oil (22°C) spreads at the air/water interface since γ_{AW} , γ_{OW} , and γ_{OA} are equal to 71.9, 29.3 and 28.0 mN/m, respectively (Table 5.1). Many food emulsions contain proteins, which can lower γ_{AW} to the extent that spreading is inhibited below a critical γ_{AW} value [8]. If this is the case, the emulsion droplets cannot spread at the air/water interface under quiescent conditions. However, during aeration, dynamic conditions exist such that there is local expansion and compression of the air bubbles. Under these conditions, we can expect that for a portion of the air/water interface, γ_{AW} will be high enough to favour oil spreading.

During the aeration of emulsions such as dairy cream, proteins adsorb at the air/water interface prior to fat globule adsorption [9,10]. It is often assumed that proteins adsorb irreversibly at air/water interfaces, in which case spreading of oil would result in compression of the protein layer

adsorbed to the remaining interface. This would result in further lowering of γ_{AW} , ultimately leading to the condition $S < 0$. In this way, adsorbed proteins should be able to limit oil spreading since less oil would be able to spread before the condition $S < 0$ is reached for the case of oil spreading at a clean air/water interface.

Table 5.1: Properties of sunflower oil and anhydrous milk fat. Density values are given for the temperature at which the spreadability of fully liquid oil emulsions was measured. The interfacial tensions γ_{OW} and γ_{OA} are shown for the three temperatures used in this study. Further, γ_{AW} for the buffer solution/air interface in the absence of surface active material, γ_{AW}^0 , is given for the different temperatures used in this study. For all γ values, an error of 0.1 mN/m applies.

System	T (°C)	ρ (g/mL)	M (g/mol)	γ_{OW} (mN/m)	γ_{OA} (mN/m)	γ_{AW}^0 (mN/m)
sunflower oil	37	-	877 ^c	30.1	27.3	69.9
sunflower oil	22	0.92 ^a	"	29.3	28.0	71.9
sunflower oil	5	-	"	28.6	28.5	74.2
milk fat	37	0.906 ^b	799 ^b	4 - 10*	29.1	69.9

^a[33] p.289, ^b[2] p.31, ^c[34] p.21, *slowly decreasing

Oil continues to spread as long as the $S \geq 0$ condition is maintained and oil molecules are available. Equation (5.1) is based on the conceptual model of an oil lens resting in the interface, which becomes progressively larger and flatter as γ_{AW} increases until, at $S = 0$, an oil film is finally formed, which may or may not be a monolayer. This model is based on macroscopic considerations (Figure 5.1a). At the microscopic level, one may view the oil droplet as a reservoir from which an oil monolayer can spread to cover the interface (Figure 5.1b) [11]. The oil continues to spread as long as γ of the spreading oil (mono)layer is lower than that of the surrounding air/water interface, that is to say as long as a surface tension gradient exists. Joos and Pintens [12] presented a theoretical model for oil spreading, based on the longitudinal wave theory [13], that predicts the distance (z) oil molecules will spread on a (thick) water layer as a function of time (t):

$$z = C|\Delta\gamma|^{1/2} \eta^{-1/4} \rho^{-1/4} t^{3/4} \quad (5.2)$$

where C is a constant and η and ρ are the viscosity and the density of the underlying liquid, respectively. In this model, the driving force for spreading is the surface tension gradient, $\Delta\gamma$, which is assumed to be uniform over the

distance from the edge of the reservoir to the edge of the spreading front (Figure 5.1b). Therefore, we can identify $\Delta\gamma = \Delta\gamma_{AW} - (\Delta\gamma_{OW} + \Delta\gamma_{OA}) = S$. Further assumptions underlying this model include (i) that oil spreads laterally away from the droplet, (ii) that the velocity of the underlying liquid decays exponentially with increasing depth into the substrate and (iii) that the propagation speed assumes a uniform expansion in all directions over the surface. Schokker et al. [14] found that the distance travelled by oil spreading out of soybean oil emulsion droplets scales with $t^{3/4}$ as predicted by Equation (5.2). Bisperink [15] recast Equation (5.2) in terms of the spreading coefficient, S ; the underlying relationship $z \propto t^{3/4}$ remained the same; and the spreading behaviour of soybean oil on a clean air/water interface was found to obey this relationship.

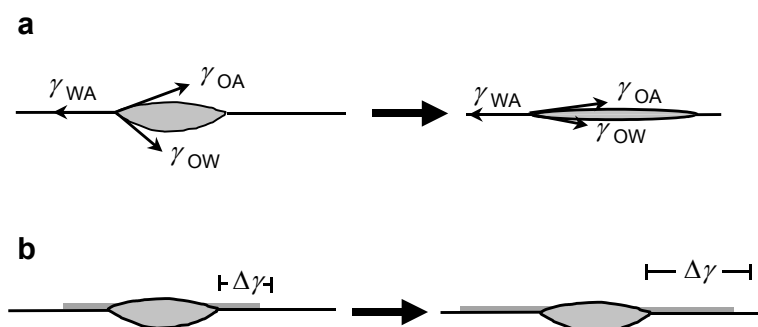


Figure 5.1: Schematic representation of two possible mechanisms for the spreading of oil at the air/water interface. In the first mechanism, (a) an oil lens resting in the interface becomes progressively larger and flatter and eventually an oil layer, covering the interface is formed; the conformation of the lens depends on the balance of the three interfacial tensions, γ_{AW} , γ_{OW} , and γ_{OA} . In the second mechanism, (b) the oil lens acts as a reservoir, from which an oil monolayer propagates over the air/water interface; the spreading of the monolayer is driven by the surface tension gradient, $\Delta\gamma$.

Equation (5.2) is of limited validity in that it was developed to describe oil spreading on clean water layers, and therefore does not take into account factors that may retard spreading such as an elastic modulus or relaxation processes that can be expected to exist in the presence of low molecular weight surfactants or adsorbed protein layers. Prins [16] proposed a model to relate the propagation speed of the spreading oil front to the surface dilational

modulus of the interface. However, Bisperink [15] showed that while this model could describe oil spreading on the surface of a dilute surfactant solution, the model could not describe the spreading of oil on a protein solution interface. It has recently been shown that certain proteins form brittle layers that can fracture, leading to inhomogeneous spreading at the air/water interface [17]. This may explain why the model proposed by Prins [16], which is based on the assumption that oil spreading proceeds homogeneously in a radial pattern, could not be successfully applied to protein systems.

Based on the arguments given above, we expect that an adsorbed protein layer may counteract oil spreading at an air/water interface to some extent. Further, in the case of whipped cream, an additional mechanism has been proposed. That is, that the presence of a network of finely distributed fat crystals within the emulsion droplets can reduce or prevent oil spreading by capillary action of the fat crystal network [1,3]. The capillary pressure, ΔP_c , of the fat crystal network is due to the Laplace pressure in the pores between the fat crystals and is given by

$$\Delta P_c = \frac{2\gamma_{OA}}{r} \cos \theta \quad (5.3)$$

where θ is the contact angle between the oil and the fat crystal, and r is the radius of the pores in the fat crystal network. By including the parameter ΔP_c into the spreading mechanism, the driving force for spreading becomes the difference between the spreading pressure, S , and the capillary pressure ΔP_c . For the static case, oil spreading occurs when the inequality in Equation (5.4) is satisfied.

$$S/d - \Delta P_c \geq 0 \quad (5.4)$$

Here, in order to obtain a 3-dimensional pressure that can be balanced against ΔP_c , we assumed that S acts over the thickness, d , of the spreading monolayer.

In this paper we test the hypothesis that the presence of crystalline fat in emulsion droplets can reduce or retard spreading of liquid oil out of emulsion droplets. The influence of solid fat content on the spreading behaviour of emulsion droplets at clean and protein-covered air/water interfaces was characterised in terms of three parameters. These are, for the case of oil spreading on clean air/water interfaces, (i) the amount of emulsion required to initiate a reduction in γ_{AW} and (ii) the rate of oil spreading out of emulsion droplets; and for the case of spreading in the presence of an adsorbed protein layer, (iii) the value of the air/water surface pressure at spreading.

5.2 Materials and Methods

5.2.1 Materials

β -Lactoglobulin was purified according to the method of de Jongh et al. [18] β -Lactoglobulin was dissolved in 20 mM imidazole buffer (pH 6.7) containing 0.1 M NaCl by stirring for 3 h at the measuring temperature of either 5, 22, or 37°C. The chemicals used for the buffer were purchased from Merck (Darmstadt, Germany, analytical grade). Buffer solutions were allowed to equilibrate overnight to the measuring temperature.

Emulsions were prepared containing 1 wt% β -lactoglobulin and 40 wt% oil ($\phi = 0.4$). Either anhydrous milk fat (butter fat, min 99.8%, Friesland Madibic Food Service, The Netherlands) or blends of fully hydrogenated palm fat (Grinsted PS101, Danisco Cultor, Denmark) and sunflower oil (Reddy, Vandermoortele, The Netherlands) were used. For the determination of γ_{OW} and γ_{OA} , the sunflower oil was further purified using silica gel 60 (70 – 230 mesh, Merck, Germany) according to the method described by Smulders [19]. This procedure was performed twice. Purified sunflower oil was flushed with N_2 gas and stored at -20°C until required. For the preparation of emulsions, the sunflower oil, hydrogenated palm fat and anhydrous milk fat were not purified. A summary of relevant interfacial tensions for anhydrous milk fat and sunflower oil at the temperatures used in the experiments is given in Table 5.1. Hydrogenated palm fat/sunflower oil (HPF/SFO) blends were prepared with mass ratios HPF/SFO of 0/100, 10/90, 35/65 and 50/50. Both the fat blends and the milk fat (MF) were warmed under gentle stirring at 65°C for 1 h to melt the fat. Prior to homogenisation, the protein solution was warmed for 1 h at 65°C, the protein solution was then mixed with the fat phase and pre-homogenised at 50°C using an Ultraturrax (T 25 basic, IKA, Staufen, Germany) equipped with an 18 mm dispersing element (S25KR-18 G, IKA). The pre-emulsion was homogenised at 50°C applying 10 passes at 7 MPa using a laboratory homogeniser (homogeniser unit HU-2.0, Delta Instruments, Drachten, The Netherlands). The droplet size distribution, as determined by light scattering, was normally distributed and the emulsions had an average droplet diameter ($d_{3,2}$) of $\sim 1 \mu\text{m}$. After homogenisation, the emulsions were quickly cooled to 7°C in an ice bath. While fat crystallisation in emulsion droplets is a complex phenomenon, rapid cooling of the emulsion is known to promote the formation of tiny crystals [2,20]. Emulsions were

stored at 7°C for a minimum of 18 h before using for the spreading experiments. Prior to the experiments, emulsions were allowed to equilibrate to the measuring temperature for 1 h in a water bath. All experiments were performed in a temperature-controlled room (5, 22 or 37°C). Unless otherwise indicated, the HPF/SFO emulsions were measured at 22°C; changing the ratio HPF/SFO varied the solid fat content of these emulsions. For the MF emulsions, the temperature of the system was varied (5, 22 or 37°C) in order to change the solid fat content of these emulsions.

5.2.2 Determination of γ_{OW} and γ_{OA}

The oil/water and oil/air interfacial tensions of the systems were measured at 1-s intervals using a roughened glass Wilhelmy plate (20 × 20 × 1 mm) suspended from a force transducer (Q 11, Hottinger Baldwin Messtechnik (HBM) GmbH, Germany). Signal detection and processing was carried out using a Spider8 control panel (HBM) and operated by Spider8 control V1.3 (HBM) software. The values of γ_{OW} and γ_{OA} reported in Table 5.1 are the average of measurements made over a 30 min time period. During this time, the interfacial tension of the system was constant. For the measurement of γ_{OW} , 200 g buffer solution was poured into a glass beaker large enough to avoid meniscus effects. To ensure that the Wilhelmy plate was properly wetted by the aqueous phase, the plate was lowered until it was completely submerged. Then, 200 g of either SFO (5, 22 or 37°C) or MF (37°C) was carefully poured onto the buffer solution. This amount was sufficient to ensure that the Wilhelmy plate was completely submerged during the measurements, so as to avoid buoyancy effects. The Wilhelmy plate was then slowly raised into the oil phase, the zero point was measured and the plate was lowered into the oil/water interface, where γ_{OW} was monitored. For the measurement of γ_{OA} , in contrast to the γ_{OW} measurements, the Wilhelmy plate was wetted by the oil phase before slowly lowering the plate into the oil/air interface.

5.2.3 Determination of spreadability and spreading rate

These experiments were performed according to the method described by Schokker et al. [14]. In this method, a stainless steel cylindrical vessel (diameter, 0.39 m) was filled with 2 L of buffer solution at the appropriate

temperature. During spreading of emulsion droplets at the air/water interface, the air/water surface tension (γ_{AW}) was monitored by the Wilhelmy plate technique. For the spreadability experiments 5- μ L aliquots of 1:100 diluted emulsion ($\phi = 0.004$) were brought onto the surface by slowly lowering a pipette with a small droplet hanging from the tip to the surface of the buffer solution in the centre of the vessel. Additions were performed at 20-s intervals until a lowering of γ_{AW} was detected. For the determination of the spreading rate, Wilhelmy plates were placed at distances of 0.01, 0.03, 0.05, 0.085, 0.10, 0.15 and 0.17 m from the centre of the vessel. A 5- μ L aliquot of undiluted emulsion ($\phi = 0.4$) was brought onto the surface as described above. The time delay between sample addition and lowering of surface tension at each of the plates was measured. In these experiments measurements were taken at 0.01-s intervals.

5.2.4 Determination of Π_{AW} at spreading

The air/water surface pressure ($\Pi_{AW} = \gamma^0_{AW} - \gamma_{AW}$, where γ^0_{AW} is the surface tension of the buffer solution/air interface in the absence of surface active material) at the point of spreading was determined for 5- μ L aliquots of emulsion ($\phi = 0.4$) injected under the quiescent surface of a 0.1 wt% β -lactoglobulin solution that had been allowed to age for 5 min. The bulk concentration of the β -lactoglobulin solution was sufficient to inhibit spontaneous oil spreading under quiescent conditions [21]. In order to lower Π_{AW} and induce oil spreading, the surface was expanded at a rate of 0.12 s⁻¹. The occurrence of oil spreading during expansion showed up as a peak in the Π_{AW} vs. time curve [8]. We define this peak value as the minimum value (empirical) of Π_{AW} required to observe oil spreading for the system, henceforth referred to as Π_{AW} at spreading. A typical curve for the evolution of Π_{AW} during expansion and the effect of oil spreading on Π_{AW} of the expanding interface is given elsewhere [8].

Experiments were performed using the roller trough set-up, a detailed description of which is given by Hotrum et al. [8]. This rectangular trough, similar to a Langmuir trough, is equipped with computer-controlled cylindrical barriers instead of the more conventional sliding barrier (Figure 2.3). The main advantage of the roller trough set-up compared to a conventional Langmuir trough is that continuous and high steady-state

expansion rates can be obtained. In the work reported here, a Teflon trough with the same inner dimensions replaced the acrylic trough described previously.

5.3 Results

5.3.1a Spreading at clean air/water interfaces: spreadability

The volume (V_e) of emulsion ($\phi_e = 0.004$) required to produce a decrease in γ_{AW} for emulsion prepared with varying amounts of solid fat was measured. The results are reported in Table 5.2 together with the calculated spreadability, SA , defined as the quotient $V_{e, \text{fully liquid}}/V_e$ where $V_{e, \text{fully liquid}}$ is the V_e for the fully liquid oil emulsion (0 HPF/100 SFO or MF 37°C). The value of SA gives an indication of the relative effectiveness of the emulsion in reducing γ_{AW} .

Table 5.2: Solid fat fraction (ϕ_{sf}), volume emulsion required to produce a decrease in γ_{AW} (V_e), and relative spreadability (SA) of the emulsion samples. The calculation of SA is described in the text.

System	T (°C)	ϕ_{sf} (emulsion)	V_e (μL)	SA (-)
0 HPF/100 SFO	22	0	35 ± 6	1
10 HPF/90 SFO	22	0.1	37 ± 6	0.95
35 HPF/65 SFO	22	0.35	54 ± 6	0.65
50 HPF/50 SFO	22	0.5	83 ± 6	0.42
MF	0	0.675		
MF	5	-	77 ± 6	0.43
MF	15	0.04		
MF	22	-	33 ± 3	1
MF	37	-	33 ± 6	1

* f solid fat for HPF/SFO system determined using pulsed nuclear magnetic resonance (pNMR) analysis (NIZO food research) and for MF system from literature [24].

For the 0 HPF/100 SFO and MF 37°C emulsions ($\phi_e = 0.004$), V_e was measured to be $35 \pm 6 \mu\text{L}$ ($SA = 1$) and $33 \pm 6 \mu\text{L}$ ($SA = 1$), respectively (Table 5.2). This is in agreement with Schokker et al. [14] who reported $V_e = 80 \mu\text{L}$ for the spreading of soybean oil emulsion with $\phi_e = 0.002$. The minimum surface tension achieved for the sunflower oil systems,

$\gamma_{AW} = 60\text{mN/m}$ (Figure 5.2), is characteristic for a triglyceride oil film on water. For the milk fat systems, a slightly lower surface tension, $\gamma_{AW} = 55\text{ mN/m}$ (data not shown) was achieved. Assuming that all of the oil spreads out of the emulsion droplets at the air/water interface, we can calculate the thickness of the spread oil layer and the area available per molecule at V_e for the 0 HPF/100 SFO and MF 37°C emulsions. For the MF 37°C emulsion, at V_e , the volume of added oil is $1.32 \times 10^{-10}\text{ m}^3$. Dividing this value by the trough area yields a thickness for the oil layer of 1.1 nm. For the same system, using the values for density and molecular weight presented in Table 5.1, at V_e , 9×10^{16} molecules of oil would be present in the interface and the area available per molecule would be 1.3 nm^2 . Similarly, for the 0 HPF/100 SFO emulsion at V_e , the corresponding layer thickness and area per molecule are 1.2 nm and 1.3 nm^2 , respectively. These values are in good agreement with literature values for a closely packed monolayer of triglyceride molecules [22], which corresponds to the point where the molecules are packed densely enough to exert a surface pressure [23].

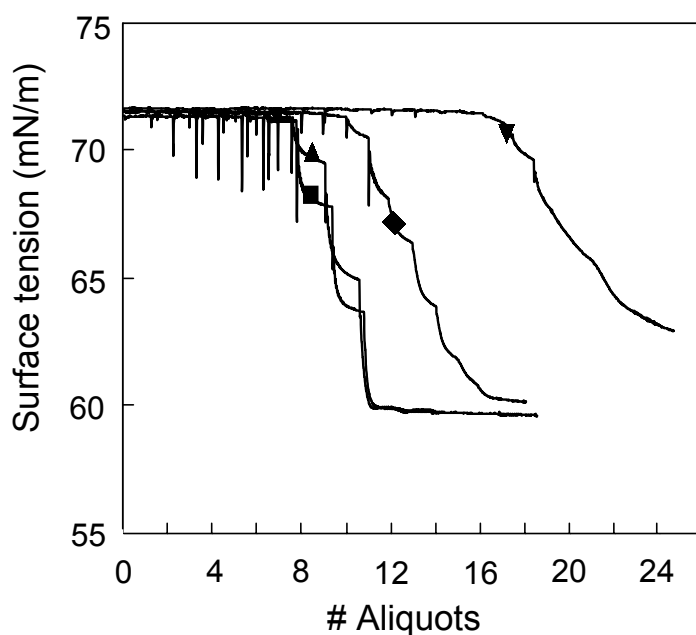


Figure 5.2: The influence of solid fat content on the number of 5- μL aliquots of emulsion ($\phi=0.004$) required to initiate a stable lowering of the surface tension of a clean air/water interface. Emulsions with mass ratios HPF/SFO of either 0/100 (▲), 10/90 (■), 35/65 (◆) or 50/50 (▼) were added at 20-s intervals.

In Figure 5.2, γ_{AW} is shown for the progressive addition of 5- μ L aliquots of emulsion ($\phi_e = 0.004$) containing HPF/SFO ratios of 0/100, 10/90, 35/65 and 50/50 to the air/water interface. It can be seen that number of aliquots added (Figure 5.2) in order to measure a decrease in surface tension, or in other words V_e increases with increasing solid fat content. The extent of this increase appears to correspond to the solid fat fraction (ϕ solid fat) of the emulsion (Table 5.2), suggesting that the spreadability of an emulsion can give a rough indication of the average ϕ solid fat in the emulsion and vice versa. Further, the spreadability results for the MF emulsions suggest ϕ solid fat = 0.57 and 0 for the MF 5°C and the MF 22°C emulsions, respectively, which seems reasonable compared to the solid fat contents reported by Walstra and van Beresteyn [24] for milk fat emulsions.

5.3.1b Spreading at clean air/water interfaces: spreading rate

The time (t) for a spreading oil front to reach a Wilhelmy plate positioned in the interface at a distance z from the origin of spreading was determined for the HPF/SFO and MF systems. The results for SFO (not emulsified) and HPF/SFO blend emulsions are given in Figure 5.3, and for MF (not emulsified) and MF emulsions in Figure 5.4. Because the solid fat content of the MF emulsions was varied by changing the temperature of the system, we measured the spreading rate of 0 HPF/100 SFO and 35 HPF/65 SFO emulsions at 5°C in addition to at 22°C as a control (Figure 5.5). The data points were fitted to a power function of the form $t = t_0 + bz^m$ (>95% confidence interval). In the fit equation, t_0 represents the time needed for the spreading oil layer to reach the first Wilhelmy plate. The values of the fit parameters are reported in Table 5.3 and the fitted functions are plotted in Figures 5.3 – 5.5. Visual comparison of the fitted curve and the data points in addition to the high R^2 values indicate that, within the experimental error, the power function fits the data well.

For the (not emulsified) SFO (22°C) and MF (37°C) oils, the exponent was found to be 1.41 ± 0.23 and 1.56 ± 0.29 , respectively (Table 5.3). Within error, these values are in agreement with the value for the exponent of 1.33 predicted from Equation (5.2) as well as with the value of the exponent determined for the spreading of soybean oil on a clean air/water surface (1.38 ± 0.15) using the same model [14]. For the emulsified oils, the values of

the exponent tended to be slightly larger than for the plain oil. This was also reported by Schokker et al. [14] for emulsified soybean oil. However, in their work as well as ours, the difference in m between bulk and emulsified oil falls within the error of the fit.

Table 5.3: Summary of the fit parameters determined by fitting the data points presented in Figures 3 - 5 to a power function of the form $t = t_0 + bz^m$ (>95% confidence interval). Residual analysis gave a random distribution.

System	T (°C)	t_0	constant, b	exponent, m	R^2
SFO only	22	-0.19 ± 0.14	23 ± 8	1.41 ± 0.23	0.99
0 HPF/100 SFO	22	0.059 ± 0.057	30 ± 14	1.82 ± 0.28	0.97
10 HPF/90 SFO	22	0.027 ± 0.098	20 ± 13	1.61 ± 0.37	0.93
35 HPF/65 SFO	22	-0.001 ± 0.105	14 ± 6	1.39 ± 0.29	0.95
50 HPF/50 SFO	22	0.008 ± 0.097	20 ± 11	1.54 ± 0.33	0.98
0 HPF/100 SFO	5	-0.066 ± 0.025	40 ± 5	1.83 ± 0.08	1
35 HPF/65 SFO	5	0.016 ± 0.081	35 ± 14	1.77 ± 0.25	0.99
MF only	37	-0.039 ± 0.098	22 ± 10	1.56 ± 0.29	0.99
MF	37	0.064 ± 0.043	60 ± 30	2.28 ± 0.30	0.99
MF	22	0.041 ± 0.052	24 ± 7	1.67 ± 0.18	0.99
MF	5	-0.075 ± 0.069	32 ± 10	1.70 ± 0.19	0.99

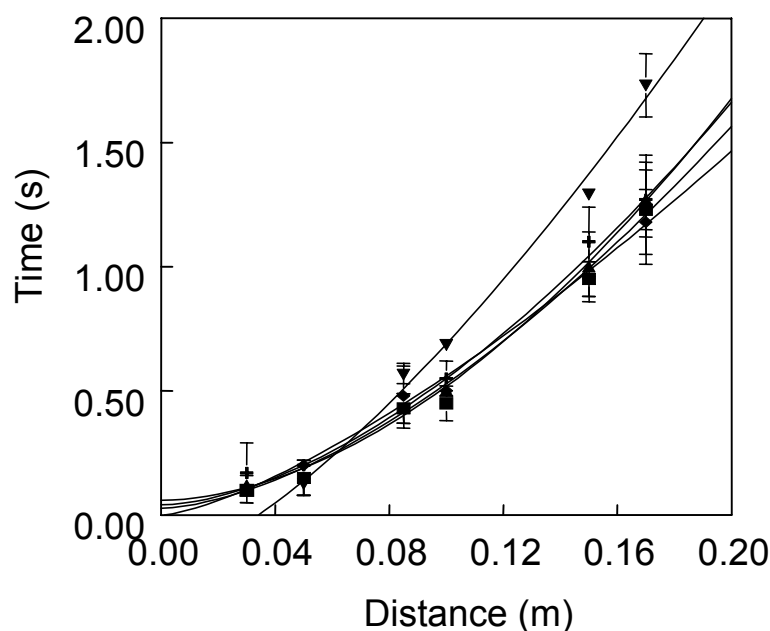


Figure 5.3: Relationship between spreading distance and time for the application of (not emulsified) SFO (\blacktriangledown) and HPF/SFO emulsion with mass ratios of either 0/100 (\blacktriangle), 10/90 (\blacksquare), 35/65 (\blacklozenge) or 50/50 (\blackplus) to a clean buffer surface. Fitted curves calculated from the fit parameters (Table 5.3) are given for each data set (solid line). All experiments performed at 22°C.

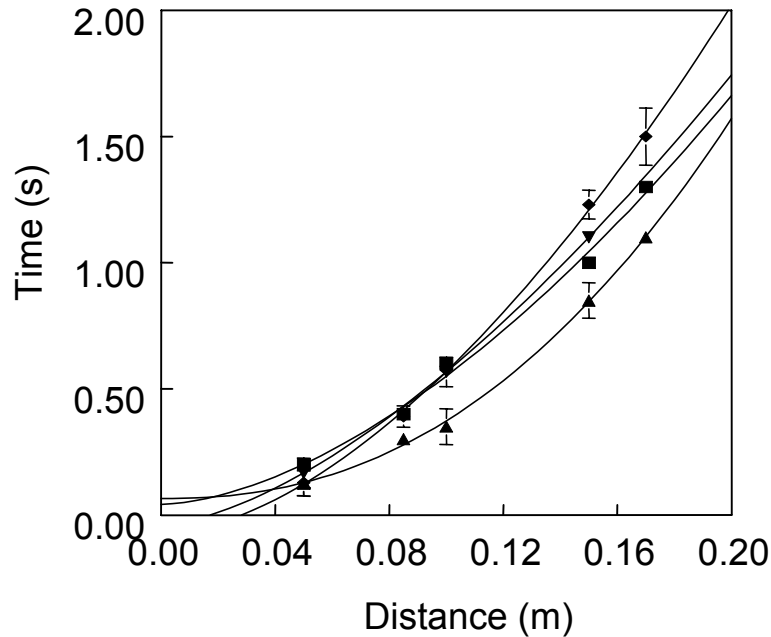


Figure 5.4: Relationship between spreading distance and time for the application of (not emulsified) MF at 37°C (▼) and MF emulsion at either 37°C (▲), 22°C (■) or 5°C (◆) on a clean buffer surface of the same temperature. Fitted curves calculated from the fit parameters (Table 5.3) are given for each data set (solid line).

The results presented in Figure 5.3 (HPF/SFO emulsions) and Table 5.3 show that the effect of solid fat content on the rate of spreading of oil out of the emulsion droplets was negligible. This also appears to be true for the MF emulsions at 5 and 22°C (Figure 5.4). The relatively large value of m for the MF 37°C emulsion is likely due to the less satisfactory fit for this system.

The temperature of the system appeared to have an effect on the spreading rate. Figures 5.4 and 5.5 show that the 5°C emulsions require more time for the oil to spread a given distance than the emulsions measured at 22°C. When spreading rate is plotted vs time (Figure 5.5, inset), the trend is clear: for the 0 HPF/100 SFO and 35 HPF/65 SFO emulsions, the spreading rate at 22°C is greater than that at 5°C over the range of times shown. The spreading rate was determined by rearranging the fitted function (Table 5.3) into an expression in terms of z :

$$z = \left(\frac{t - t_0}{b} \right)^{\frac{1}{m}} \quad (5.5)$$

of which the derivative yielded an expression for spreading rate, dz/dt :

$$\frac{dz}{dt} = \frac{1}{m} \left(\frac{t - t_0}{b} \right)^{\frac{1}{m}-1} \cdot \frac{1}{b} \quad (5.6)$$

Spreading rates were then calculated by substituting the values of the fit parameters (Table 5.3) into Equation 5.6. An explanation for the observed temperature dependence of the spreading rate is given in the discussion.

5.3.2 Spreading in the presence of an adsorbed protein layer: Π_{AW} at spreading

In Table 5.1, γ_{OW} and γ_{OA} are given for SFO and MF. The MF was measured at 37°C, at which temperature the oil was liquid. It was not possible to measure γ_{OW} and γ_{OA} for MF at 22 or 5°C since milk fat was solid at these temperatures. For MF at 37°C, γ_{OW} was found to decrease slowly in time, indicating the gradual adsorption of surface active material, probably in the form of phospholipids, mono- and diglycerides, which are known to make up ~ 1 wt% of milk fat [2]. However, we do not expect this to have a significant influence on the value of Π_{AW} at spreading since, due to the dynamic nature of the spreading process, the values for γ_{OW} and γ_{OA} will be closer to the values measured for the pure interface. Previously, we have observed that the value of Π_{AW} at spreading is in line with this assumption [8]. Further, since both MF and SFO are composed of a mixture of triglycerides, for the calculation of the predicted Π_{AW} for $S > 0$ (Table 5.4), we will assume that the γ_{OW} and γ_{OA} values measured for the pure SFO interfaces can serve as reasonable approximations of the γ_{OW} and γ_{OA} expected for the pure MF interfaces.

Temperature has a significant effect on interfacial tension. The decrease in γ_{AW}^0 of the buffer solution with increasing temperature (Table 5.1), can be attributed to the temperature dependence of γ_{AW} for pure water [25]. For γ_{OW} at the sunflower oil/water interface, the interfacial tension was found to increase with increasing temperature indicating a negative excess entropy of this interface. This temperature dependence of γ_{OW} has also been reported in the literature. Krog [26] and Gaonkar [27] reported a similar increase in γ_{OW} with increasing temperature for sunflower oil/water and soybean oil/water interfaces, respectively. Finally, γ_{OA} was found to decrease with increasing

temperature. This trend has also been reported in the literature for γ_{OA} of pure triglycerides [28] and a variety of vegetable oils [29]. Due to the temperature dependence of γ_{OA} and γ_{OW} , the minimum value of γ_{AW} required for spreading based on Equation (5.1) is shifted to slightly higher γ_{AW} values with increasing temperature. However, the predicted values of Π_{AW} at spreading (Table 5.4), where $\Pi_{AW} = \gamma_{AW}^0 - \gamma_{AW}$, are additionally influenced by the temperature dependence of γ_{AW}^0 .

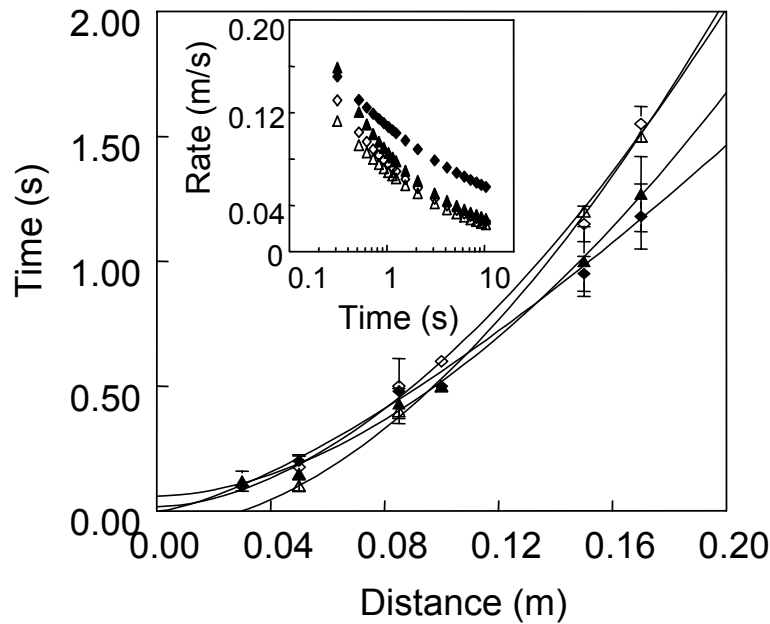


Figure 5.5: Relationship between spreading distance and time for the application of HPF/SFO with mass ratios of either 0/100 (\blacktriangle) and 35/65 (\blacklozenge) to a clean buffer surface at 22°C (closed symbols) and at 5°C (open symbols). Fitted curves calculated from the fit parameters (Table 5.3) are given for each data set (solid line). **Inset:** spreading rate vs. time for the same system as above. Although the error in the calculated spreading rate values was large (not shown), the trend is clear. Calculation of spreading rate is described in the text.

Measured values of Π_{AW} at spreading for the HPF/SFO blend and MF emulsions are reported in Table 5.4. The experimental value for the 0 HPF/100 SFO 22°C emulsion is in agreement with our previous results for the entering and spreading of emulsion droplets at the air/water interface [8,21] and with the predicted value of Π_{AW} required for spreading. Further, comparison of the results reported in Table 5.4 for the other HPF/SFO blends measured at 22°C suggests that there is no significant effect of crystalline fat

on the value of Π_{AW} at spreading. For the MF 22°C emulsion, Π_{AW} at spreading is also in reasonable agreement with the predicted value, supporting that it was a reasonable assumption to use the values of γ_{OA} and γ_{OW} for sunflower oil in the calculation of Π_{AW} required for $S > 0$ (Table 5.4).

Table 5.4: Predicted and measured values for Π_{AW} at spreading. The predicted Π_{AW} at spreading for each of the measuring temperatures (5, 22 and 37°C) was calculated by substituting γ_{OW} and γ_{OA} of sunflower oil and γ^0_{AW} of the buffer solution (Table 5.1) into Equation (5.1). Experiments were performed at the temperature indicated. For the predicted Π_{AW} values, an error of 0.3 mN/m applies.

System	T (°C)	Π_{AW} for $S = 0$ predicted (mN/m)	Π_{AW} at spreading measured (mN/m)
0 HPF/100 SFO	5	17.1	17.0* \pm 0.8
0 HPF/100 SFO	22	14.6	14.1 \pm 1.0
0 HPF/100 SFO	37	12.5	15.9 \pm 1.0
10 HPF/90 SFO	22	14.6	15.2 \pm 0.3
35 HPF/65 SFO	22	14.6	15.4 \pm 0.2
50 HPF/50 SFO	22	14.6	13.7 \pm 1.1
MF	5	17.1	17.2* \pm 0.3
MF	22	14.6	16.6 \pm 1.0
MF	37	12.5	16.3 \pm 0.5

* spontaneous spreading

The measured values of Π_{AW} at spreading for the MF 37°C and 0 HPF/100 SFO 37°C emulsions of 16.3 \pm 0.5 mN/m and 15.9 \pm 1 mN/m, respectively, are significantly higher than the predicted value of 12.5 mN/m. The reason for this discrepancy is not entirely understood; one possibility is that the assumption that γ_{OW} and γ_{OA} are equal to that of the pure surfaces is no longer valid at this temperature. The oils used for emulsion preparation contained impurities in the form of mono- and diglycerides (and phospholipids in the case of milk fat), which display temperature dependent surface behaviour. This will primarily affect γ_{OW} .

For the HPF/SFO blend and MF emulsions at 5°C, the emulsion spread spontaneously, meaning no expansion of the interface was required. The calculated and measured values of Π_{AW} at spreading for 5°C are in agreement with one another (Table 5.4). Thus, for the 5°C systems, the predicted

temperature dependence of Π_{AW} for $S > 0$ calculated based on γ_{OW} and γ_{OA} for SFO appears to hold for both the SFO and MF systems: if this were not the case, spontaneous spreading would not be observed.

5.4 Discussion

5.4.1a Spreading at clean air/water interfaces: spreadability

Liquid oil was observed to spread out of the emulsion droplets, unimpeded by the presence of a fat crystal network within the droplets (Table 5.2). Based on Equations (5.3) and (5.4), we can estimate the pore radius, r , between fat crystals in a fat crystal network required for the pressure balance $2\gamma_{OA}\cos\theta/r = S/d$. For smaller r , we expect the capillarity of the fat crystal network to be strong enough to withstand the spreading pressure.

For the calculation, we will assume that the contact angle, θ , between the liquid oil and the fat crystal is zero and that γ_{OA} is equal to 28 mN/m. Further, for a clean air/water interface at 22°C, $S = 14.6$ mN/m for the sunflower oil system. Assuming that this pressure acts over the thickness of a triglyceride monolayer of ~ 1 nm (Results, section 5.3.1a), we obtain $S/d = 1.46 \times 10^7$ Pa. Substituting these values into Equations (5.3) and (5.4) yields $r = 4$ nm, implying that ΔP_c will only exceed S/d when the radius of all pores between the fat crystals is less than 4 nm. This is very small, and we can expect that under most conditions, the fat crystal network in the emulsion droplet [20,30,31] will be such that at least a few, if not most, pores are larger than 4 nm. Therefore, it is reasonable to assume that the capillarity of the fat crystal network cannot prevent oil spreading. This finding is contrary to the hypothesis presented in literature that one of the stability mechanisms of whipped cream [1,3] is impeded oil spreading at the air bubble surface due to the presence of a fat crystal network. Possibly, in natural whipped cream, where the fat crystals can form a very finely distributed, densely packed structure under certain temperature treatments [20,30], the permeability of the fat crystal network may be low enough to contribute to reduced oil spreading; but even then, the complete absence of pores with a radius greater than 4 nm seems unlikely. Moreover, if the contact angle is not zero, which may well occur, the capillary pressure is even smaller.

5.4.1b Spreading at clean air/water interfaces: spreading rate

The presence of crystalline fat had no significant influence on the rate of oil spreading out of emulsion droplets for either the HPF/SFO or MF emulsions (Figures 5.3 and 5.4, Table 5.3). This implies that for the systems containing crystalline fat, the release of oil from the fat crystal network is not the rate-determining step for oil spreading.

The temperature of the system, however did appear to have an effect on the spreading rate (Figure 5.3, inset). For the 0 HPF/100 SFO emulsions, the spreading rate at 22°C was greater than that at 5°C over the range of times shown. This is in agreement with the spreading theory presented in Equation (5.2), which predicts that the spreading rate of oil on a clean water surface is dependent on the viscosity and density of the underlying liquid, in this case water. In particular, the viscosity of water is temperature dependent and as a result, we would expect approximately a 10% decrease in spreading rate due to the decrease in the viscosity of water with a lowering in temperature from 22 to 5°C. The differences in spreading rate (Figure 5.5, inset) appear to be equal to or greater than 10%.

It was mentioned earlier that in the case of aerated emulsions, adsorbed proteins are expected to be present at the air bubble surface [9], and in this sense it would have been desirable to measure the spreading rate of oil in the presence of an adsorbed protein layer. However, Equation (5.2) does not account for the influence of an adsorbed protein layer on the rate of oil spreading. Prins [16] suggested that adsorbed proteins may be able to reduce the rate of oil spreading to an extent related to the surface elastic modulus of the protein film, but a model describing the spreading rate of oil in the presence of an adsorbed protein layer has not yet been developed. In addition, the applied method is not suitable for detecting oil spreading at a protein-covered air/water interface as the technique cannot distinguish between oil spreading itself and the resulting compression of the protein layer. Moreover, fracture of the adsorbed protein layer results in an inhomogeneous spreading pattern [17]; the current method is only valid when oil spreads homogeneously in a radial pattern over the surface.

5.4.2. Spreading in the presence of an adsorbed protein layer: Π_{AW} at spreading

It appears that the presence of crystalline fat had a negligible effect on the value of Π_{AW} at spreading. This makes sense: the value of S , Equation (5.1), is based on the balance of interfacial tensions of the liquid phases, and is therefore independent of the presence of a solid phase.

The interfacial tensions of the liquid phases are however temperature dependent, leading to an increase in the predicted value of Π_{AW} for $S > 0$ with decreasing temperature (Table 5.4). This resulted in spreading under quiescent conditions for the MF 5°C system. The spontaneous spreading at 5°C is not a result of the presence of solid fat in the emulsion: the fully liquid 0 HPF/100 SFO emulsion also displayed spontaneous spreading at this temperature. Instead, the occurrence of spontaneous spreading is most likely the result of the temperature dependence of Π_{AW} of the bulk 0.1% β -lactoglobulin solutions. At 22 and 37°C the solutions give $\Pi_{AW} = 19$ and 20 mN/m, respectively, after a 5 min equilibration period. But at 5°C, Π_{AW} is only 17 mN/m after 5 min, under which conditions $S > 0$ (Table 5.4). The observation of spontaneous oil spreading for the 5°C emulsions supports this.

It appears that compared to at 22 or 37°C, the surface activity of the protein at 5°C is reduced. This is in qualitative agreement with Suttiprasit and McGuire [32] who observed that at 2°C, the adsorption of β -lactoglobulin to a hydrophobic silicon surface yielded lower adsorbed amounts than when the experiment was performed at 27 or 52°C. Determination of the cause for the decrease in Π_{AW} with decreasing temperature is beyond the scope of this paper, however a possible explanation may be that at low temperature proteins have less of a tendency to unfold than at higher temperatures. This would lead to lower surface pressures for the same adsorbed amount.

The lower Π_{AW} of the adsorbed protein layer observed for β -lactoglobulin at 5°C appears to facilitate oil droplet entering and spreading. We would expect the dynamic surface pressure of the β -lactoglobulin solutions to be similarly influenced by temperature. This may be of practical relevance to the whipping of cream, and suggests that the need for low temperature during whipping may be two-fold. First, to ensure the presence of crystalline fat, which provides structure to the final product and second, to facilitate entering and spreading of emulsion droplets, which would promote interaction

between emulsion droplets at the air/water interface leading to (faster) formation of a partially coalesced network.

5.5 Concluding Remarks

The importance of the presence of crystalline fat to the development of firmness and structure in aerated emulsions such as whipped cream is well established [1-5]. However, there is a lack of understanding of the role played by crystalline fat in the air bubble stability during whipping. Some authors have suggested that a fat crystal network within the emulsion droplets may contribute to air bubble stability by reducing the spreading of liquid oil out of the emulsion [1,3]. In this paper, we have made an attempt to test this hypothesis. To this end, we have investigated the influence of the presence of crystalline fat in the emulsion on the spreading behaviour of oil at the planar air/water interface.

For the systems studied in this paper, the presence of crystalline fat did not change the spreading rate of oil out of emulsion droplets onto a clean air/water interface. Further, the decreased spreadability of emulsions containing crystalline fat could be fully accounted for by the increased ϕ solid fat content of the emulsions. Moreover, rough calculations indicate that, with the exception of extremely the case of finely distributed fat crystals, the capillary pressure of a crystalline fat network would not be expected to be sufficient to counteract the spreading pressure that exists at a clean air/water interface. Finally, in the case where protein was present at the air/water interface, the presence of crystalline fat did not influence the value of Π_{AW} at spreading. Based on the above findings, we do not expect that the presence of a fat crystal network is the main parameter controlling oil spreading out of emulsion droplets at the air/water interface during the preparation of aerated emulsions such as whipped cream.

The temperature dependence of protein adsorption at the air/water interface, however, may be important for droplet entering and spreading. After a 5 min equilibration time, at 5°C, the Π_{AW} of a 0.1% β -lactoglobulin solution was lower than the Π_{AW} for the same solution at 22 or 37°C, which resulted in spontaneous spreading for the 5°C systems. In relation to the aeration of emulsions by whipping, this implies a reduction in the minimum expansion rate required for the entering and spreading of emulsion droplets at the air/water interface, which may facilitate the whipping process. In terms

of reducing spreading of oil at the air/water interface, it is more likely that adsorbed protein, rather than the presence of crystalline fat, plays a central role. However, in order to confirm this, further investigation into the spreadability and spreading rate of oil droplets at protein-covered air/water interfaces is required.

Acknowledgements

The authors thank Franklin Zoet for performing experiments, and the Laboratory for Microbiology, Wageningen University for the use of their 37°C facility. Further, Friesland Madibic Food Service, The Netherlands and Danisco Ingredients, Denmark are gratefully acknowledged for providing the anhydrous milk fat and the fully hydrogenated palm fat, respectively.

References

- [1] Darling, D. F. (1982). Recent advances in the destabilization of dairy emulsions. *Journal of Dairy Research*, 49, 695-712.
- [2] Mulder, H. and Walstra, P. (1974). *The Milk Fat Globule*. Wageningen: Pudoc.
- [3] Brooker, B. E. (1993). Stabilisation of air in foods containing fat - a review. *Food Structure*, 12, 115-122.
- [4] Kalab, M. (1985). Microstructure of dairy foods. 2. Milk products based on fat. *Journal of Dairy Science*, 68, 3234-3248.
- [5] Schmidt, D. G. and van Hooydonk, A. C. M. (1980). A scanning electron microscopical investigation of the whipping of cream. *Scanning Electron Microscopy*, III, 653-658.
- [6] Prins, A. (1986). Some physical aspects of aerated milk products. *Netherlands Milk and Dairy Journal*, 40, 203-215.
- [7] Harkins, W. D. and Feldman, A. (1922). Films. The spreading of liquids and the spreading coefficient. *The Journal of the American Chemical Society*, 44(12), 2665-2685.
- [8] Hotrum, N. E., van Vliet, T., Cohen Stuart, M. A. and van Aken, G. A. (2002). Monitoring entering and spreading of emulsion droplets at an expanding air/water interface: a novel technique. *Journal of Colloid and Interface Science*, 247(1), 125-131.
- [9] Brooker, B. E., Anderson, M. and Andrews, A. T. (1986). The development of structure in whipped cream. *Food Microstructure*, 5, 277-285.
- [10] Smith, A. K., Kakuda, Y. and Goff, H. D. (2000). Changes in protein and fat structure in whipped cream caused by heat treatment and addition of stabilizer to the cream. *Food Research International*, 33, 697-706.
- [11] Heslot, F., Cazabat, A. M., Fraysse, N. and Levinson, P. (1992). Experiments on spreading droplets and thin films. *Advances in Colloid and Interface Science*, 39, 129-145.
- [12] Joos, P. and Pintens, J. (1977). Spreading kinetics of liquids on liquids. *Journal of Colloid and Interface Science*, 60(3), 507-513.
- [13] Lucassen, J. (1968). *Trans. Faraday Soc.*, 64, 2221.
- [14] Schokker, E. P., Bos, M. A., Kuijpers, A. J., Wijnen, M. E. and Walstra, P. (2003). Spreading of oil from protein stabilized emulsions at air/water interfaces. *Colloids and Surfaces B: Biointerfaces*, 26(4), 315-327.
- [15] Bisperink, C. G. J. (1997). *The influence of spreading particles on the stability of thin liquid films*. Thesis: Wageningen Agricultural University, The Netherlands.
- [16] Prins, A. (1989). Foam stability as affected by the presence of small spreading particles. *New York*.

- [17] Hotrum, N. E., Cohen Stuart, M. A., van Vliet, T. and van Aken, G. A. (2003). Flow and fracture phenomena in adsorbed protein layers at the air/water interface in connection with spreading oil droplets. *Langmuir*, 19, 10210-10216.
- [18] de Jongh, H. H. J., Gröneveld, T. and de Groot, J. (2001). Mild isolation procedure discloses new protein structural properties of β -lactoglobulin. *Journal of Dairy Science*, 84, 562-571.
- [19] Smulders, P. E. A. (2000). *Formation and stability of emulsions made with proteins and peptides*. Thesis: Wageningen University.
- [20] Precht, D. (1988). Fat crystal structure in cream and butter. In N. Garti and K. Sato, *Crystallization and polymorphism of fats and fatty acids* (pp. 305-361). New York: Marcel Dekker.
- [21] Hotrum, N. E., Cohen Stuart, M. A., van Vliet, T. and van Aken, G. A. (2003). Entering and Spreading of Protein Stabilised Emulsion Droplets at the Expanding Air/Water Interface. In E. Dickinson and T. van Vliet, *Food Colloids, Biopolymers and Materials* Cambridge: Royal Society of Chemistry.
- [22] Harkins, W. D. (1952). *Physical Chemistry of Surface Films*. New York: Reinhold Publishing Corporation.
- [23] Adamson, A. W. and Gast, A. P. (1997). *Physical Chemistry of Surfaces*. New York: John Wiley and Sons.
- [24] Walstra, P. and van Beresteyn, E. C. H. (1975). Crystallization of milk fat in the emulsified state. *Netherlands Milk and Dairy Journal*, 29, 35-65.
- [25] *CRC Handbook of Chemistry and Physics*. (2003) Boca Raton: CRC Press LLC.
- [26] Krog, N. J. (1991). Thermodynamics of interfacial films. In M. El-Nokaly and D. Cornell, *Microemulsions and emulsions in foods* (pp. 138-145).
- [27] Gaonkar, A. G. (1992). Effects of salt, temperature and surfactants on the interfacial tension behavior of a vegetable oil/water system. *Journal of Colloid and Interface Science*, 149(1), 256-260.
- [28] Chumpitaz, L. D. A., Coutinho, L. F. and Meirelles, A. J. A. (1999). Surface tension of fatty acids and triglycerides. *Journal of the American Oil Chemists' Society*, 76(3), 379-382.
- [29] Flingoh, Oh, C. H. and Let, C. C. (1992). Surface tensions of palm oil, palm olein and palm stearin. *Elaeis*, 4(1), 27-31.
- [30] Walstra, P. (1967). On the crystallization habit in fat globules. *Netherlands Milk and Dairy Journal*, 21, 166-191.
- [31] Lopez, C., Bourgaux, C., Lesieur, P., Bernadou, S., Keller, G. and Ollivon, M. (2002). Thermal and structural behaviour of milk fat 3. Influence of cooling rate and droplet size on cream crystallization. *Journal of Colloid and Interface Science*, 254, 64-78.
- [32] Suttiprasit, P. and McGuire, J. (1992). The surface activity of α -lactalbumin, β -lactoglobulin and bovine serum albumin. II. Some molecular influences on adsorption to hydrophilic and hydrophobic silicon surfaces. *Journal of Colloid and Interface Science*, 154(2), 327-336.
- [33] Walstra, P. (2003). *Physical Chemistry of Foods*. New York: Marcel Dekker.
- [34] Kloek, W. (1998). *Mechanical properties of fats in relation to their crystallization*. Thesis: Wageningen Agricultural University, The Netherlands.

Chapter 6:

Elucidating the relationship between the spreading coefficient, surface-mediated partial coalescence and the whipping time of cream

Abstract

The influence of whisk rotational speed, protein concentration, protein type and the presence of low molecular weight surfactant on the whipping time of emulsions was investigated. Increasing the rotational speed, decreasing the protein concentration or adding emulsifier all resulted in shorter whipping times. Further, creams stabilised by WPI had shorter whipping times than creams stabilised by sodium caseinate. The influence of whisk rotational speed, protein concentration, protein type and the presence of low molecular weight surfactant on the whipping time of recombined cream can be explained in terms of a model predicting how these variables promote fat droplet adsorption and spreading at the air bubble surface during whipping. This model is fundamentally different from earlier models that attempted to describe the influence of the variables investigated on the whipping behaviour of cream in terms of their influence on the static properties of the adsorbed layer at the fat droplet surface as such.

6.1 Introduction

The air bubbles in whipped cream are stabilised by adsorbed fat globules that are connected via a network of partially coalesced fat globules [1-8]. Partial coalescence is the state of fused fat droplets that are kept from complete merging into a single spherical shape by the presence of crystalline fat present within the fat droplet [9]. In general, the outline of the original individual droplets is maintained. In a study on the whipping of emulsions, van Aken [8] distinguished three stages in the whipping process which, depending on the time to reach the endpoint of whipping, either appear as distinct phases or may overlap to some extent. In the first stage, large air bubbles are introduced and broken up into smaller ones by the whipping action of the whisks. This initial foam is predominantly stabilised by protein [1,2]. The second stage is characterised by gradual accumulation of fat droplets on the surface of the air bubbles. This process has been well characterised; a number of electron microscopy studies clearly show fat droplets adhered to the air bubble surface [2,5,7,10]. Finally, in the third stage, a partially coalesced network of fat droplets is built up which acts to trap the air bubbles, retain the serum phase and give stiffness to the whipped cream. At the maximum stiffness, the endpoint of whipping has been reached, further whipping leads to the formation of butter granules and foam collapse.

The second stage of whipping is particularly interesting as during this stage air bubbles are in a constant state of formation, break-up and coalescence. Due to the dynamic nature of the air bubble interface, during this stage, fat droplets can attach and release some liquid fat, which spreads onto the bubble surface. The close proximity of adhered droplets leads to interfacial fat globule flocculation and aggregation [3,6], which we will refer to as surface-mediated partial coalescence. It should be mentioned that air is not essential for partial coalescence to occur; shear-induced partial coalescence, which is the result of sticking of emulsion droplets when they collide as a result of convection is also possible [9,11]. For example, cream can be churned into butter in the absence of air [6,12], however, churning proceeds much faster in the presence of air [6]. A schematic representation of both surface-mediated and shear-induced partial coalescence is given in Figure 6.1. Although shear-induced partial coalescence will undoubtedly also occur during the whipping of cream, it seems likely that during the second stage of whipping, when air bubbles are being created and destroyed, surface-

mediated partial coalescence will dominate. If this is the case, then the air bubble surface can be viewed as the primary location for droplet interaction leading to partial coalescence, and ultimately the build-up of foam structure. The entering and spreading of droplets in the air-water surface is the critical first step in this surface-mediated process.

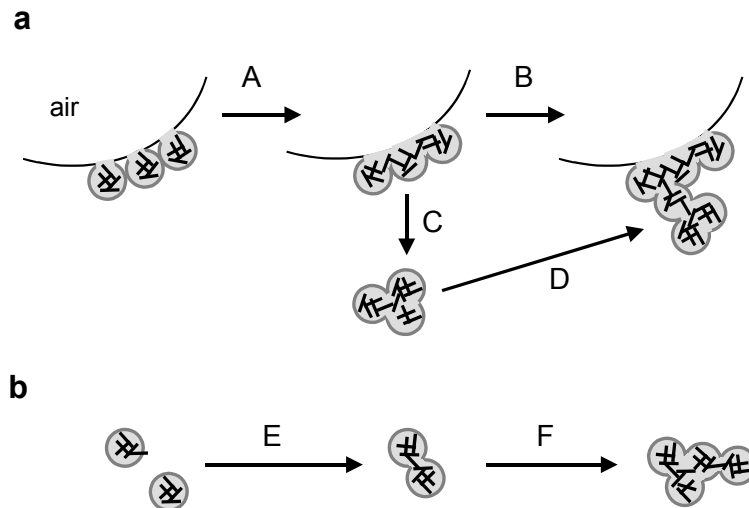


Figure 6.1 Schematic depiction of two possible mechanisms for partial coalescence. In the surface-mediated mechanism (a), air bubbles play an important role. When $S > 0$ (Equation (6.1)) fat droplets can attach to the protein-covered air bubble surface and interfacial flocculation takes place; partial coalescence (A) of the interfacial flocs ensues. If, at this point, the bubble bursts (C), a partially coalesced fat clump remains. If the air bubble remains stable (B), a fat clump from the bulk may partially coalesce with the adsorbed fat clump (D). The shear-induced mechanism for partial coalescence (b) is independent of the presence of air. Partial coalescence (E) occurs when two droplets collide and the fat crystals in the droplets pierce the film between them. Larger fat clumps can form (F) when small clumps collide and partially coalesce with other clumps or free droplets.

Whether or not oil spreading will occur is dependent on the balance of surface tensions (γ) at the three-phase boundary between the oil (O), water (W) and air (A) interfaces [13,14]. This balance of forces is described by the spreading coefficient, S :

$$S = \gamma_{AW} - (\gamma_{OW} + \gamma_{OA}) \quad (6.1)$$

When S is positive, oil spreads. A triglyceride oil with medium to long chain fatty acids, such as soybean, sunflower, or liquid butter oil, can spread at the clean air/water interface since $S > 0$ for such an oil [14-16]. Oil spreading can be inhibited if γ_{AW} becomes so low that the condition $\gamma_{AW} > \gamma_{OW} + \gamma_{OA}$ is no longer satisfied. This can occur due to the presence of an adsorbed protein layer [14], which may influence the adhesion of fat droplets to the air bubble surface during the whipping of cream since, in whipped cream, the initial air bubble surfaces [1,2] are stabilised by adsorbed protein. However, because whipping is a dynamic process, likely the surface tension of the air bubbles is also dynamic, meaning that for protein-stabilised air bubbles, S can become positive due to an increase in γ_{AW} resulting from local surface expansion of the air bubbles. The presence of adsorbed proteins at the bubble surface can serve to limit the amount of oil spreading out of the fat droplets. In earlier work [3,17] it was suggested that the fat crystal network present in the emulsion droplets would help to limit the spreading of liquid oil out of emulsion droplets adhered to the air bubble surface. However, recently, Hotrum et al. [16] have shown that the capillary pressure present in a fat crystal network would not, under most circumstances, be sufficient to withstand the spreading pressure exerted on a fat droplet resting in the air/water interface.

In previous papers we have reported investigations on emulsion droplet spreading at the expanding planar air/water interface [14,18,19]. A summary of the findings most relevant to the whipping of cream is given in Figures 6.2 and 6.3. The data is presented in terms of air/water surface pressure, $\Pi_{AW} = \gamma_{AW}^0 - \gamma_{AW}$, where $\gamma_{AW}^0 = 72$ mN/m is the surface tension of the clean air/water interface at 22 °C.

Figure 6.2 gives the steady state surface pressures, Π_{SS} , that were measured at the air/solution interface when this is subjected to various relative expansion rates for sodium caseinate or whey protein isolate (WPI) solutions. Π_{SS} is observed to decrease with increasing expansion rate and decreasing protein concentration. Further, lower Π_{SS} values during expansion are achieved with WPI than with sodium caseinate for all expansion rates at a given concentration; this is due to the higher surface activity of sodium caseinate compared to WPI [14].

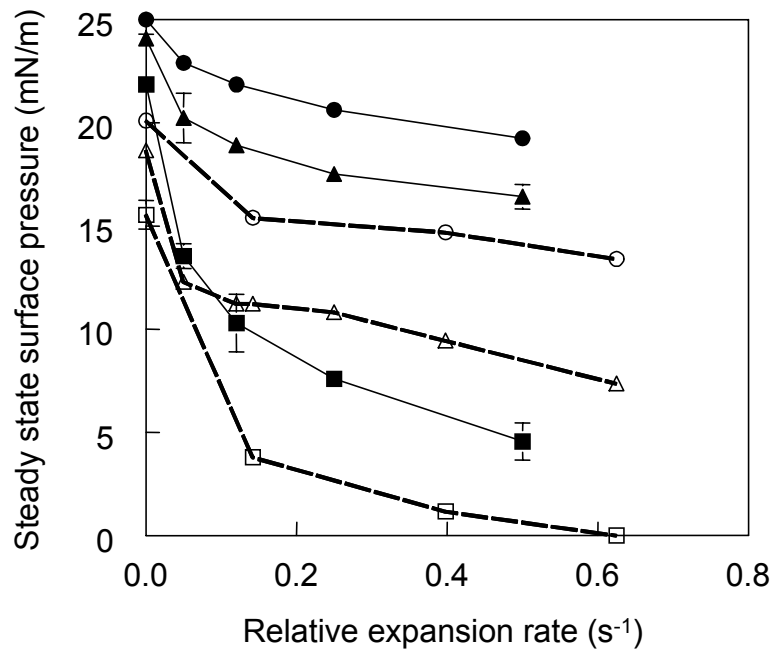


Figure 6.2 Steady state surface pressure vs. relative expansion rate; sodium caseinate (closed symbols), WPI (open symbols) ■ 0.01 wt%, ▲ 0.1 wt% and ● 1 wt%, respectively.

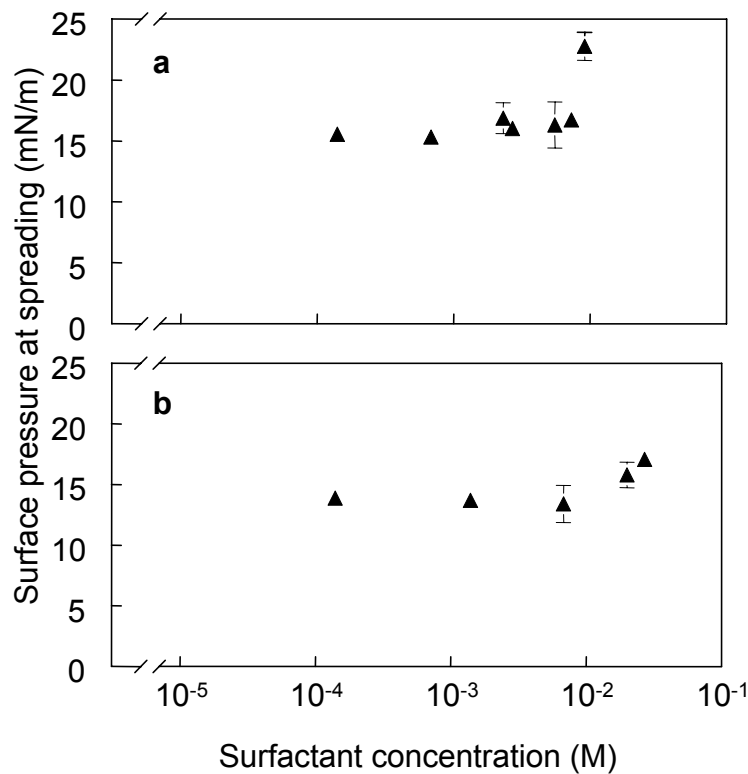


Figure 6.3 Surface pressure at spreading vs. surfactant concentration for β -lactoglobulin-stabilised emulsions containing (a) added Tween 20 (concentration in the aqueous phase) or (b) added Span 80 (concentration in the oil phase).

The spreading behaviour of protein-stabilised sunflower oil emulsions was investigated for sodium caseinate and WPI solutions at the same concentrations and expansion rates as those reported in Figure 6.2. In these experiments, it was observed that oil droplet spreading occurred at protein concentrations and expansion rates that yielded $\Pi_{SS} \leq 15$ mN/m [14,18]. Oil droplet spreading was never observed for these systems when $\Pi_{SS} > 15$ mN/m. Thus, for the sunflower oil system the value of 15 mN/m represents a critical surface pressure, Π_{cr} , below which spreading can occur. Using known values for γ_{OW} and γ_{OA} one can easily show that Π_{cr} is precisely the value satisfying the condition $S = 0$. Moreover, for protein-stabilised emulsions, the value of Π_{cr} implies $\gamma_{OW} = \gamma'_{OW}$ during spreading. The data in Figure 6.2 indicate that a minimum expansion rate is required in order to reach Π_{cr} for a given protein type and concentration. The relatively high value of $\Pi_{cr} \sim 15$ mN/m indicates that the air/water interface does not need to be completely void of adsorbed protein for spreading to occur.

Further, Hotrum et al. [19] have shown that low molecular weight surfactants, or emulsifiers, are able to shift Π_{cr} to higher values due to their ability to lower γ_{OW} at the expanding oil/water interface during oil spreading, thus shifting the balance of forces in Equation (6.1). This facilitates oil droplet spreading since for higher Π_{cr} less rigorous surface expansion conditions will be required to reach the critical surface pressure. Figure 6.3 shows that for sunflower oil emulsion droplets stabilised by β -lactoglobulin the Π_{cr} required for spreading increases with increasing concentrations of either Tween 20 (Figure 6.3a) or Span 80 (Figure 6.3b), reaching 22 mN/m in the case of added Tween 20 and 17 mN/m in the case of Span 80.

In this paper, we aim to investigate the influence of whipping speed, protein type, protein concentration and the presence of low molecular weight (lmw) surfactants on the duration of the whipping process in order to elucidate the role of the spreading behaviour of emulsion droplets at the air/water interface in the whipping process. The trends in the whipping results will be discussed in terms of our previous findings regarding the influence of these same parameters on the spreading behaviour of emulsion droplets at the planar air/water interface that are presented in Figures 6.2 and 6.3.

6.2 Materials and Methods

6.2.1 Materials

Whey protein isolate, WPI, (BiPRO, Lot no. JE 052-9-420, Davisco Foods International, Le Sueur, MN 56058) and sodium caseinate (Sodium caseinate S, DMV International, Veghel, The Netherlands) were used in the preparation of protein solutions and emulsions. WPI and caseinate powders contained 95% and 86% protein, respectively (Biuret standard assay, in agreement with manufacturer's specifications). Proteins were dissolved in 20 mM imidazole buffer (pH 6.7) containing 0.1 M NaCl by stirring for 1 h at room temperature. The chemicals used for the buffers were purchased from Merck (Darmstadt, Germany, analytical grade). For the investigation into the influence of lmw surfactant on the whipping properties of cream, either water-soluble Tween 20 (polyoxyethylene sorbitan monolaurate, Merck), or oil-soluble Span 80 (sorbitan monooleate, Fluka, Switzerland) was used.

6.2.2 Emulsion preparation

Emulsions were prepared containing 40 wt% fat and 1 wt% protein. The fat phase consisted of a blend of 35 wt% fully hydrogenated palm fat (Grinsted PS101, Danisco Cultor, Denmark) and 65 wt% sunflower oil (Reddy, Vandermoortele, Roosendaal, the Netherlands). The fat blend was warmed under gentle stirring at 65°C for 1 h to melt the fat. Prepared protein solutions were warmed to 65°C, prior to mixing with the fat phase. The mixture was then pre-homogenised at 65°C using an Ultraturrax (IKA, Staufen, Germany). Finally, the emulsions were prepared by homogenisation at 2 MPa in a Rannie laboratory homogeniser, warmed at 65°C, for 10 passes of the pump. After homogenisation, emulsions were rapidly cooled in an ice bath to 7°C. Emulsions were stored overnight at 7°C before performing the experiments. The emulsions had an average droplet diameter ($d_{3,2}$) of $\sim 1 \mu\text{m}$ as determined by light scattering using a Coulter Laser LS230 (Coulter Electronics, Mijdrecht, The Netherlands). For emulsions with added Span 80, the required amount of surfactant was dissolved in the fat blend during warming. In the case of added Tween 20, an emulsion with a slightly higher fat and protein content was prepared. After homogenisation and initial cooling, this emulsion was diluted with Tween 20 dissolved in buffer to give the desired concentration, followed by gentle mixing.

6.2.3 Whipping of emulsions

Emulsions were whipped at 7°C in an automated whipping apparatus (Ledoux b.v., Dodewaard, The Netherlands). The same instrument was also used by van Aken [8] in a study on the aeration of natural whipped cream. A 250-mL emulsion sample was gently poured into a stainless steel or glass beaker (diameter, 9.6 cm) which was placed inside the thermostat jacket of the whipping apparatus, allowing the temperature to be controlled within 0.5°C during whipping. The whipping action was provided by two whisks (radius, 20 mm; length, 113 mm, composed of six, 1 mm stainless steel wires) rotating in a planetary motion pattern, designed to maximise the incorporation of air and to maintain homogeneous whipping conditions over the entire volume. The electrical current required to maintain a constant rotational speed was monitored during the whipping process. This current is a measure of the energy dissipation in the system and is characteristic of its mechanical properties. At the endpoint of whipping, the whipped emulsion reaches a maximum stiffness, which is registered as a peak in the electrical current signal. We define this peak as the endpoint of whipping and refer to the time to reach this peak as the whipping time. Unless otherwise stated, all experiments were performed using a rotational speed of 584 rpm.

6.3 Results

In Figure 6.4, the power transferred by the whisks is plotted as a function of time for various whipping speeds applied to WPI-stabilised model cream. The peak defining the endpoint of whipping can be clearly seen. The whipping times measured for our model creams were significantly longer and had lower values for the peak of maximum resistance than those reported for natural cream whipped using the same apparatus [8]. However, the shape of the curves in Figure 6.4 and the microscopy images in Figure 6.5 suggest that despite the longer whipping times, the whipping process for our model cream follows a similar mechanism to that of natural whipping cream. For example, for the cream whipped at a rotational speed of 584 rpm (Figure 6.4), the three stages of whipping described by van Aken [8] can be clearly identified. In the first stage, large air bubbles are incorporated into the emulsion and broken up into smaller bubbles, this is characterised by a small increase in the power-input signal (Figure 6.4). During this first stage, the foam is considered to be

protein-stabilised [1,2]. A few emulsion droplets are observed to begin to adhere to the air bubble surface, but the air bubbles are not yet fully coated (Figure 6.5b). In the second stage of whipping, the coating of emulsion droplets at the air bubble surface gradually becomes denser (Figure 6.5c) and there is a gradual slight increase in the power transferred by the whisks (Figure 6.4), which is related to the increasing viscosity of the system. Finally, in the third stage there is a sharp increase in the power input (Figure 6.4); during this stage the size of the fat clumps increases (Figure 6.5d) and the cream becomes stiff as a network of partially coalesced emulsion droplets is formed.

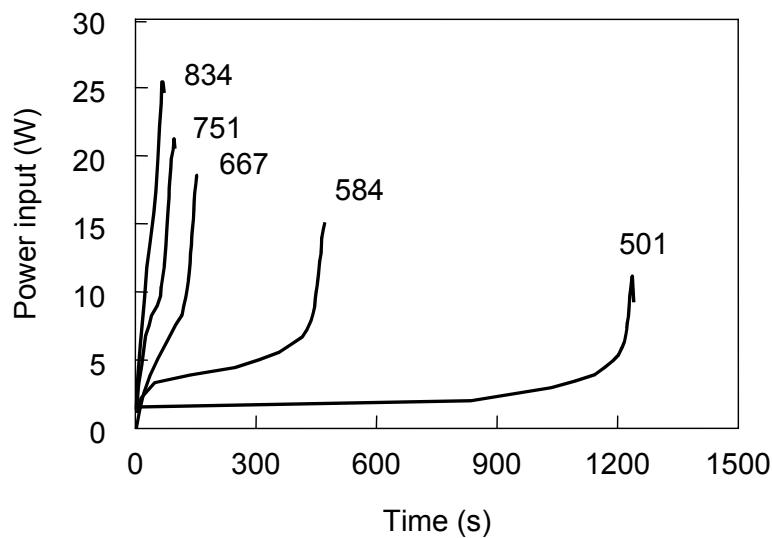


Figure 6.4 Power input transferred by the whisks vs. time during the whipping of WPI-stabilised model cream. Numbers near the curves denote the rotational speed of the whisks in rpm.

In addition, in Figure 6.4 we see that whipping time increases with decreasing rotational speed. The whipping time is re-plotted in Figure 6.6 as a function of rotational speed for WPI-stabilised model cream as well as for sodium caseinate-stabilised model cream and, for reference, for natural cream. The whipping times for natural cream are in agreement with the results reported by van Aken [8]. For all three systems, the whipping time begins to increase sharply for whipping speeds lower than 600 rpm (Figure 6.6). Van Aken [8] attributes the strong dependence of whipping time on rotational speed to a variation in the rate of transformation of free fat globules into

clumps driven by surface-mediated partial coalescence during the second stage of whipping.

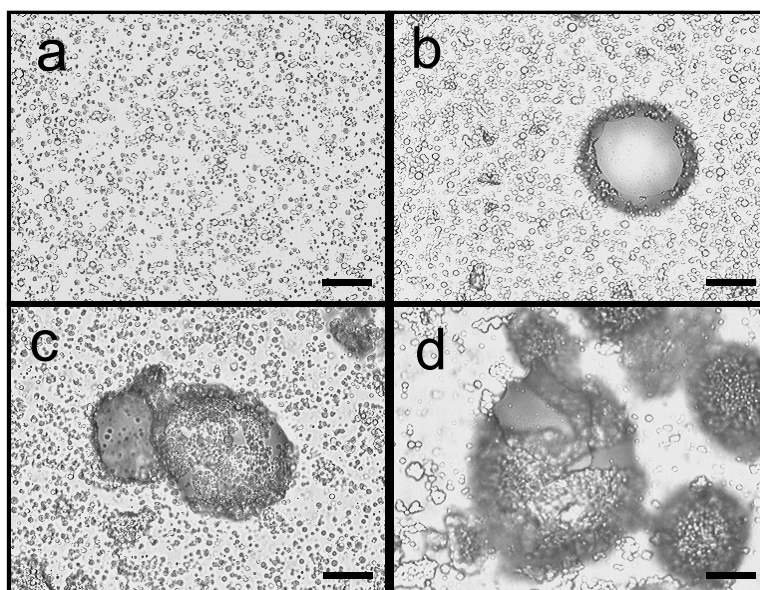


Figure 6.5 Light micrographs of WPI-stabilised model cream whipped at a rotational speed of 584 rpm. (a) before whipping, (b) after 50 sec, (c) after 290 sec and (d) after 473 sec. Time to reach endpoint of whipping: 473 sec. Length of bar = 100 μm .

Further, Figure 6.6 also shows that WPI-stabilised creams give shorter whipping times than sodium caseinate-stabilised creams, a trend that was also observed by van Camp et al. [20] for butterfat emulsions stabilised by WPI compared to those stabilised by sodium caseinate. This observation suggests that the transition from free fat droplets to clumped fat proceeds faster for WPI-stabilised creams than for sodium caseinate-stabilised creams. In an earlier paper [21] we observed that β -lactoglobulin forms brittle adsorbed layers at the air/water interface compared to β -casein, which forms more fluid-like layers. The former type of adsorbed layer (β -lactoglobulin) leads to entering and spreading of oil droplets over a much larger area in a single event, while the latter type (β -casein) results in more controlled emulsion droplet entering and spreading. If this is also the case for WPI compared to sodium caseinate, it may help explain the shorter whipping times observed for the WPI-stabilised compared to the sodium caseinate-stabilised creams (Figure 6.6). However, WPI is also less surface active than

sodium caseinate (Figure 6.2), which may also have a significant effect on the whipping time of the emulsions, as we will explain in the discussion section.

Protein concentration had an effect on the whipping time of WPI-stabilised model cream (Figure 6.7). The whipping time does not change much between the creams containing 0.6 and 1 wt% WPI, however there is a significant increase in the whipping time when the protein concentration is increased from 1 to 3 wt%. The effect of protein concentration on whipping time suggests fat clumping proceeds faster for the 0.6 and 1 wt% WPI creams than for the 3 wt% WPI cream. These results are also in qualitative agreement with van Camp [20], who observed a decrease in whipping time with decreasing whey protein concentrate (WPC) concentration (from 3.1 to 0.42 wt%), which below 1.6 wt% appeared to level off to a plateau value for whipping time. Further, these results are in qualitative agreement with Needs and Huitson [10], who observed a 50% decrease in whipping time for natural cream from which the milk serum proteins had been removed compared to unadulterated cream. We observed a slight decrease in the overrun of the emulsions with increasing protein concentration (Figure 6.7). Needs and Huitson [10] reported no significant effect of protein concentration on the overrun, nor did van Camp [20] in the case of WPC-stabilised model creams. This difference between our experimental results and the literature could be due to a difference in the whipping apparatus used.

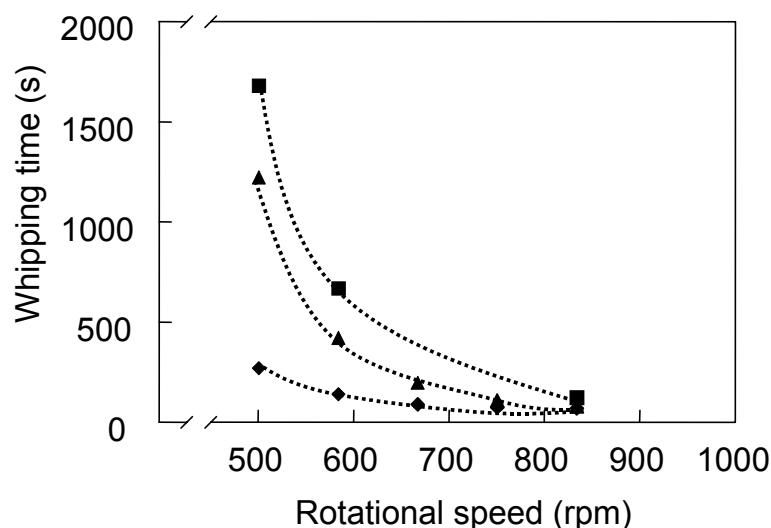


Figure 6.6 The influence of rotational speed on whipping time for model creams stabilised by either WPI (▲) or sodium caseinate (■) and for natural cream (◆). Dotted lines help to distinguish between data sets.

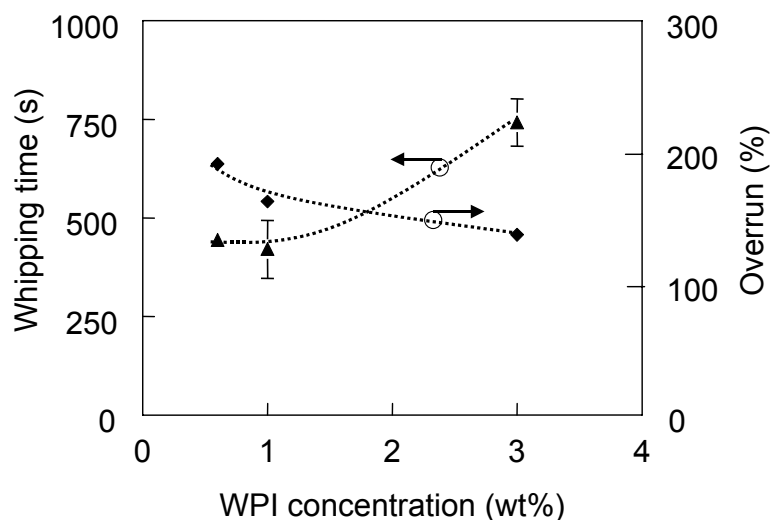


Figure 6.7 The influence of protein concentration on whipping time (▲) and overrun (◆) of WPI-stabilised emulsions. Dotted lines help distinguish between data sets. Whisk rotational speed: 584 rpm.

The influence of added low molecular weight surfactant on the whipping time and overrun of the model creams was also investigated. In Figure 6.8 the whipping times are shown for WPI-stabilised emulsions containing added Tween 20 (Figure 6.8a) or Span 80 (Figure 6.8b). In both cases we observed a decrease in whipping time with increasing surfactant concentration; the effect being stronger for Tween 20 than for Span 80, especially at lower concentrations. For the emulsions containing 2.7 and 5.5 mM Tween 20, the whipping time was decreased to such an extent that it was similar to that of natural cream whipped at the same rotational speed (Figure 6.6). A decrease in whipping time in the presence of added low molecular weight surfactant has also been reported for recombined cream to which glycerol monostearate had been added [22]. Further, the results are in qualitative agreement with the observation reported in the literature, that destabilisation of ice cream mix emulsions subjected to shear in the presence of air bubbles proceeds more rapidly in the presence of added emulsifier [23,24]. Over the range of concentrations used, the overrun was not influenced by the addition of Span 80 (Figure 6.8b). In the case of Tween 20 (Figure 6.8a) the cream containing 5.5 mM Tween 20 gave a lower overrun (~110%) compared to the other samples.

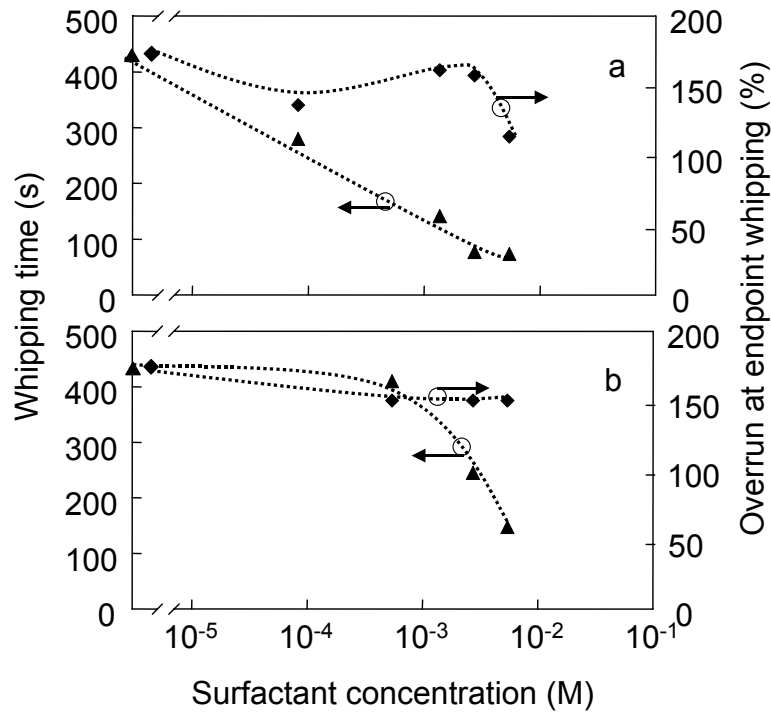


Figure 6.8 Whipping time (▲) and overrun (◆) of WPI-stabilised emulsions with added (a) Tween 20 (water phase) or (b) Span 80 (oil phase). Dotted lines help distinguish between data sets. The values measured in the absence of surfactant are shown on the primary y-axis before the break. Whisk rotational speed: 584 rpm.

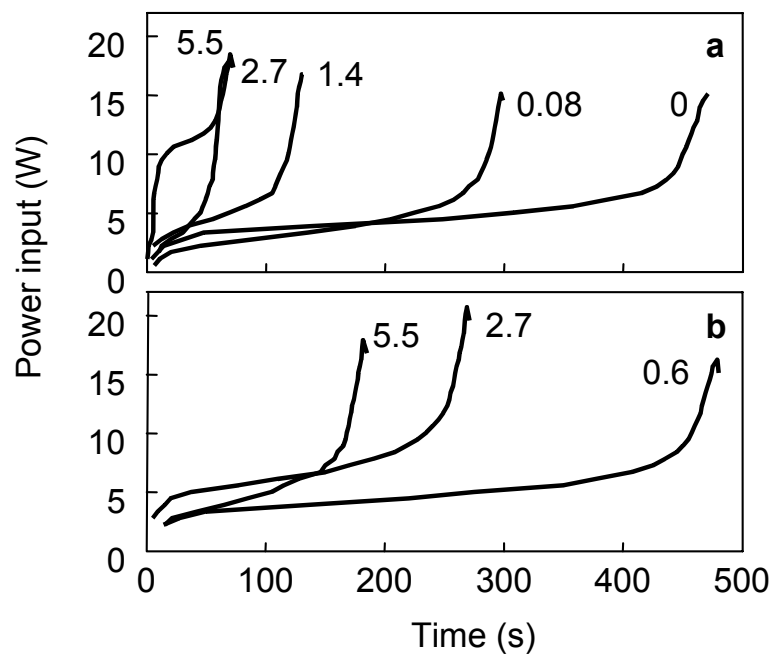


Figure 6.9 Power input transferred by the whisks vs. time for the whipping of model cream containing 1% WPI with added (a) Tween 20 or (b) Span 80. Numbers near the curves denote the lmw surfactant concentration in mM. Whisk rotational speed: 584 rpm.

The shape of power-input profile for the cream containing 5 mM Tween 20 (Figure 6.9) also differed from the other samples, which in addition to the low overrun may suggest that there is an optimum between accelerating the whipping process and forming a whipped cream with desirable structural characteristics. The power-input profiles for the remaining model creams with added surfactant (Figure 6.9) were similar in shape to those for the WPI-stabilised model cream in the absence of surfactants (Figure 6.3). The only difference was that with increasing surfactant concentration, a steady decrease in the length of the second stage of whipping was observed, which strongly suggests that surfactants play an important role in the adhesion and subsequent surface-mediated partial coalescence of emulsion droplets at the air/water interface. The sharpness of the peak in the third stage of whipping, the stage characterised by the build-up of a partially coalesced network, did not appear to differ between systems in the presence (Figure 6.9) or absence (Figure 6.3) of surfactant.

6.4 Discussion

We have demonstrated that whipping speed, protein type, protein concentration and the presence of low molecular weight surfactant all influence the whipping time of the model creams (Figures 6.6-6.8). Changes in whipping time are mainly due to a variation in the length of the second stage of whipping. This stage is characterised by the accumulation of fat globules at the air/water interface. Thus, our results strongly suggest that the rapidity and ease with which emulsion droplets can attach to and spread at the air/water interface determine the whipping time. We propose that the influence of the variables investigated on the whipping time can be explained in terms of the effect they have on the spreading behaviour of emulsion droplets at the planar air/water interface.

Brooker et al. [2] proposed that the incorporation of air is not sufficient stimulus per se to cause fat droplets to penetrate the air/water interface on a large scale. In our work on the spreading behaviour of emulsion droplets at the planar air/water interface [14], we established that an adsorbed protein layer can effectively inhibit droplet entering and spreading provided it maintains a pressure exceeding a critical value, Π_{cr} . During aeration, air bubbles are initially protein-stabilised [1,2]; thus, it seems reasonable to assume that during whipping, fat droplet adsorption and spreading can only

occur at the portion of the air bubble surface for which the air/water surface pressure is lower than Π_{cr} . This leads to the following scenario.

During the second stage of whipping, bubbles are in a dynamic state of formation, break-up and coalescence during which air bubble surfaces are continually expanded and compressed. As a result, at a given moment in time there will be a distribution of dynamic air/water surface pressures; ranging from low values for newly formed air bubble surfaces to high values for portions of the air bubble surface that are compressed. This distribution is represented schematically in Figure 6.10a. The total area under the curve represents the sum of the surface area of the individual air bubbles, or the total air bubble surface available in the whipped cream. The Π_{cr} required for fat droplet spreading is indicated by a vertical dotted line. The area under the curve to the left of this line is shaded to indicate that for this fraction of the total air bubble surface, the air/water surface pressure will be low enough for adsorption and spreading of fat droplets to occur. The remainder of the bubble area is inactive.

Adsorption and spreading of fat droplets at the air bubble surface is the precursor to surface-mediated droplet coalescence (Figure 6.1), which is a main determining factor for the whipping time of cream. Thus, we expect that manipulating the fraction of the total bubble surface area for which $S > 0$, will influence the ease and rapidity of fat droplet adhesion and spreading, ultimately governing the whipping time of the system. In this way, the spreading behaviour of emulsion droplets at the planar air/water interface is directly related to the whipping behaviour of cream.

First, let us assume that the situation in Figure 6.10a represents a reference case. If the surface pressure distribution is shifted to the left with respect to the reference case, as in Figure 6.10b, we expect the fraction of the total bubble surface area for which $S > 0$ to increase and the whipping time to decrease. In our experiments at the planar air/water interface (Figure 6.2) we observed that, for a protein solution, lower steady state surface pressures (i.e. a shift in the surface pressure distribution in Figure 6.10a to the left) could be achieved by increasing the relative expansion rate, decreasing the protein concentration or using WPI instead of sodium caseinate. Similarly, for the whipped model creams, increasing the rotational speed (Figures 6.4 and 6.6), decreasing the protein concentration (Figure 6.7) or using WPI instead of sodium caseinate (Figure 6.6) resulted in shorter whipping times.

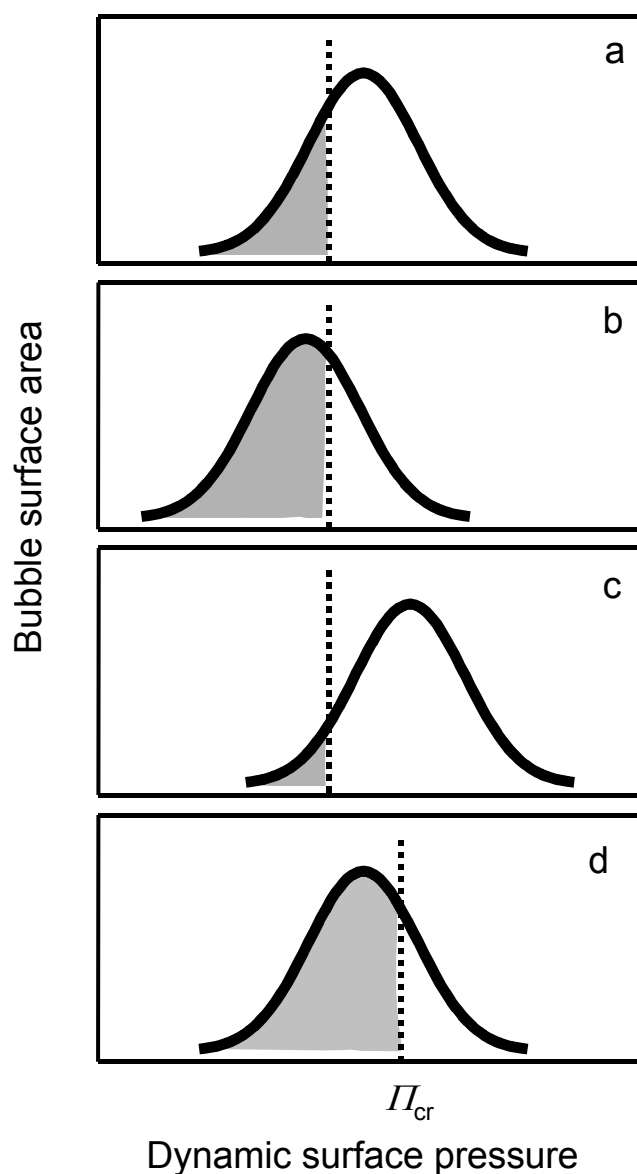


Figure 6.10. Schematic representation of the distribution of surface pressure values present at the surface of air bubbles during whipping. Vertical line indicates the critical surface pressure for spreading. For a given system (a), the shaded area under the curve indicates the fraction of the air bubble surface area for which fat droplet spreading can occur. This area can be increased or decreased by shifting the surface pressure distribution to the left (b) or to the right (c), respectively. In addition, if the critical surface pressure is shifted to a higher value (d) the fraction of the bubble surface area for which $S > 0$ will increase. As explained in the discussion section, increasing the proportion of the bubble surface area for which $S > 0$ leads to shorter whipping times, whereas decreasing the area leads to longer whipping times.

Conversely, if the surface pressure distribution is shifted to the right with respect to the reference case, as in Figure 6.10c, we expect the fraction of the total bubble surface area for which $S > 0$ to decrease and the whipping time to increase. This can be achieved by decreasing the relative expansion rate/rotational speed, increasing the protein concentration or using sodium caseinate instead of WPI. The experimental results for both expansion of planar air/water interface (Figure 6.2) and aeration by whipping (Figures 6.4, 6.6, and 6.7) confirm this, supporting the concept that the whipping time is related to the ease with which fat droplets can adhere to and spread at the air/water interface.

The line of reasoning depicted by Figure 6.10 can also be used to explain why the model creams stabilised by either 0.6 or 1 wt% WPI had similar whipping times, while the cream stabilised by 3 wt% WPI had a significantly longer whipping time (Figure 6.7). Spreading can occur as long as $S > 0$. If, for the 1 wt% WPI cream, the majority of the surface pressure distribution is already to the left of the critical surface pressure, then shifting the distribution even further to the left by lowering the protein content will no longer significantly influence the whipping time. However, increasing the protein concentration will shift the distribution to the right and with that, the whipping time of the cream will increase.

For the variables discussed above (rotational speed, protein type and protein concentration) the value of Π_{cr} was constant. However, if Π_{cr} can be shifted to higher Π_{AW} values, then we would expect $S > 0$ for an even greater proportion of the air bubble surface, leading to shorter whipping times without having to shift the position of the surface pressure distribution. This is depicted schematically in Figure 6.10d. The dynamic surface pressure distribution is constant with respect to Figure 6.10a, but shifting Π_{cr} to the right has increased the shaded area under the curve. In earlier work on spreading behaviour of emulsion droplets at the planar air/water interface [19], it was observed that surfactants facilitate droplet spreading by shifting Π_{cr} to higher Π_{AW} values. The value of Π_{cr} was increased from 15 mNm up to 17mN/m or 22 mN/m in the case of Span 80 or Tween 20, respectively (Figure 6.3). Correspondingly, in the whipping experiments (Figure 6.9) we observed a significant decrease in length of the second stage of whipping with increasing surfactant concentration. Thus, the decrease in whipping time in the presence of surfactants further strengthens our hypothesis that whipping

time is dependent on the rapidity and ease with which emulsion droplets can adhere to and spread at the air/water interface. It should be mentioned that the whipping time of the WPI-stabilised model creams is observed to begin to decrease (Figure 6.8) at surfactant concentrations that are considerably lower than those required for an increase in the value of Π_{cr} for β -lactoglobulin-stabilised emulsion (Figure 6.3). In addition to promoting surface-mediated partial coalescence as proposed in this paper, surfactants are known to promote shear-induced partial coalescence [3], which can also lead to faster clumping rates and shorter whipping times. The discrepancy between the surfactant concentration required to initiate a decrease in whipping time and that required to initiate an increase in Π_{cr} is a reminder that the effect of shear-induced partial coalescence on the whipping process cannot be entirely neglected.

Until now, researchers have tried to explain the influence of whipping speed, protein concentration, protein type and the presence of low molecular weight surfactant on the whipping behaviour of cream in terms of the static properties of the emulsion droplets and their adsorbed layers, such as adsorbed amount, relative strength of the adsorbed protein layer, size and orientation of fat crystals, or contact angle of the fat crystals at the oil/water interface. These properties of the emulsion droplets are of relevance to the probability of a fat crystal piercing the film between colliding droplets. The piercing probability is an important parameter controlling the rate of shear-induced partial coalescence and probably a significant parameter controlling the formation of a network of partially coalesced fat droplets during the third stage of the whipping process. However, we expect that these properties of the emulsion droplets are less important for the adhesion and spreading of emulsion droplets at the air/water interface, which we expect to be an important parameter controlling surface-mediated partial coalescence. Therefore, an explanation for the rate of partial coalescence based solely on the static properties of the emulsion droplets fails when applied to aerated emulsions. The conceptual model presented in Figure 6.10 demonstrates that the influence of rotational speed, protein concentration, protein type and the presence of emulsifiers on the whipping behaviour of cream (Figures 6.6-6.8 and [8,10,20,22-24]) can be well accounted for in terms of the influence of these variables on the spreading behaviour of emulsions. This model (Figure 6.10), when combined with the existing knowledge of the factors

promoting shear-induced partial coalescence, can more fully account for the dependence of the whipping time of the model emulsions on the experimental system parameters (rotational speed, protein concentration, protein type and presence of emulsifiers). The industry has long been aware of the fact that in order to improve the whipping properties of recombined cream, emulsifiers must be added. The mechanism of surface-mediated partial coalescence and how it can be controlled (Figure 6.10) helps to explain why this is so.

It would be interesting to determine if the model presented in Figure 6.10 can be applied to explain why homogenised cream tends to have much longer whipping times than natural cream [5,7]. In homogenised cream, adsorbed caseins and whey proteins [25] stabilise the fat droplets. In natural cream, the fat droplets are stabilised by the milk fat globule membrane, which comprises a complex mixture of proteins, phospholipids, neutral glycerides (including mono- and diglycerides), and other components. Phospholipids, mono- and diglycerides, which are known to be fairly surface active, together account for ~ 41 wt% of the total membrane [6]. Conceivably, the abundant presence of these small, surface active molecules in the MGF_M could shift Π_{cr} to a higher value compared to the Π_{cr} for homogenised cream, where the droplets are predominantly protein stabilised (e.g. Figure 6.10d compared to Figure 6.10a) and in this way lead to shorter whipping times for natural cream. However, detailed information regarding the spreading behaviour of fat globules from natural and homogenised cream at the air/water interface is required if we wish to accept or reject this hypothesis.

6.5 Summary

In our experiments at the planar air/water interface we found that oil spreading can be controlled by manipulating the expansion rate of the air/water interface, bulk protein concentration, protein type and the balance of forces at the three-phase boundary. It is generally accepted that during the whipping of natural and recombined cream fat droplets adhere to the air/water interface where they partially coalesce with neighbouring droplets leading to structure development in the foam. Presumably, the faster this surface-mediated partial coalescence occurs, the shorter the time required to reach the endpoint of whipping. In this work, we observed that an increased whipping speed, decreased protein concentration, or the addition of lmw surfactant lead to shorter whipping times. Further, shorter whipping times

were observed for WPI-stabilised cream compared to cream stabilised by sodium caseinate. In all cases, the decrease in whipping time was due to a decrease in the length of the second stage of whipping; the stage characterised by the adhesion of fat droplets to the air bubble surface. The decrease in whipping time could be accounted for by considering the influence of whisk rotational speed, protein concentration, protein type and lmw surfactant concentration on the fraction of bubble surface area for which fat droplet spreading is possible. The same parameters that promote droplet spreading at the air/water interface result in a decrease in the whipping time of our model creams. Correlating the whipping time of cream with the spreading behaviour of fat droplets at the air/water interface represents a new insight into the mechanisms involved in the whipping of cream.

Acknowledgements

The authors thank Serena Avino and Sören Stinner for performing experiments. Danisco Ingredients, Denmark is gratefully acknowledged for providing the fully hydrogenated palm fat.

References

- [1] Anderson, M., Brooker, B. E. and Needs, E. C. (1987). The role of proteins in the stabilization/destabilization of dairy foams. In E. Dickinson, *Food Emulsions and Foams* (pp. 100-109). London: Royal Society of Chemistry.
- [2] Brooker, B. E., Anderson, M. and Andrews, A. T. (1986). The development of structure in whipped cream. *Food Microstructure*, 5, 277-285.
- [3] Darling, D. F. (1982). Recent advances in the destabilization of dairy emulsions. *Journal of Dairy Research*, 49, 695-712.
- [4] Goff, H. D. (1997). Instability and partial coalescence in whippable dairy emulsions. *Journal of Dairy Science*, 80, 2620-2630.
- [5] Graf, E. and Müller, H. R. (1965). Fine structure and whippability of sterilized cream. *Milchwissenschaft*, 20(6), 302-308.
- [6] Mulder, H. and Walstra, P. (1974). *The Milk Fat Globule*. Wageningen: Pudoc.
- [7] Schmidt, D. G. and van Hooydonk, A. C. M. (1980). A scanning electron microscopical investigation of the whipping of cream. *Scanning Electron Microscopy*, III, 653-658.
- [8] van Aken, G. A. (2001). Aeration of Emulsions by whipping. *Colloids and Surfaces A: Physicochemical and Engineering Aspects*, 190, 333-354.
- [9] van Boekel, M. A. J. S. and Walstra, P. (1981). Stability of oil-in-water emulsions with crystals in the disperse phase. *Colloids and Surfaces*, 3, 109-118.
- [10] Needs, E. C. and Huitson, A. (1991). The contribution of milk serum proteins to the development of whipped cream structure. *Food Structure*, 10, 353-360.
- [11] Boode, K. and Walstra, P. (1993). Partial coalescence in oil-in-water emulsions 1. Nature of the aggregation. *Colloids and Surfaces A: Physicochemical and Engineering Aspects*, 81, 121-137.
- [12] Labuschagne, J. H. (1963). *Churning in the absence of air*. Thesis: Wageningen Agricultural University, The Netherlands.

- [13] Harkins, W. D. and Feldman, A. (1922). Films. The spreading of liquids and the spreading coefficient. *The Journal of the American Chemical Society*, 44(12), 2665-2685.
- [14] Hotrum, N. E., van Vliet, T., Cohen Stuart, M. A. and van Aken, G. A. (2002). Monitoring entering and spreading of emulsion droplets at an expanding air/water interface: a novel technique. *Journal of Colloid and Interface Science*, 247(1), 125-131.
- [15] Schokker, E. P., Bos, M. A., Kuijpers, A. J., Wijnen, M. E. and Walstra, P. (2003). Spreading of oil from protein stabilized emulsions at air/water interfaces. *Colloids and Surfaces B: Biointerfaces*, 26(4), 315-327.
- [16] Hotrum, N. E., Cohen Stuart, M. A., van Vliet, T. and van Aken, G. A. (2004). Spreading of partially crystallized oil droplets on an air/water interface. *Accepted to Colloids and Surfaces A: Physicochemical and Engineering Aspects*.
- [17] Brooker, B. E. (1993). Stabilisation of air in foods containing fat - a review. *Food Structure*, 12, 115-122.
- [18] Hotrum, N. E., Cohen Stuart, M. A., van Vliet, T. and van Aken, G. A. (2003). Entering and Spreading of Protein Stabilised Emulsion Droplets at the Expanding Air/Water Interface. In E. Dickinson and T. van Vliet, *Food Colloids, Biopolymers and Materials* Cambridge: Royal Society of Chemistry.
- [19] Hotrum, N. E., Cohen Stuart, M. A., van Vliet, T. and van Aken, G. A. (2004). Oil droplet spreading in the presence of proteins and low molecular weight surfactants. *Submitted*
- [20] van Camp, J., van Calenberg, S., van Oostveldt, P. and Huyghebaert, A. (1996). Aerating properties of emulsions stabilized by sodium caseinate and whey protein concentrate. *Milchwissenschaft*, 51(6), 310-315.
- [21] Hotrum, N. E., Cohen Stuart, M. A., van Vliet, T. and van Aken, G. A. (2003). Flow and fracture phenomena in adsorbed protein layers at the air/water interface in connection with spreading oil droplets. *Langmuir*, 19, 10210-10216.
- [22] Zadow, J. G. and Kiesecker, F. G. (1975). Manufacture of recombined whipping cream. *The Australian Journal of Dairy Technology*, 30(3), 114-117.
- [23] Pelan, B. M. C., Watts, K. M., Campbell, I. J. and Lips, A. (1997). The stability of aerated milk protein emulsions in the presence of small molecule surfactants. *Journal of Dairy Science*, 80, 2631-2638.
- [24] Goff, H. D. and Jordan, W. K. (1989). Action of emulsifiers in promoting fat destabilization during the manufacture of ice cream. *Journal of Dairy Science*, 72, 18-29.
- [25] Darling, D. F. and Butcher, D. W. (1978). Milk-fat globule membrane in homogenized cream. *Journal of Dairy Research*, 45, 197-208.

Summary

The whipping of cream has both fascinated and baffled scientists for decades. Whipped cream is an example of an aerated emulsion: through the incorporation of air bubbles, a three-phase partially crystallised fat-in-water emulsion (cream) is transformed into a four-phase system (whipped cream). Several types of cream can be distinguished including natural cream, homogenised cream and recombined cream; all can be considered to be dispersions of oil (fat) in a continuous aqueous phase. In order to be able to form the partially coalesced fat droplet network which provides structural stability to the whipped cream, creams must contain a mixture of liquid and solid fat. Irrespective of the type of cream, when whipped, the adhesion and partial wetting of the air bubble surface with liquid fat from the droplets is a critical step in the development of this partially coalesced fat droplet network. However, at the time work on this thesis started, information in scientific literature describing the parameters controlling the entering and spreading of emulsion droplets at the air/water interface was sparse. In this thesis, we set out to deepen our knowledge concerning the parameters that are of relevance to the entering and spreading of emulsion droplets at the air/water interface; this was the subject of investigation in Chapters 2-5. Moreover, our aim was to determine whether a link exists between the entering and spreading behaviour of emulsion droplets at the air/water interface and the whipping properties of cream, which was addressed in Chapter 6.

In Chapter 2, we began by characterising the entering and spreading behaviour of protein-stabilised emulsion droplets at quiescent and expanding air/water interfaces. For this purpose an apparatus was developed which consisted of a Langmuir trough in which the air/water interface could be continuously expanded by means of rollers in the place of the traditional sliding barrier. When sodium caseinate and whey protein isolate-stabilised emulsion droplets were injected under the surface of sodium caseinate and whey protein isolate solutions, respectively, it appeared that the droplets entered and spread at the air/water interface only if the air/water surface pressure did not exceed a threshold value of ~ 15 mN/m, which we termed the critical surface pressure. This condition could be satisfied either under quiescent conditions for low protein concentrations or by continuous expansion of the interface at higher protein concentrations. The existence of a critical surface pressure of ~ 15 mN/m for sunflower oil spreading out of

protein-stabilised emulsion droplets indicates that the air/water interface does not need to be completely void of adsorbed protein in order for spreading to occur.

In Chapter 3, we took a more in-depth look at oil spreading at the air/water interface for protein-stabilised emulsion droplets, in this case added under the surface of a spread protein layer. By using a spread protein layer, adsorption of protein from the underlying bulk solution could be neglected. The essentially irreversible nature of protein adsorption allowed manipulation of the air/water surface tension by expansion of the air/water surface such that oil droplet spreading could be induced. From the morphology of the spreading emulsion, clear differences in the surface flow behaviour of different protein films could be observed. The proteins investigated represent a series exhibiting an increased tendency to form a coherent protein film at the air/water interface in the order β -casein (pH 6.7) < β -lactoglobulin (pH 6.7) < soy glycinin (pH 3). In the case of β -casein, the protein film flowed and oil spread in a radial fashion. The β -lactoglobulin and soy glycinin films on the other hand fractured during expansion and oil spread in the cracks in the protein film, making the broken structure visible. The observation of film fracture serves as strong visual evidence for an inhomogeneous distribution of protein molecules in the protein film during large-scale deformation of protein films formed from certain proteins. The thermodynamic criteria for oil spreading were not influenced by the mechanical properties of the protein film.

It is well known that emulsifiers, or low molecular weight (lmw) surfactants can increase the sensitivity of emulsions to coalescence and partial coalescence under shear. This effect is even stronger for emulsions sheared in the presence of air. In Chapter 4, in an attempt to better understand the mechanism by which lmw surfactants promote emulsion droplet coalescence in the presence of air, we investigated the influence of lmw surfactant on the spreading behaviour of emulsified oil at the air/water interface. Two non-ionic lmw surfactants, polyoxyethylene sorbitan monolaurate (Tween 20, water-soluble) and sorbitan monooleate (Span 80, oil-soluble), were used. The maximum value of the air/water surface pressure allowing oil spreading was significantly higher in the presence of sufficiently high concentrations of Span 80 (17 mN/m) or Tween 20 (22 mN/m), than in the absence (or at low concentrations) of surfactant (15 mN/m). These results demonstrate that the

presence of lmw surfactants can facilitate oil droplet spreading at the air/water interface. The increase in the critical surface pressure for spreading implies a shift in the balance of forces at the oil/water/air phase boundary, which is likely due to the fact that lmw surfactants are more effective than proteins in lowering the oil/water surface tension under the dynamic conditions encountered during oil droplet spreading. This may be relevant to the aeration of emulsions: an increase in the value of the air/water surface pressure for which oil spreading can occur may explain the increased instability against (partial) coalescence of emulsions with added lmw surfactant compared to protein-only stabilised emulsion droplets when these systems are sheared in the presence of air. This explanation can be seen as an alternative to the explanation that the decreased stability against coalescence results from a decrease in the mechanical strength of the adsorbed protein layer when lmw surfactant molecules adsorb and displace protein molecules from the oil/water interface.

It is known that in order to build up a network of partially coalesced emulsion droplets, both liquid and crystalline fat must be present in the droplets. Some authors have speculated that the presence of crystalline fat in emulsion droplets may reduce or retard oil spreading, which is considered to be one of the mechanisms by which crystalline fat provides stability and structure to aerated emulsions such as whipped cream. In Chapter 5, the influence of crystalline fat in the emulsion droplets on the droplet spreading behaviour was investigated. The influence of crystalline fat on the amount and rate of oil spreading out of emulsion droplets onto either a clean or a protein-covered air/water interface was measured for β -lactoglobulin-stabilised emulsions prepared with either anhydrous milk fat or a blend of hydrogenated palm fat and sunflower oil. At a clean interface, the liquid oil present in the emulsion droplets was observed to completely spread out of the droplets unimpeded by the presence of a fat crystal network. Further, the rate of oil spreading was not influenced by the presence of crystalline fat. At a protein covered interface, the spreading behaviour of the emulsion droplets containing crystalline fat was evaluated in terms of the value of the surface pressure at the point of initiation of oil spreading; this value was unaffected by the presence of crystalline fat. Based on these results, we concluded that it is unlikely that the role of crystalline fat in stabilising air bubbles in systems such as whipped cream is to reduce oil spreading at the air/water interface.

Finally, in Chapter 6, we presented a model in which we draw a parallel between the spreading behaviour of emulsion droplets at the air/water interface and the whipping properties of recombined cream. The influence of whisk rotational speed, protein concentration, protein type and the presence of lmw surfactant on the whipping time of recombined cream was investigated. Increasing the rotational speed, decreasing the protein concentration, or adding lmw surfactant all resulted in shorter whipping times. Further, creams stabilised by whey protein isolate had shorter whipping times than creams stabilised by sodium caseinate. Moreover, the addition of lmw surfactant lead to a significant decrease in the whipping time of the emulsions. In the presented model, the influence the experimental variables on whipping time could be well correlated with their ability to promote oil spreading at the air/water interface. This model is fundamentally different from earlier, less successful, models that attempted to describe the influence of whipping speed, protein concentration, protein type and the presence of lmw surfactant on the whipping behaviour of cream in terms of their influence on the static properties of the adsorbed layer at the fat droplet surface or the contact angle between fat crystals and the oil/water interface.

This thesis represents a contribution towards understanding the physical principles underlying the spreading behaviour of emulsion droplets at the air/water interface. It is generally accepted that during the whipping of cream, fat droplets adhere to the air/water interface, where they can partially coalesce with neighbouring droplets. This is a key step in the development of whipped cream structure. Presumably, the faster droplets can partially coalesce at the air/water interface, the shorter the time required to whip the cream to its maximum stiffness. We have demonstrated that the same parameters that promote emulsion droplet spreading also improve the whippability of cream. We therefore conclude that emulsion droplet spreading is a key parameter controlling the interaction between emulsion droplets at the air/water interface during whipping. We expect that the improved understanding of mechanisms of emulsion droplet spreading presented in this thesis will enable the food industry to take a more strategic approach to product formulation. In a wider frame of reference, we expect that the work presented here can improve our understanding of the stability of emulsions when they come into contact with air in general, for example as a result of processing operations including stirring, pouring, or mastication.

Samenvatting

Het opkloppen van slagroom heeft wetenschappers al tientallen jaren gefascineerd en verbaasd. Opgeklopte room is een voorbeeld van een beluchte emulsie: een drie-fasen systeem, namelijk een (gedeeltelijk gekristalliseerde) olie-in-water emulsie (room) wordt door het inbrengen van luchtbellens omgezet in een vier-fasen systeem (slagroom). Voor de ontwikkeling van stevigheid in geslagen room is het essentieel dat er bij het kloppen een driedimensionaal netwerk van gedeeltelijk samengevloeiende emulsiedruppels ontstaat. Algemeen wordt aangenomen dat tijdens het opkloppen van room emulsiedruppels adsorberen aan de ingeslagen luchtbellens, waarover ze vervolgens gedeeltelijk kunnen spreiden. Wanneer tijdens het opkloppen luchtbellens coalesceren, worden de gedeeltelijk gespreide emulsiedruppels naar elkaar toe gedreven, waarna ze gedeeltelijk samenvloeien (partiële coalescentie). Partiële coalescentie is alleen mogelijk wanneer de emulsiedruppels zowel vloeibaar als vast vet bevatten. Bij het begin van dit onderzoek was er in de wetenschappelijke literatuur weinig bekend over de factoren die een rol spelen bij het adsorberen en spreiden van emulsiedruppels aan lucht/water-grensvlakken. Sindsdien hebben we onze kennis op dit gebied sterk uitgebreid. Het onderzoek waaruit deze kennis is voortgekomen, staat beschreven in de hoofdstukken 2-5. In hoofdstuk 6 wordt beschreven hoe het adsorptie- en spreidgedrag van emulsiedruppels aan het lucht/water grensvlak correleert met het opklopproces, en met de eigenschappen van de slagroom.

In hoofdstuk 2 worden adsorptie en spreiding van eiwit-gestabiliseerde emulsiedruppels aan stilstaande en expanderende lucht/water-grensvlakken beschreven. Om deze processen te bestuderen, werd een nieuwe meetmethode ontwikkeld, bestaande uit een aangepaste Langmuirtrog waarin het lucht/water-grensvlak doorlopend geëxpandeerd kon worden door middel van draaiende cilinders in plaats van de gebruikelijke bewegende barrières. In de experimenten werden natriumcaseïnaat of wei-eiwitisolaat-gestabiliseerde emulsiedruppels geïnjecteerd onder het oppervlak van respectievelijk natriumcaseïnaat- en wei-eiwitisolaat-oplossingen. Het bleek dat de emulsiedruppels alleen konden adsorberen en spreiden wanneer de oppervlaktedruk van het lucht/water-grensvlak lager was dan ~ 15 mN/m. Dit gold zowel voor stilstaande grensvlakken bij lage eiwitconcentraties, als voor expanderende grensvlakken bij hogere

eiwitconcentraties. Deze drempelwaarde hebben we de kritische oppervlaktedruk genoemd. Deze kritische oppervlaktedruk van ~ 15 mN/m impliceert dat het lucht/water-grensvlak niet volledig vrij hoeft te zijn van geadsorbeerd eiwit om de emulsiedruppels toch te laten spreiden.

In hoofdstuk 3 wordt het onderzoek naar het spreidgedrag van eiwitgestabiliseerde emulsiedruppels aan lucht/water-grensvlakken met een gespreide eiwitlaag beschreven. Het gebruik van gespreide eiwitlagen als modelsysteem heeft als voordeel dat adsorptie van eiwit uit de onderstaande oplossing verwaarloosd kan worden, waardoor specifieke aspecten van het spreidgedrag van emulsiedruppels voor diverse eiwitsystemen beter onderzocht konden worden. Doordat eiwit vrijwel niet desorbeert van lucht/water-grensvlakken, kon de oppervlaktedruk van het grensvlak zodanig ingesteld worden dat spreiden van emulsiedruppels al dan niet plaatsvond. Bij het spreiden van de emulsiedruppels werden duidelijke verschillen in het stromingsgedrag van verschillende geadsorbeerde eiwitlagen waargenomen. Eiwitten vormen een min of meer coherente film aan het lucht/water grensvlak: van de onderzochte eiwitten varieerde de sterkte van de eiwitlaag in de volgorde β -caseïne < β -lactoglobuline < soya glycinine. In het geval van β -caseïne vloeide de eiwitlaag in radiale richting uit als gevolg van spreiding van emulsiedruppels. De eiwitlagen van β -lactoglobuline en soya glycinine braken daarentegen tijdens het expanderen, en de olie spreidde in de scheuren van de eiwitlaag. Deze waarneming vormt een visueel bewijs dat eiwitlagen niet homogeen zijn tijdens grote vervormingen.

Partiële coalescentie van emulsiedruppels aan het lucht/water-grensvlak is een belangrijk proces tijdens het opkloppen van room. Het is bekend dat de aanwezigheid van emulgatoren de gevoeligheid van emulsies voor partiële coalescentie vergroot en daarmee het opklopgedrag bevordert. De huidige opvatting over het mechanisme hiervan is dat emulgatoren de eiwitten van het water/olie-grensvlak verdringen, waardoor de mechanische sterkte van de eiwitlagen afneemt. Onze alternatieve hypothese is dat emulgatoren het adsorptie- en spreidgedrag van emulsiedruppels bevorderen, doordat zij tijdens het spreiden de olie/water grensvlakspanning kunnen verlagen. Om deze hypothese te testen, hebben we de invloed van emulgatoren op het spreidgedrag van emulsiedruppels onderzocht, wat in hoofdstuk 4 beschreven staat. Hierbij hebben we twee niet-ionogene emulgatoren gebruikt:

het water-oplosbare polyoxyethyleen-sorbitan-monolaureaat (Tween 20) en het olie-oplosbare sorbitan-monooleaat (Span 80). De kritische oppervlaktedrukken voor het spreiden van emulsiedruppels gestabiliseerd door β -lactoglobuline/Tween 20 (22 mN/m) en β -lactoglobuline/Span 80 (17 mN/m) bleken significant hoger dan die voor eiwitgestabiliseerde emulsiedruppels (15 mN/m). Deze resultaten laten zien dat de aanwezigheid van emulgatoren het spreiden van emulsiedruppels bevordert door het evenwicht van krachten aan het lucht/water/olie-grensvlak te verschuiven. Emulgatoren zijn effectiever dan eiwitten in het verlagen van de oppervlaktespanning van het olie/water-grensvlak onder de dynamische omstandigheden zoals tijdens het spreiden van emulsiedruppels. Dit heeft tot gevolg dat de emulsiedruppels al bij een lagere grensvlakspanning aan de luchtbellen zullen adsorberen en spreiden, waardoor de opkloptijd wordt verkort. Dit mechanisme vormt dus een alternatief voor/aanvulling op de huidige opvatting dat emulgatoren het opklopedrag bevorderen doordat ze eiwitten van het water/olie-grensvlak verdringen.

Om een netwerk van partieel gecoalesceerde emulsiedruppels te verkrijgen, is het essentieel dat de emulsiedruppels zowel vloeibaar als vast vet bevatten. Diverse onderzoekers hebben gesuggereerd dat de aanwezigheid van vast vet in emulsiedruppels het spreiden van olie vertraagt of vermindert. In hoofdstuk 5 is het onderzoek naar de invloed van vast vet op het spreidgedrag van emulsiedruppels beschreven. De kritische oppervlaktedruk voor spreiding op een lucht/water-grensvlak met een geadsorbeerde eiwitlaag was onafhankelijk van het gehalte vast vet. Ook de snelheid waarmee de olie spreidde op een schoon lucht/water-grensvlak bleek onafhankelijk van het gehalte vast vet. De hoeveelheid olie die uit de met β -lactoglobuline gestabiliseerde emulsiedruppels kon spreiden, kwam overeen met de beschikbare hoeveelheid vloeibaar vet in de emulsiedruppels, maar gezien het grote aantal beschikbare emulsiedruppels in room is dit niet een beperkende factor. We concludeerden dat het onwaarschijnlijk is dat onder normale omstandigheden het opkloppen van room beïnvloed wordt door vertraagde of verminderde spreiding van olie als gevolg van de aanwezigheid van vast vet.

In hoofdstuk 6 wordt een model gepresenteerd waarin het spreidgedrag van emulsiedruppels op het lucht/water-grensvlak wordt gerelateerd aan opklopeigenschappen van gerecombineerde room. Opklopexperimenten met

gerecombineerde room lieten zien dat verhogen van de klopsnelheid, verlagen van de eiwitconcentratie, of toevoegen van emulgator in een verkorte opkloptijd resulteerde. Gerecombineerde room gestabiliseerd door wei-eiwitisolaat had een kortere opkloptijd dan gerecombineerde room gestabiliseerd door natriumcaseïnaat. Het effect van deze variabelen correleert met het gemak waarmee emulsiedruppels adsorberen aan en spreiden op het lucht/water-grensvlak bij vergelijkbare omstandigheden als tijdens het opkloppen. Het gepresenteerde model is fundamenteel anders dan eerdere modellen die de invloed van de bestudeerde variabelen op de opkloptijd beschreven. Deze modellen gingen er veelal vanuit dat het opklopedrag wordt bepaald door de mechanische eigenschappen van de geadsorbeerde eiwitlaag aan het oppervlak van de emulsiedruppels, terwijl ons model uitgaat van de adsorptie- en spreidingseigenschappen van de emulsiedruppels.

Het onderzoek beschreven in dit proefschrift draagt bij aan het begrip van de fysische principes welke ten grondslag liggen aan het spreidgedrag van emulsiedruppels aan het lucht/water-grensvlak, alsook aan de ontwikkeling van structuur tijdens het opkloppen van slagroom. In dit proefschrift hebben we laten zien dat de factoren die het spreiden van emulsiedruppels bevorderen, dezelfde zijn als die de opkloppen van room verbeteren. Dit betekent dat het spreiden van emulsiedruppels aan lucht/water grensvlakken een belangrijke factor is in de ontwikkeling van de structuur in opgeklopte slagroom: hoe sneller de emulsiedruppels kunnen adsorberen en spreiden op de luchtbel, hoe sneller ze partieel kunnen coalesceren, en hoe korter de tijd totdat de slagroom zijn maximale stevigheid bereikt. Onze nieuwe inzichten inzake de interactie tussen emulsiedruppels en luchtbellen tijdens het opkloppen, zullen de levensmiddelenindustrie in staat stellen hun productontwikkeling gericht te sturen. Verder zal het onderzoek ook bijdragen aan een beter begrip van de stabiliteit van emulsies wanneer deze met lucht in contact komen, bijvoorbeeld bij processtappen als roeren, pompen en gieten, maar ook bij het bewerken van voedsel in de mond.

List of Publications

Journals

- Hotrum, N.E.**, van Vliet, T., Cohen Stuart, M.A., van Aken, G.A. (2002) Monitoring entering and spreading of emulsion droplets at an expanding air/water interface: a novel technique, *Journal of Colloid and Interface Science* **247**: 125.
- van Aken, G.A., Blijdenstein, T.B.J., **Hotrum, N.E.** (2003) Colloidal destabilisation mechanisms in protein-stabilised emulsions, *Current Opinion in Colloid and Interface Science* **8**: 371.
- Hotrum, N.E.**, Cohen Stuart, M.A., van Vliet, T., van Aken, G.A. (2003) Flow and fracture in adsorbed protein layers at the air/water interface in connection to spreading oil droplets, *Langmuir* **19**: 10210.
- Hotrum, N.E.**, Cohen Stuart, M.A., van Vliet, T., van Aken, G.A. Spreading of partially crystallized oil droplets on an air/water interface. *Accepted for publication in Colloids and Surfaces A: Physicochemical and Engineering Aspects*.
- Hotrum, N.E.**, Cohen Stuart, M.A., van Vliet, T., van Aken, G.A. Oil droplet spreading in the presence of proteins and low molecular weight surfactants. *Submitted 2004*.
- Hotrum, N.E.**, Cohen Stuart, M.A., van Vliet, T., Avino, S.F., van Aken, G.A. Elucidating the relationship between the spreading coefficient, surface-mediated partial coalescence and the whipping time of cream. *To be submitted 2004*.

Conference Proceedings

- Hotrum, N.E.**, Cohen Stuart, M.A., van Vliet, T., van Aken, G.A. (2003) Entering and spreading of protein-stabilized emulsion droplets at the expanding air-water interface, *in Food Colloids, Biopolymers and Materials* (T. van Vliet and E. Dickinson, Eds.), Royal Society of Chemistry, Cambridge, p. 192.
- Hotrum, N.E.**, Cohen Stuart, M.A., van Vliet, T., van Aken, G.A. (2003) Insertion and spreading of emulsion droplets at the air/water interface: relevance to aerated food systems, *in Proceedings of the Third World Congress on Emulsions, Lyon, September 24-27, 2002*.
- Hotrum, N.E.**, Cohen Stuart, M.A., van Vliet, T., van Aken, G.A. Proposing a relationship between the spreading coefficient and the whipping time of cream, *in Food Colloids, Interactions, Microstructure and Processing* (E. Dickinson, Ed.), Royal Society of Chemistry, Cambridge, *Submitted 2004*.

Acknowledgements

Dit proefschrift is het resultaat van vier jaar onderzoek bij het WCFS, Fysko en Food Physics. Je kunt zien dat ik de afgelopen vier jaar een beetje overal heb gezeten, en ik denk dat ik het beste van al die werelden heb kunnen ervaren.

Het werk dat beschreven staat in dit proefschrift is gereed gekomen met de hulp en medewerking van anderen, welke ik hier wil bedanken. In de eerste plaats wil ik mijn promotor, Martien Cohen Stuart, en mij co-promotoren, George van Aken en Ton van Vliet, bedanken voor hun begeleiding, betrokkenheid, vele ideeën en constructief kritiek. Het was een waardevolle ervaring om met jullie te hebben mogen samenwerken.

Franklin Zoet, van jou heb ik veel geleerd over het opzetten en plannen van experimenten. Ook heb je een groot gedeelte van de in dit proefschrift beschreven experimenten uitgevoerd. Kortom, je bent onmisbaar geweest. Ook dank ik Renate Ganzevles, die in het kader van haar afstudeervak bij Fysko een grote bijdrage geleverd heeft aan het werk dat in hoofdstuk 3 beschreven staat. Renate, onze samenwerking heb als erg prettig ervaren en ik ben blij dat je mijn paranimf wilt zijn. I'd also like to thank Serena Avino and Sören Stinner for their hard work in generating the experimental results that are described in Chapter 6.

Ronald Wegh, Hennie van Beek, Gert Nieuwboer, Jan Theunissen en de medewerkers van het werkplaats dank ik voor hun technisch deskundigheid die de "roller trog" en "Trurnit methode" mogelijk gemaakt heeft.

Alle medewerkers van het SEF-project, Fysko, Food Physics en PDQ dank ik voor hun medewerking en de goede sfeer op het werk. Mijn kamergenoten, Carline, Anneke, Theo, Jeannet, Catriona, Hilde, Paolo, Farid, en Olga, wil ik in het bijzonder bedanken voor de interessante discussies en de gezelligheid. Mede dankzij jullie heb ik met veel plezier hier gewerkt. Anneke, behalve collega ben je ook een vriendin en ik ben blij dat je mijn paranimf wilt zijn.

Mijn schoonfamilie ben ik dankbaar voor de warme omgeving, waardoor ik mij vanaf de eerste dag thuis voelde in Nederland.

Thanks to Mum and Dad for their encouragement, support and having the courage to let me be me. Amy, thanks for your interest and enthusiasm and for cheering me on from a distance.

Finally, dearest Erix, my partner, mentor and friend; on the path of life, I'm thankful to be travelling with you.

Curriculum Vitae

Natalie Elizabeth Hotrum was born on October 16, 1975 in Point-Claire, Canada. From 1977-1989 she lived in Toronto, where she attended primary and middle school. From 1989-1997 she lived in Edmonton, Canada. In 1993, she graduated from Ross Sheppard Composite High School. In the same year, she began her university education in the Faculty of Science at the University of Alberta. In the spring of 1997 she graduated with a Bachelor of Science; Chemistry major, Biological Sciences minor.

In May 1997 she joined Prof. D. G. Dalgleish's research group as an M.Sc. student at the Department of Food Science, University of Guelph, Canada. From May 1998-May 1999 she carried out her thesis research project at the Institute of Food Nutrition and Human Health, Massey University, New Zealand, under the supervision of Prof. H. Singh. Upon returning to the University of Guelph, she successfully defended her thesis entitled "Interactions between κ -carrageenan and β -lactoglobulin in gelling and non-gelling aqueous systems" thus completing the Master of Science degree in June, 1999.

From August 1999 to March 2004, Natalie worked as a Ph.D. student at the Wageningen Centre for Food Sciences in collaboration with the Laboratory for Physical Chemistry and Colloid Science at Wageningen University, The Netherlands. The work carried out during this period is described in this thesis.

The research described in this thesis was part of the research programme “Structure and Functionality” of the Wageningen Centre for Food Science and was carried out at Wageningen University, The Netherlands.

Cover Front, CSLM image of whipped recombined cream, Henrie van Aalst, Unilever R&D, The Netherlands

Back, Protein layer morphology made visible by spreading emulsion droplets

Printing Ponsen & Looijen BV, Wageningen